THE EFFECTS OF CLIMATIC CONDITIONS AND BRICK CONTENT ON RECYCLED ASPHALT PAVEMENT AND RECYCLED CONCRETE AGGREGATE AS UNBOUND ROAD BASE

By

RYAN F. SHEDIVY

A thesis submitted in partial fulfillment
of the requirements for the degree of

MASTER OF SCIENCE

GEOLOGICAL ENGINEERING

at the

UNIVERSITY OF WISCONSIN-MADISON

FALL 2012

THE EFFECTS OF CLIMATIC CONDITIONS AND BRICK CONTENT ON RECYCLED ASPHALT PAVEMENT AND RECYCLED CONCRETE AGGREGATE AS UNBOUND ROAD BASE

Students Name

Campus ID Number

Approved:

Signature Date

Tuncer B. Edil, Professor

Signature Date

James M. Tinjum, Assistant Professor

Executive Summary

This study evaluates the use of recycled concrete aggregate (RCA) and recycled asphalt pavement (RAP) as an unbound road base. This investigation looked at the climatic behavior (i.e., temperature effects, wet/dry cycling) of RAP and RCA and the effects of brick content on the resilient modulus and plastic strain (as an index) of RCA. The two chapters of this thesis individually discuss each one of these studies. The recycled materials used in this study came from a large geographical area covering eight U.S. states including California, Colorado, Michigan, Minnesota, New Jersey, Ohio, Texas and Wisconsin. Basalt and a quartz/granite/limestone blend meeting Minnesota Department of Transportation's Class 5 gradation standard were used as control materials.

Resilient modulus tests were conducted on the materials according to protocol 1-28a of the National Cooperative Highway Research Program (NCHRP). Modifications were made to the triaxial cell for resilient modulus to accommodate varying temperatures (7 °C to 50 °C) to test the materials at. The Power function proposed by Moosazedh and Witczak (1981) and NCHRP models were fitted to the resilient modulus test data to estimate resilient modulus as a function of stress state. The NCHRP model provided higher coefficients of determination than the Power function model. A summary resilient modulus (SRM) was calculated from the Power function and NCHRP models at a bulk stress of 208 kPa, which is typical for a base

course and the recommended bulk stress value for NCHRP 1-28a. External LVDT data provided more reliable SRM values than internal LVDT data.

The effects of temperature on resilient modulus of the RAP and RCA were evaluated using NCHRP 1-28a protocols at 7, 23, 35, and 50 °C. No decrease in SRM was observed in the RCA and natural aggregates tested. A decrease in SRM of approximately 37% and 30% was observed for both TX and CO RAP, respectively, tested between the 23 °C and 35 °C temperatures; however, this decreasing trend did not continue between 35 °C and 50 °C where it stabilized. This decrease in SRM is suggestive of a critical temperature between 23 °C and 35 °C where the physical characteristics of the asphalt binder coating the aggregates is altered.

The increased temperature caused the strain rate to increase in all RAPs, but no effects occurred in the natural aggregates or RCAs tested. NJ RAP had the highest strain rate, followed by TX RAP and then CO RAP. Most of the increase in strain rate occurred within the first 1,000 cycles (conditioning phase) of the resilient modulus test. Total cumulative plastic strains achieved in RAPs were generally high (> 7%), which is similar to results reported in the literature, but increased temperature increased the rate at which the plastic strain was achieved. Due to this trend, RAP that is placed and compacted during the warmest time of the year could act to reduce the total plastic strain accumulation after pavement is laid.

A procedure to evaluate the effects of wetting and drying of RAP and RCA on particle degradation was developed. Two RCAs, two RAPs, and two natural aggregates were tested at 5, 10, and 30 wet/dry cycles. Micro-Deval and particle

size distribution tests were conducted on the materials after their specificed wet/dry cycle. No trend was observed in Micro-Deval loss percentage or particle size distribution due to wet/dry cycles, which suggests that wetting and drying of recycled material has no effect on particle degradation.

One of the most costly and time consuming impurities to remove before and during crushing of recycled materials is brick because of its extensive use as a façade material covering concrete buildings. To study if brick is a major impurity in RCA, compaction tests and resilient modulus tests were completed on RCA mixed with brick at 0, 10, 20, and 30% brick by mass. Four RCAs were used: NJ, OH, MN, and TX. Compaction tests were completed at 0% and 30% brick on all RCA materials except NJ RCA due to lack of materials. When compared to 0% brick specimens, optimum moisture content increased and dry unit weight decreased in all RCAs mixed with 30% brick. This was attributed to brick having higher absorption and lower specific gravity and dry unit weight than RCA. Water drained out of the compaction molds if more water than OMC was added, not allowing maximum dry unit weight to decrease. No apparent trends were observed between SRM and brick content three of the four RCAs tested, but a decrease in plastic strain was observed with increased brick content.

Acknowledgments

I would like to thank my academic and research advisors, Professors Tuncer B. Edil and James M. Tinjum, for their guidance and support over the past year during my masters program and over the entire last six years in the Geological Engineering program at the University of Wisconsin. I would also like to thank Professors Craig Benson and Dante Fratta for their support and advice throughout my time at the University of Wisconsin. It has been a wonderful experience and I have gained numerous lifelong skills I will cherish throughout my life and career.

I would also like to thank everyone affiliated with the Geological Engineering program at UW-Madison. My undergraduate advisor, Jean Bahr, for helping make graduating so much easier because of her tremendous organization skills. Xiaodong (Buff) Wang for helping me out with all the tests I completed and helping me trouble shoot any problems I ran into. I would also like to thank Bill Lang for teaching me the laboratory skills I needed to know to be productive in the structures lab.

I would especially like to thank all the other undergraduate and graduate students in the Geological Engineering program at the University of Wisconsin, especially Jeff Lin and Andrew Ruetten for enduring all of those days in the compaction and structures labs crushing brick and mixing aggregate. Special thanks also to Ozlem Bozyurt for helping me start this project as her undergraduate assistant. I would also like to thank my colleagues Kongrat Nakkaew, Erica Hagen,

Steve Schubert, Jiannan Chen, Ali Soleimanbeigi, and Tirupan Mandal for helping me with this project.

Another group of people I could not have completed this without out my good friends Andrew Keene, Joe Scalia, Lauren Meyer, Nikki Woodward, Erin Hunter, Chris Bareither, Jordan Radke, Eric Schrauben, Dan Abel, Damian Naylor, David Larson, Ian Olson, Dan Shedivy, Matt Regner, Justin Marita, Andre Perkins, and Nick and Michelle Howe. Thanks for taking my mind off of work sometimes and helping me get through everything.

Most of all I would like to thank my family: my parents (Gary and Toni Shedivy), my brother and sister-in-law (Justin and Margo Shedivy), my sister and brother-in-law (Heidi and Brett Sjoberg), my nieces (Avery and Freya), and especially my girlfriend, Christie Rosebraugh. All of you have provided me with the everyday support and encouragement I needed to get to where I am today. Without all of you I would not have been able to accomplish this. This thesis is dedicated to all of you.

The results in this study are based on work supported by the TPF-5 (129) Recycled Unbound Materials Pool Fund administered by The Minnesota Department of Transportation and the Recycled Materials Resource Center (RMRC), which is supported by the Federal Highway Administration. The opinions, findings, conclusions, or recommendations expressed herein are those of the author(s) and do not necessarily represent the views of the sponsors.

TABLE OF CONTENTS

LIST OF TABLES

LIST OF FIGURES

1. The Effects of Wet/Dry Cycling on Particle Degradation and Temperature on Resilient Modulus of Recycled Concrete Aggregate and Recycled Asphalt Pavement

1.1 INTRODUCTION

There are over 6.5 million km of roads in the United States (US) (FHWA 2010). The most common raw material used in road construction and reconstruction is natural aggregate, created by crushing rock. Use of natural aggregates has increased from approximately 229 million metric tons in 1950 to 1.15 billion metric tons in 2011, of which 82% was used as construction material, mainly for road construction (USGS 2011). Access to natural aggregates has become more difficult because of reduced "ideal" sites caused by increasing environmental regulations and previous depletion of resources (Carpenter et al. 2007). The price of natural aggregates has increased due to increased demand in conjunction with a decreased supply near building locations (Robinson and Brown 2002). With decreased supply and increased demand, alternatives for natural aggregate have been considered.

Sustainable alternatives to natural aggregate that are increasing in use are recycled asphalt pavement (RAP) and recycled concrete aggregate (RCA). RAP is produced by removing and crushing asphalt pavement, while RCA is a collection of concrete acquired from demolition of buildings, runways, and roadways (Kuo et al. 2002, Guthrie et al. 2007, FHWA 2008). As of 1998, only 80% of all asphalt concrete aggregate debris was recycled, with the remaining 20% landfilled (Wilburn 1998). Concrete is even less recycled. Approximately 50% of concrete debris is recycled.

The use of RAP and RCA as a substitute for natural aggregate can also reduce costs. The majority of costs from using natural aggregate are incurred from transportation of the material from the quarry to the job site (Robinson and Brown 2002). By recycling old roadway material on-site, the transportation costs are reduced significantly. Furthermore, there are no costs associated with mining or tipping fees for the construction and debris (C&D) waste. The only additional costs incurred are associated with crushing, sorting, and handling the material on-site.

In addition to the benefit of cost savings, greenhouse gas emissions can be reduced by using RAP and RCA (Horvath, 2003). Mining emits greenhouse gases through the stripping of vegetation surrounding the mine and using fossil fuels to operate machinery. The use of recycled materials will reduce the need for mining and, in turn, reduce the greenhouse gas emissions produced by mining.

Although RAP and RCA are currently used as an alternative road base material, studies characterizing the mechanical properties of the materials are lacking (Bennert et al. 2000, Nataatmadja and Tan 2001, Guthrie et al. 2007, FHWA 2008). Specifically, the thermo-mechanical behavior, influence of wetting and drying, and the effects of freeze-thaw cycles have not been thoroughly investigated (Bozyurt 2011). RCA and RAP perform well at room temperature, but the climatic effects (i.e., freeze-thaw, temperature, and wet/dry) associated with the use of these materials year-round in varying climates need to be investigated to recommend more accurate design procedures based on location

The effects of temperature on the resilient modulus and plastic deformation of RCA and RAP when used as unbound base course has not been investigated. RAP

contains a temperature-sensitive material, asphalt binder, which becomes less viscous as temperature increases (Griffin et al. 1959). RCA also can contain asphalt binder as a deleterious material. To investigate the effects that temperature has on RAP when used as an unbound base course, resilient modulus tests were conducted at varying temperatures. From this test, plastic strain could be calculated for each material at each temperature. Natural aggregates were used as a control material.

Wetting and drying is a typical test conducted on concrete to evaluate the effects of wetting and drying on soil-cement losses, water content changes, and volume changes (ASTM D559). There is no wet/dry standard for testing unbound aggregate. A procedure was developed for wet/dry testing of unbound aggregates to see the effects the process had on particle degradation. RAP, RCA, and natural aggregates were subjected to varying wet/dry cycles and both particle size distributions (PSDs) and Micro-Deval tests were performed before and after the wetting and drying.

Road base aggregates have to withstand constant variation in temperature in temperate climates. During the spring and fall, road bases can undergo multiple cycles of freezing and thawing daily. Freezing and thawing of aggregates can have detrimental effects on the aggregate because of expansion and contraction of the water inside the pore space of the aggregate. When water freezes within the pore space of the compacted aggregate, aggregates can foul and produce excess fines, reducing the competency of the road base. To investigate this climatic effect, material was compacted at optimum moisture content (OMC) and subjected to varying freeze-thaw cycles. Resilient modulus tests were then conducted on the specimens to evaluate the effects of freeze-thaw on stiffness.

1.2 BACKGROUND

1.2.1 Recycled Unbound Base Materials

Researchers have investigated the use of RCA in road base or subbase courses to provide a viable option for the reuse of this C&D waste (Poon and Chan 2005). RCA is used predominantly in pavement construction as replacement for natural aggregates and cement-treated subbase layers (Saeed et al. 2006). Molenaar and Niekerk (2002) investigated the engineering properties of RCA and suggested that good-quality road base or subbase can be built from these materials. The Federal Highway Administration (2008) reported that, when compared to natural aggregates, RCA has lower density, higher water absorption, higher soundness mass loss, and higher content of foreign material. In most cases, however, the properties of RCA are within the specifications for base course or concrete aggregate.

Park (2003) investigated the characteristics and performance of RCA as road base and subbase for concrete pavement by comparing the engineering properties of RCA with those of crushed stone aggregate. The performance characteristics were evaluated based on compatibility, shear resistance, and stability of RCA; and the mechanical properties were evaluated in the field using a falling weight deflectometer to determine deflections. RCA had the same compactibility as crushed stone aggregate and shear resistance equal to or better than crushed stone aggregate. Park (2003) concluded that the RCA can be used as base and subbase materials in place of crushed stone aggregate for supporting a concrete pavement system.

The National Asphalt Pavement Association (NAPA) (2009) reported that asphalt pavement is the most recycled material in the US. The US highway construction

industry annually produces more than 100 million tons of RAP that is recycled into new pavements (NAPA 2009). According to FHWA (2011), RAP is a valuable and high-quality material that may demonstrate good performance as a granular road base and a replacement for more expensive virgin aggregate.

Guthrie et al. (2007) conducted free-free resonant column tests on RAP and natural aggregate blends to evaluate the effects of percentage change of RAP on the stiffness of road base. Blends were prepared according to the following RAP and natural aggregate percentages: 100/0, 75/25, 50/50, 25/75, and 0/100. Stiffness was determined after compaction at OMC, after a 72-h period of heating at 60 ^{0}C to simulate summer conditions; and after a 10-d period of capillary soaking followed by a 24-h period of submersion to simulate conditions of field saturations. At OMC, the stiffness decreased with the addition of 25% RAP, then increased with the addition of 50%, 75%, and 100% RAP. When the material was heated for 72-h, the stiffness increased with the addition of 25% RAP and then decreased with the addition of 50%, 75%, and 100% RAP. According to Guthrie et al. (2007), the decrease in stiffness is related to the softening behavior of asphalt due to heat. In the soaked condition, the stiffness of the material behaved similar to the samples in the dry condition, but with stiffness values between 40% and 90% lower.

Kim et al. (2007) investigated the stiffness of base course containing different ratios of RAP and natural aggregate. Resilient modulus tests were conducted on the recycled material in accordance with National Cooperative Highway Research Program testing protocol 1-28A (NCHRP 1-28a). The 50% aggregate-50% RAP specimens developed stiffness equivalent to the 100% aggregate specimens at lower confining

pressures (~ 20 kPa); at higher confinement (~ 120 kPa), the RAP specimens were stiffer.

Bennert et al. (2000) compared the mechanical properties of two types of C&D waste, RCA and RAP, with dense-graded aggregate base course, used in roadway base applications in New Jersey. The RAP and RCA were mixed at varying percentages with the dense-graded aggregate base course. Bennert et al. (2000) found that the pure RAP and RCA samples had higher stiffness than the dense-graded aggregate base course, and the stiffness of the base course increased with an increase in RAP and RCA content. The pure RCA specimens accumulated the least amount of permanent strain. Even though pure RAP was stiffer than the dense-graded aggregate base course, the RAP accumulated the greatest amount of permanent strain. Bennert et al. (2000) reported that the resulting contrast between the pure RAP resilient modulus and its permanent deformation might be due to the breakdown of asphalt binder under loading.

1.2.2 Resilient Modulus

The design of roadway pavement relies on proper characterization of the load-deformation response of the pavement layers (Tian et al. 1998). Base and subgrade deform when subjected to repeated loads from vehicular traffic. The M_r defines the nonlinear elastic response of pavement geomaterials, such as unbound aggregate base and subbase, under repeated traffic loads. The resilient behavior of unbound aggregate layers is affected by the stress state experienced because of wheel loading and the physical properties of aggregate (Pan et al. 2006). The M_r is a linear-elastic modulus

obtained from dynamic loading, defined as the ratio of the cyclic deviator stress to the resilient (recoverable) strain, and is defined as:

$$M_r = \left({}^{\sigma_d}/_{\varepsilon_r} \right) \quad (1.1)$$

where ε_r is the recoverable elastic strain and σ_d is the applied deviator stress.

Design of pavements and rehabilitation of layered pavement systems use M_r as an essential parameter in the design process (Heydinger et al. 2007). The M_r is a key input in NCHRP 1-37 (mechanistic-based pavement design approach), which is being evaluated for adoption by numerous state highway agencies (Pan et al. 2006). The performance of pavement is dependent on the stiffness of the pavement structure under specified traffic loads and environmental conditions. Generally, a high M_r for a base course infers a stiffer base course layer, which increases pavement life. The resilient response of granular material is important for the load-carrying ability of the pavement and the permanent strain response, which characterize the long-term performance of the pavement and rutting phenomenon (Lekarp et al. 2000).

1.2.3 Freeze-Thaw Effect on RAP and RCA

Seasonal variation in moisture and temperature occurs in most areas of the US. The M_r of road base and subbase tends to change throughout the pavement's life due to these seasonal variations. The freeze-thaw (F-T) cycling of pavement profiles may significantly influence pavement performance and is a major climatic behavior evaluation factor of base course materials. The M_r of an aggregate base/subbase is thought to increase during freezing and drying and decrease during thawing and wetting (Kootstra et al. 2009). Therefore, pavement design in regions where variations in

temperature and moisture are appreciable should consider these factors (Zaman and Zhu 1999).

Bozyurt (2011) studied the effects of F-T cycling on some of the same materials used in this study. Those materials were CA, MN, and TX RAP; Class 5; and MI, TX, and CA RCA. Specimens were prepared at room temperature and then subjected to 0, 5, 10, and 20 F-T cycles. After the appropriate F-T cycle, resilient modulus tests were conducted on the recycled materials. Bozyurt (2011) found that the SRM of the RAPs decreased with increased number of F-T cycles, but at a slower overall rate than Class 5. This decrease was attributed to particle degradation and progressive asphalt binder weakening. SRM of the RCA decreased from zero to five F-T cycles, but increased in SRM between 5 and 20 F-T cycles. This behavior was attributed to progressive generation of fines and hydration of the cement paste. Results can be seen in Figure A.5 to Figure A.8 in the Appendix.

1.2.4 Temperature Effects on Resilient Modulus

Roads in certain climates can experience a large range and/or fluctuation in temperature. While road surface courses experience this hot and cold weather directly, the road base course is insulated by the surface course and does not experience as great a fluctuation in temperature. Unbound base course typically comes from rock that has been crushed. Rock contains no material that is affected by the temperature change experienced by road base courses, but recycled materials can contain components that could make them susceptible to temperature.

RAP contains bituminous asphalt, a material that exhibits decreased viscosity with increased temperature (Griffin et al. 1959, Roberts et al. 1996, Lee et al. 2008, West et al. 2010). Because bituminous asphalt coats many of the aggregates in RAP, a decrease in viscosity has the potential to impact the particle interlocking of the material during or after compaction. A decrease in asphalt stiffness due to a decrease in viscosity is also observed as a result of increased temperature. Asphalt binder increases in stiffness but becomes brittle in nature at temperatures below freezing (Marasteanu and Anderson 1996). Materials with asphalt binder also observe increased strain at elevated temperature (Soleimanbeigi 2012). Soleimanbeigi (2012) observed an exponential increase in secondary compression index with increased temperature with a recycled asphalt shingles/bottom ash mixture. Kim and Labuz (2007) investigated the effects of various natural aggregate/RAP blends on M_r and cumulative plastic strain and found both cumulative plastic strain and M_r increased with increasing RAP content.

Wen et al. (2011) studied the effects of temperature on M_r for natural aggregate base course mixed at 0%, 20%, 40%, and 60% RAP. The materials were mixed at OMC and compacted to 95% maximum dry unit weight, then subjected to -20 °C, 20 °C, and 60 °C temperatures. The results showed that there was little effect to M_r with increase of temperature from 20 °C to 60 °C on the 0% and 20% RAP. For the 40% and 60% RAP mixes, there was up to 5% and 30% decreases, respectively in M_r with increased temperature from 20 °C to 60 °C. The decrease in M_r with increased temperature in the 40% and 60% RAP mixtures was attributed to the reduction in asphalt stiffness with temperature increase. A decrease in M_r with increased RAP

content was observed on the specimens tested at -20 °C. The opposite effect was observed with the RAP mixtures at 20 °C; M_r increased with increased RAP content, a characteristic observed at UW-Madison.

1.2.5 Wet/Dry Cycling

Unbound base courses experience numerous wetting and drying cycles throughout their lifetime. These wet/dry cycles are mostly caused from influxes in precipitation, but can also stem from other sources such as water table increases and flooding. Aggregates used in road construction should be weather resistant so they do not degrade and breakdown when subjected to wetting and drying (Wu et al. 1998). Bozyurt (2011) investigated the effects of weathering and handling of RAP and RCA using the Micro-Deval test (AASHTO T-327). RAP and RCA had higher Micro-Deval losses than the Class 5 natural aggregate control material, but both recycled materials had lower losses than the recommendation for natural aggregate in design manuals (i.e., DOT specifications).

The wet/dry cyclic test is a standard test used in concrete. This test has been used to evaluate the effects on soil-cement losses and volume changes with increased cycles on concrete (ASTM D559). Previous studies have not been completed to evaluate the effects of wet/dry cycles on unbound aggregates, nor has any standard been developed.

1.3 MATERIALS

The recycled materials used in this study were obtained from various states in the US. Three RAPs and three RCAs were collected and named according to the state of origin. The materials represent coarser, medium, and finer gradations based on their grain size (D_{50}, C_c, and C_u). The reference base courses studied and used as the controls in this study were a gravel meeting Class 5 aggregate specifications for base course per the Minnesota Department of Transportation and crushed basalt from Senegal, Africa. The basalt was material studied previously by a visiting scholar at the University of Wisconsin-Madison.

Six recycled materials and two conventional base courses were used in the first part of this investigation. Three of the recycled materials were recycled asphalt pavement (RAP) and three were recycled concrete aggregate (RCA). The recycled materials used in this study were obtained from a wide geographical area, covering four different states: California, Colorado, New Jersey, and Texas. The Class 5 aggregate was composed of quartz, granite and carbonates (limestone and dolomite). The ratio of quartz/granite to carbonates is 2.1. The percentage of mineral type in Class 5 aggregate was 68% for Quartz/Granite and 32% for Carbonates. Percent quartz/granite (aggregate and concrete) and percent carbonate of gravel (aggregate and concrete) of gravel are 43% and 20%, respectively. The crushed basalt was 100% basalt crushed in Senegal, Africa and transported to the University of Wisconsin by a visiting Senegalese scholar to mechanically characterize, and the remaining unused material was used for this study.

The RAP received from the Colorado DOT was collected from hundreds of reclaimed highways. Although the RAP came from varied sources, the aggregates for the production of the asphalt originated from rock in Colorado, most from quarries in Morrison and Golden and some aggregates were sourced from the Platte River.

The material provided by the New Jersey DOT (NJ DOT) is from stockpiles for demolition projects, primarily in New Jersey. The material in the stockpiles is in flux since NJ DOT constantly adds new loads and removes content for different purposes.

The CA RCA provided by the California DOT is broken concrete rubble from the demolition of structures. Stockpiling in California is usually done three times a year. These stockpiles are not added to throughout their life-cycle. If stockpiled material is still unavailable during visits from subcontractors, new material is used to create a new stockpile.

The RCA sent by the Texas DOT is from a commercial source; therefore, the individual sources of aggregate or material characteristics included in the RCA are not known. The Texas RAP is from a highway project where the contractor milled the "binder" course after approximately 1.5 years of service.

A summary of the index properties and soil classifications is shown in Table 1.1. The materials used in this study are classified as non-plastic per ASTM D 2487, the Unified Soil Classification System (USCS). The recycled materials (three RCAs and three RAPs) classified as A-1-a and Class 5 and basalt aggregates classified as A-1-b according to the AASHTO soil classification system (ASTM D 3282). Specific gravity (G_s) and absorption tests were conducted according to AASHTO T 85. Asphalt content was determined by ASTM 6307. The modified Proctor compaction test (ASTM D 1557)

was performed to determine the optimum moisture content (w_{opt}) and maximum dry unit weight (γ_{dmax}). The particle size distribution (PSD) for the investigated materials were determined according to ASTM D 422 and are shown in Figure 1.1a and Figure 1.1b, along with upper and lower bounds reported in literature (Bennert et al. 2000, Bejarano et al. 2003, Blankenagel and Guthrie 2006, Guthrie et al. 2007, Saeed 2008, Kuo et al. 2002).

1.4 METHODS

1.4.1 Resilient Modulus

Resilient modulus tests were performed on compacted specimens according to NCHRP 1-28a Procedure Ia, which applies to base and subbase materials. The materials used in this study classify as Type I material in NCHRP 1-28A, which requires a 152-mm diameter and 305-mm high specimen for resilient modulus testing (NCHRP 2004). Specimens were prepared at OMC and compacted to 95% of maximum modified Proctor density. Specimens were compacted in six lifts of equal mass within 1% of the target dry unit weight and 0.5% of target moisture content to ensure uniform compaction (NCHRP 2004).

Resilient modulus tests were conducted with internal and external linear variable displacement transducers (LVDT). External LVDTs have an accuracy of ± 0.005 mm, and internal LVDTs have an accuracy of ± 0.0015 mm. Clamps for the internal LVDTs were built in accordance with NCHRP 1-28A specifications. Internal LVDTs were placed at quarter points of the specimen to measure the deformations over the half-length of the specimen, whereas external LVDT measured deformations of the entire specimen

length. An MTS Systems Model 244.12 servo-hydraulic machine was used for loading the specimens. Loading sequences, confining pressures and data acquisition were controlled from a computer running LabView 8.5 software.

Various factors influence the M_r including loading conditions (confining and deviatoric stresses), physical properties (water content, void ratio, matric suction), and soil properties (particle size distribution and plasticity). The most important factors are stress conditions. Because of this, multiple models have been proposed to examine the relationship between M_r and stress factors (i.e., deviatoric and confining stresses). The two models used in this study were the Power model proposed by Moosazedh and Witczak (1981) and the NCHRP model. Both are described below. First the M_r for each load sequence was obtained by averaging the M_r from the last 5 cycles of each test sequence. The M_r data were fitted with the Power function model proposed by Moosazedh and Witczak (1981)

$$M_r = k_1 \times \left(\frac{\theta}{p_a}\right)^{k_2} \tag{1.2}$$

where M_r is resilient modulus, θ is bulk stress, p_a is atmospheric pressure (101.4 kPa), and k_1 and k_2 are empirical fitting parameters. The constant k_1 is unique to a given material and is independent of k_2. k_2 represents the effect of stress on the modulus and varies within narrow limits (0.45 to 0.62 for granular base (Huang 2003)). k_1 and k_2 are material-dependent parameters. The range of k_1 varies greatly and its value is largely controls M_r predicted. Bulk stress is another means of quantifying confining pressure and deviator stress in a single term and is defined as the sum of the three principle stresses. Bulk stress is defined as

$$\theta = \sigma_1 + \sigma_2 + \sigma_3 \tag{1.3}$$

where σ_1, σ_2, and σ_3 are the principal stresses acting on the specimen.

The M_r data were also fitted with the NCHRP model(NCHRP 2004) defined

$$M_r = k_1 . p_a . \left(\frac{\theta - 3k_6}{p_a}\right)^{k_2} . \left(\frac{\tau_{oct}}{p_a} + k_7\right)^{k_3} \quad (1.4)$$

where k_1, k_2, k_3, k_6, and k_7 are constants, p_a is atmospheric pressure (101.4 kPa), τ_{oct} is octahedral shear stress, and θ is bulk stress.

For every specimen tested, it is important that the M_r values calculated at the end of each cycle and used to determine the SRM are accurate. To determine the accuracy of the values calculated, a coefficient of variance was determined for the last five M_r values of each sequence, which are averaged to calculate the M_r of a sequence. M_r values with a coefficient of variation above 8% were not used to calculate the SRM of the specimen.

For base course, the SRM corresponds to the M_r at a bulk stress of 208 kPa, as suggested by Section 10.3.3.9 of NCHRP 1-28a. SRM is used to determine the layer coefficient, which is a required input in the AASHTO pavement design equation (Tian et al. 1998). The Power function (Eq. 1.2) is a simple model that is widely used for granular materials. The estimated SRM per the Power function model was compared to the measured modulus. Statistical analysis indicated that results from the Power function model are significant at a 95% confidence level, and the model represents the data reasonably well for RCA (R^2 = 0.85) and for RAP (R^2 = 0.90) (Bozyurt 2011).

1.4.2 Temperature Effects on Resilient Modulus

The effect of temperature on the engineering properties of the tested materials was determined by completing M_r tests at varying temperatures. M_r tests were carried out on specimens at four different temperatures: 7 °C, 23 °C, 35 °C, and 50 °C. The lower and upper bounds were selected because of the limits imposed by the equipment used that would allow for the NCHRP 1-28a standard to be followed. Specimens were compacted at OMC and at 95% maximum modified dry unit weight and prepared according to the NCHRP 1-28a standard as outlined in Section 1.4.1.

Due to the hydraulics needed for the M_r test, the equipment could not be moved to a temperature controlled room for the tests to be conducted at varying temperatures. Instead of controlling the temperature around the entire platform of the hydraulic actuator, the temperature control was limited to the acrylic cell containing the specimen. Figure 1.2a and Figure 1.2b show the M_r setup of the temperature-controlled cell with hot water and with cold water, respectively. The NCHRP 1-28a standard specifies that air must be used as the confining fluid during the M_r test. Due to air being used as the confining fluid, temperature-controlled water was circulated through 15.2-m of 6.35-mm-diameter copper coil wrapped around the inside of the acrylic cylinder to heat or cool the specimen through heating or cooling the confining air. The temperature the specimen could reach was limited due to the confining air insulating the heat transfer from the copper coil to the specimen.

The temperature-controlled water was heated in a 152-mm permeameter using a Watlow FIREROD immersion heater, which operated at 100 °C. A thermocouple was placed inside the water-filled permeameter to determine the temperature of the

circulating water. The thermocouple was connected through a data logger, which was controlled by a LabVIEW program that turned the heater on and off to regulate the circulating water temperature. Water was circulated from the permeameter to the copper coil using a 2650 L/h magnetically driven pump that was placed outside of the permeameter. 6.35-mm-diameter Tygon tubing was used to transfer the water from the permeameter to the copper coil and back. A similar setup was used for the 7 °C temperature goal, except a freezer was used to hold a 75-L container of water. The 2650 L/h pump was placed inside the 75-L container and 6.35-mm-diameter tubing was again used to transfer water from the reservoir to the copper coil and back. For tests at 35 °C, and 50 °C, a blanket was wrapped around both the acrylic cell and the water reservoir to limit heat dissipation. For tests conducted at 7 °C, a blanket was wrapped around the acrylic cell and placed over the freezer to reduce cold air dissipation.

To determine the specific temperatures to test the material at, calibration of the equipment was conducted to determine the limiting temperature of the equipment. Class 5 aggregate was used as the calibration material. To determine the temperature of the specimen at a given time while heating or cooling, three thermocouples were compacted into the specimen. The thermocouples were compacted at mid-height of the specimen and placed in the middle, outside, and halfway between the middle and outside. After the first test, only one thermocouple at the center of the specimen was necessary because there was little temperature change from edge to center after equilibration. Using one thermocouple compacted inside the specimen also reduced disturbance to the specimen. Thermocouples were placed within the cell to determine the air temperature and in the water reservoir to measure water temperature.

As seen in Figure 1.3a to Figure. 1.3c, constant temperature was achieved within 15-h of the temperature of the water being circulated. The maximum water temperature achieved with the Watlow heater was 76 °C, which corresponded to an air temperature of 58 °C and specimen temperature of 50 °C (± 1 °C). Although the likelihood of a base course reaching 50 °C is very minimal once pavement is installed, this temperature is possible to achieve during compaction and before pavement is installed, which insulates the base course. 7 °C (± 1 °C) was the lowest temperature the specimen would reach when circulating 0 °C water, marking the minimum temperature tested. The specimens were also tested at room temperature (23 °C) as a control. The 35 °C temperature was set as a temperature between room (23 °C) and 50 °C to help evaluate any trend and because this temperature is more of a realistic maximum temperature base course will experience after being insulated by pavement. Figure 1.3a to Figure 1.3c show the thermocouple data for the calibration at each temperature except 23 °C.

Quality control compaction tables for each specimen tested are presented in Table 1.2 to Table 1.3. All specimens were compacted within the NCHRP 1-28a standard of ± 0.5% of OMC. The majority (84%) of the specimens were compacted within ± 1% of the target dry density, in accordance with the NCHRP 1-28a standard. The five specimens (16%) that were compacted outside of the 1% target were the Class 5 specimens and the 7 °C TX RAP specimen. The TX RAP specimens were around 6 to 7% above the target dry density, but were all within 0.6% standard deviation of one another. Because the four TX RAP specimens are within only 0.6% standard deviation of one another, these tests were considered valid because they were all representative

of one another. As for the one Class 5 specimen, it was 0.1% above being rounded to 1%. Further testing could not be completed to correct the errors due to lack of material.

1.4.3 Wet/Dry Cycling of Unbound Recycled Materials

The procedure for wet/dry cycling of unbound recycled materials was based upon a similar procedure for compacted soil-cement mixtures (ASTM D559). Unlike ASTM D559, the recycled aggregate is unbound, so an apparatus was created to contain the material in its compacted state while still allowing water to flow through the aggregate. Loss of material was not weighed due to the unbound nature of the material. This test was conducted to evaluate the effects of wet/dry cycles on particle degradation of the material, not loss of material.

To replicate the in-field conditions of the recycled materials and natural aggregates tested, aggregates were compacted in the same mold used for M_r testing following the same steps as used in Section 1.4.1. All specimens were compacted at OMC and at 95% maximum modified Proctor dry unit weight. Once compacted, specimens were extruded from the mold and placed into the wet/dry apparatus.

A wet/dry apparatus had to be fabricated to hold the specimens intact throughout the entire wetting and drying of the material. Due to the unbound nature of the aggregate, loss of material existed, but minimizing the loss was important. One sheet of non-woven geotextile was wrapped around the specimens and held in place using ten rubber bands (Figure 1.4). Two 152-mm-diameter pieces of non-woven geotextile were also used on the top and bottom of the cylindrical specimens. The non-woven

geotextile used in this test kept the specimens intact while still allowing water to freely move through.

Two 152-mm-square plates were placed on the top and bottom of the specimen and locked into place using four 38-cm threaded rods. Each plate had approximately twenty 6.35-mm holes drilled into it to allow for water to enter and exit the specimen. The plates used for the RAP were made from polyvinyl chloride (PVC) and the plates used to hold the RCA and natural aggregates specimens were made from aluminum. Aluminum was used for RCA and natural aggregate because of the high temperature (100 °C) oven used to dry the material. PVC was used for the RAP because of availability and applicability in the lower temperature (50 °C) oven used to dry RAP. Eight bolts and washers threaded through the 38-cm rods were used to tighten the plates to the specimens.

Calibration of the wetting and drying time of the aggregates was conducted to determine the time for full saturation and drying. Specimens were placed in 114-L drums filled with tap water to achieve saturation. Saturation was achieved quickly (< 30-min) without vacuum as opposed to five hours as dictated by ASTM D559. Saturation was defined as the point when the weight of the specimen did not change more than ± 0.05 kg after a 30-min increment. To be conservative, all materials were submerged in water for one hour during the wetting cycle.

For drying, RAP and RCA/natural aggregate specimens were placed in ovens at 50 °C and 100 °C. 50 °C drying temperature was selected for RAP to reduce the potential for softening of the asphalt binder because aged asphalt binder found in RAP starts to soften around 60 °C (Read and Whiteoak 2003). 100 °C drying temperature was

selected for the RCA and natural aggregates because these materials did not contain any temperature-sensitive material, and the higher temperature decreased drying time for these hydrophilic materials. Calibration tests revealed that the RAPs, RCAs, and natural aggregates were considered dry after 22-h in their respective ovens. Dry was defined as the weight of the material not changing more than +\- 0.05 kg after a 30-min increment. RAP was able to dry after the same amount of time, but at a lower temperature than the RCAs and natural aggregates because it is a hydrophobic material.

Specimens were put through a 1-h wetting and 22-h drying cycle to complete one wet/dry cycle. A new specimen was created for each of the five, ten, and thirty wet/dry cycle procedures. Once the specimen completed its final cycle, pictures were taken for documentation of the intact specimen and then specimens were broken apart from their compacted state and dried for PSD and Micro-Deval tests.

PSDs (ASTM D422) were completed on all coarse-grained materials after the last wet/dry cycle. There were no deviations from the ASTM D422 standard. PSDs were also carried out on each material at 0 wet/dry cycles, but after compaction. Micro-Deval tests were conducted on all material following AASHTO T-327. All specimens were prepared as an oven dried sample of 19.0-mm except Class 5 and NJ RAP because of lack of material at certain particle sizes. All Class 5 wet/dry specimens used only 1000-g of material for each Micro Deval test. 250-g were retained on the 16 mm sieve, 250 g on the 12.7-mm sieve, and 500-g on the 9.7-mm sieve. NJ RAP was not tested at 5 cycles due to lack of material. NJ RAP specimens had 750-g retained on the 6.35-mm sieve and 750-g retained on the 4.76-mm sieve.

1.5 RESULTS AND DISCUSSION

1.5.1 Temperature Effects on Resilient Modulus

1.5.1.1 Temperature and Summary Resilient Modulus

The effects of temperature on SRM can be seen in Table 1.4 for both internal and external LVDT calculated SRMs using both NCHRP and Power fitting models. More detailed NCHRP SRM fitting parameters at varying temperatures for RCA/Basalt/Class 5 and RAP are shown in Table 1.5 and Table 1.6, respectively. Table 1.7 and Table 1.8 display the Power model fitting parameters at varying temperatures for RCA/Basalt/Class 5 and RAP, respectively. The NCHRP external LVDT SRM values are plotted in Figure 1.5a through Figure 1.5d. NCHRP modeled SRM as opposed to the Power modeled SRM was plotted because the coefficient of determination was higher on average than that of the Power modeled SRM. The NCHRP modeled SRM is the SRM used in the Mechanistic Empirical Pavement Design Guide (MEPDG).

Figure 1.6a and Figure 1.6b show a 1:1 comparison of internal SRM to external SRM using the NCHRP model and the Power model, respectively. As observed by many other studies (Bozyurt 2011, Camargo et al. 2012), the calculated internal SRM was higher than the external SRM. The ratio of internal to external SRM from this study was on average 1.7, similar to findings by Camargo et al.'s (2012) of an average of 1.5 on base course. Table 1.5 and Table 1.6 show the internal to external SRM ratio for the SRMs calculated using the NCHRP model. Table 1.7 and Table 1.8 show the internal to external SRM ratio for the SRMs calculated using the Power model.

The 1.7 internal to external SRM ratio in this study is much lower than previous data collected and reported from the UW-Madison's Recycled Materials Resource Center, which had ratios closer to 3 (Bozyurt 2011). Figure 1.7a and Figure 1.7b show the comparison between SRM calculated earlier by Young-Hwan Son at UW-Madison and SRM calculated in this study at room temperature (23 °C) on the same material. As seen in these figures, Son's 2011 internal SRM values were much higher (270% of the original value) than those calculated in this study. Whereas Son's external SRM values were slightly higher (130% of the original value) than the SRM values from this study, but much closer than the internal SRMs. This difference is attributed to malfunctioning internal LVDTs used by Son. The internal LVDTs used by Son were thought to be calibrated incorrectly, recording incorrect displacements which increased the overall internal SRMs for each material tested. Son's internal LVDTs were also different from the LVDTs used in this study and had a shorter range for recording displacement. This shorter range did not allow the entire M_r test to proceed without resetting the interior LVDTs in the middle of the test, which could have altered the data collected and led to higher SRM values. Son's external LVDTs were calibrated correctly and SRM calculated from these LVDTs is considered accurate.

The values for Son's internal SRM data were reported in a previous task report (Task IB) submitted to this project. This internal SRM is not considered accurate and should not be used. The interior LVDTs used for this study are considered calibrated and the SRM values calculated from these LVDTs is considered accurate. Due to this problem with internal LVDTs, comparisons in previous task report data should only be

done using external SRM values. External SRM values yielded much more consistent values than internal SRM values (Bozyurt 2011).

To analyze change in SRM with temperature for each material, coefficients of variations were calculated for the samples with enough material to run replicate M_r tests at 23 °C (i.e., Basalt, Class 5, TX RCA, and CA RCA) (Table 1.9). Any fluctuation in SRM outside of the coefficient of variation for the specific material was deemed a statistically significant change in SRM. For RCA samples, there appeared to be a decreasing trend in CA RCA with increasing temperature, but this decreasing trend was not outside of the coefficient of variation for CA RCA replicate tests completed (14%). A decreasing trend in SRM (28% decrease) was observed from 7 °C to 23 °C for TX RCA, but no trend was observed between 23 °C and 50 °C. The decrease in TX RCA from 7 °C to 23 °C is outside of the 19% coefficient of variation, indicating that the lower temperature could result in stiffening of the RCA, a common behavior of aggregates (Huang 2004). NJ RCA showed the same decreasing trend in SRM (27% decrease) from 7 °C to 23 °C, but lack of material did not allow for replicates to be completed on the material at room temperature to justify if this change in SRM was within the coefficient of variation between replicate tests.

For natural aggregate samples, both Basalt and Class 5 did not show any trends outside of the 7% and 17% coefficients of variation, respectively. Because of the lack of change in SRM outside of the coefficients of variation for each material, no change in SRM with temperature was observed in either natural aggregate.

Due to lack of material, no RAP replicates at room temperature could be tested to determine the coefficients of variation under this study. Previous SRM data on RAP

from the same sources but different studies was evaluated (Table A.2 and Table A.3), but was not used to the abnormally high coefficients of variation suggesting a difference in testing method and analysis between the studies. Without coefficients of variation to determine the possible percentage change in SRM between replicates, results for RAP had to be analyzed using other statistical means. As seen from Figure 1.5b, there is little trend between the three RAPs tests from 7 °C to 23 °C or from 35 °C to 50 °C, but there is a noticeable step drop in SRM for CO RAP and TX RAP between 23 °C and 35 °C. NJ RAP does not exhibit this step drop in SRM, indicating a possible error in the test or NJ RAP has a different characteristic than CO RAP and TX RAP that makes it not susceptible to temperature change. For this reason, replicate tests could have confirmed this lack of change in SRM, but a limited quantity of material available did not allow for this; therefore, the SRM data collected for NJ RAP was not evaluated any further.

As seen in Figure. 1.5b, NJ RAP has the least fluctuation in SRM at varying temperatures, but both TX RAP and CO RAP have dramatic (37% and 30%, respectively) differences in SRM between 23 °C and 35 °C, but all SRM values for the RAPs were still approximately the same or higher than the SRM values for the RCAs and natural aggregates tested at 35 °C. Little change (< 13 MPa or 9%) in SRM is observed in any of the RAPs from 7 °C to 23 °C and 35 °C to 50 °C. Due to the lack of material not allowing replicate tests to determine the coefficients of variation for each RAP, the six SRMs for all RAPs at 7 °C and 23 °C were grouped together and the six SRMs for all RAPs at 35 °C and 50 °C were grouped together for a statistical analysis. Figure 1.8a shows this grouping of the data. Averages were taken of each grouping to

determine the average step drop in SRM (24% decrease) of the RAP from 23 °C to 35 °C. Figure 1.8b shows the difference in average SRM of each grouping with the standard deviation. From Figure 1.8a and Figure 1.8b, it is observed that there is a trend of decrease in SRM for RAPs between 23 °C and 35 °C of approximately 24% on average. This trend of a decrease in M_r with increased temperature was also observed by Wen et al. (2011), but between the temperatures of 20 °C and 60 °C and at RAP contents of 60% to natural aggregate. Wen et al. (2011) saw a decrease in M_r of 30% with the increase in temperature.

The 60% decrease in SRM between 23 °C and 35 °C could be attributed to the asphalt in the material reaching its softening point, where the asphalt binder starts to behave less viscously (Read and Whiteoak 2001). This softening point typically occurs between 45 °C and 80 °C, so another explanation may be warranted for this decrease. Wen et al. (2011) claimed the decrease in M_r between the RAP he tested at 20 °C and 60 °C was due to decreased asphalt stiffening with temperature increase, but 60°C is within the softening point range of asphalt, whereas 35 °C is not. With a decrease in viscosity of the material, the asphalt binder coating the aggregates reduces in shear strength, decreasing the stiffness of the material under loading. It is recommended that further M_r tests on RAP at temperature between 23 °C and 35 °C be completed so that a more accurate temperature at which the SRM starts to decrease can be determined. It is also recommended that further M_r tests at these temperatures be done with other RAPs so that this trend can be further evaluated. Table 1.10 shows the ratios of SRM values at 23 °C and SRM values at 35 °C or 50 °C. The average of the external SRM ratios between 23 °C and 35 °C was 1.4. To be conservative, a reduction factor of 1.5

can be considered when evaluating the SRM of a 100% RAP base course to accommodate the effects of temperature on the SRM of RAP. More M_r tests on 100% RAP at different temperature can be performed to further analyze this decreasing trend in SRM with temperature.

1.5.1.2 Temperature and Plastic Strain (as an Index)

The noticeable difference in SRM between 23 °C and 35 °C for TX RAP and CO RAP indicates that there is a temperature at which the asphalt starts to behave less viscously when loaded. This temperature range is much lower than the typical softening point of asphalt binder (between 45 °C and 80 °C according to Read and Whiteoak (2003)). This behavior was not observed in NJ RAP through SRM values, but was observed when evaluating the strain rates of each specimen during the first sequence of the M_r test that conditions the specimen. No data is used to calculate M_r during this phase. During the conditioning phase NJ RAP experienced the highest strain rates of any material at 35 °C and 50 °C. CO and TX RAPs did not have as high strain rates during the conditioning phase at these temperatures.

Figure 1.9a and Figure 1.9b show this quick increase in strain rate for RAPs during the 100, 500, and 900 cycles of the conditioning phase at different temperatures. From Figure 1.9a and Figure 1.9b it can also be observed that NJ RAP had the fastest strain rate increase among the RAPs, followed by TX and CO RAP. A better comparison can be made between each material's strain rates during the first 100 cycles through the bar graphs displayed in Figure 1.10 at different temperatures. This figure displays the large impact temperature has on strain rate for RAPs, but the little

impact it had on materials without asphalt (i.e. RCA and natural aggregate). This trend can be seen throughout the entire conditioning phase in Figure 1.11a to Figure 1.11b. NJ RAP had the highest strain rate at each temperature, followed by TX RAP and then CO RAP.

Figure 1.12a and Figure 1.12b show the effects temperature had on cumulative plastic strain of the RAP, RCA, and natural aggregate throughout the M_r test. For RAPs, a trend of increasing plastic strain with increased temperature was observed. This trend supports the theory that strain rate increases with increased temperature in RAP when used as an unbound base course. There was no apparent trend observed for the RCAs and natural aggregates tested except that there is little to no effect and the plastic strains stay relatively constant regardless of temperature.

Further support of the increasing plastic strain with RAP temperature theory is evident in Figure 1.13 and Figure 1.14, which show the effect of temperature on cumulative plastic strain during the conditioning phase and during the remainder of the M_r test. An exponentially increasing cumulative plastic strain trend with increasing temperature was observed during the first sequence of the M_r test for all RAPs. The opposite trend in plastic strain is seen in the remaining 30 sequences with a decreasing trend observed. Figure 1.13 shows that, except for the cumulative plastic strain values at 7 °C, total cumulative plastic strain for RAPs at each temperature are consistent. These observed trends in Figure 1.13 and Figure 1.14 show that increasing temperature in RAPs results in faster accumulation of plastic strain without increasing total cumulative plastic strain. The low total cumulative plastic strain for all RAPs at 7 °C shown in Figure 1.14 was attributed to the rigidity of the asphalt coating the aggregates

at near freezing conditions (Griffin et al. 1959). Figure 1.13 shows that NJ RAP had the largest increase in plastic strain with increase in temperature, followed by TX RAP and CO RAP, similar to the findings in strain rate.

Figure 1.15 to Figure 1.18 show the effects of temperature on cumulative plastic strain for the RCAs and natural aggregates tested. Little plastic strain is accumulated during the first sequence in the RCA and natural aggregate specimens. No change in cumulative plastic strain outside of the expected margin of error due to instrumentation and rounding is observed in any of the RCAs or natural aggregates at varying temperatures. RAP exhibited the highest plastic strains for all materials tested, which was a trend also observed by Kim and Labuz (2007) where plastic strains in RAP at room temperature were greater than two times those of natural aggregate. This trend of higher plastic strain with material containing asphalt was also observed in Ebrahimi et al. (2012) where recycled pavement material containing asphalt exhibited higher plastic strains than natural aggregate. This increase in plastic strain was attributed to the viscous creep of the asphalt coating the aggregates in the recycled pavement material and it was suggested that this deformation could lead to rutting in flexible pavements. Although this was the case, Ebrahimi et al. (2012) found that the overall life of the road would be increased using recycled pavement material as opposed to other materials because of the higher M_r of the material. Class 5 also had high (~8%) plastic strains for base course material. All values of cumulative plastic strain can be seen in Table 1.11 to Table 1.13.

A problem associated with these high (> 6%) total cumulative plastic strain values in the RAP and Class 5 material is the problem with long term performance of

the pavement. High strain values lead to long-term rutting issues in the pavement, which decreases pavement life (Huang 2003). Because of this increased total cumulative plastic strain and increased strain rate due to temperature, further tests should be conducted on compaction of RAP at higher temperatures. As seen from the increased strain rates at increased temperatures, compaction at increased temperatures could decrease the total cumulative plastic strain accumulated in RAPs. In addition, the temperature effects on hydraulic conductivity of RAP should be evaluated. The softening of the asphalt binder under loading can decrease pore space, reducing hydraulic conductivity of the material. High hydraulic conductivity in road base is important to allow water to drain away from the pavement system.

The mechanism causing this increased plastic strain at higher temperatures in RAP is hypothesized to be the asphalt coating the aggregates. The asphalt coating decreases roughness of the aggregates; therefore, decreasing contact friction angles. RAP has characteristically lower maximum dry unit weights when compacted than RCA and natural aggregate, which is attributed to the poor compaction ability of asphalt-coated aggregates (Bozyurt 2011). The asphalt coating also becomes more viscous at higher temperatures, which could allow for the specimens to consolidate due to decreased friction angles.

1.5.2 Wet and Dry Cycling

Particle degradation due to wet/dry cycling was evaluated through PSDs and Micro-Deval tests conducted after compaction, but before wetting and drying (0 cycles), and after 5, 10, and 30 cycles of wetting and drying. Figure 1.19 to Figure 1.24 show

the PSDs for all four cycles. Figure 1.24 does not include wet/dry cycle five because of the lack of NJ RAP available during this test. For the natural aggregates, no change in PSD is observed outside of the expected error from the sample collected. For CA and TX RCA, no trends are observed; but for CA RCA, both 0 and 5 cycle are shown having finer material than the 10 and 30 cycle material. This is also observed for the 0 cycle TX RCA material. This observation is assumed to be due to the error in sampling the specimen for PSD material and not because of the wet/dry process. This assumption is made because the PSD of the material changes throughout the barrel the material is stored in. Outside of this measurement error, there is no observable change in PSD with the change in number of wet/dry cycles. A similar result can be observed for the TX and NJ RAP (Figure 1.23 and Figure 1.24, respectively).

During the wetting and drying processes, the loss of fines was documented. Fines migrated to the bottom of the cylinders during drying and were lost during wetting. The amount of fines lost was negligible (< 20 g) in relation to the size of the specimen, but a noticeable trend of increasing fines content with increased wet/dry cycles was observed in the PSDs. Figure 1.25 shows this trend observed in the natural aggregate and RCA specimens. No trend was observed for the RAP material. Figure 1.26 to Figure 1.31 show pictures of each specimen after 5, 10, and 30 cycles. From these figures it can be observed that both RAPs tested were able to stay much more intact than the RCAs and natural aggregates through the wetting and drying. This does not show that RAP will behave better through wetting and drying *in situ*, but does show that RAP when compacted, has higher cohesive properties than both RCA and natural aggregate. This increased cohesion could be due to the drying temperature of the

material being 50 °C, which may have altered the asphalt binder within the RAP, bonding particles together.

Micro-Deval testing was completed on the materials to evaluate the effects of wet/dry cycles on abrasion resistance. Samples were collected for Micro-Deval analysis from the tested specimens. The Micro-Deval tests results can be observed as percent loss in Figure 1.32. No trend was observed in any of the materials because all percent losses were within the single operator coefficient of variation 3.4%. All losses were similar (within 3.4% COV) to previous Micro-Deval studies conducted at 0 wet/dry cycles (Bozyurt 2011). Table 1.14 shows the exact values of the Micro-Deval losses for each material tested at each wet/dry cycle.

1.6 CONCLUSIONS

Temperature effects were investigated by resilient modulus tests at four different temperatures: 7, 23, 35, and 50 °C on three RAPs, three RCAs, and two natural aggregates. Increased temperature decreased the SRM of TX and CO RAP, but no change in SRM for NJ RAP was observed. Temperature did not affect the SRMs of any natural aggregate or RCA specimens tested. All RAP specimens were found to be affected to some degree by increased temperature because of the asphalt content. There was a step drop in SRM of greater than 30% between the specimens tested at 23 °C and 35 °C for both TX and CO RAP; however, this trend did not continue between 35 °C and 50 °C. This trend was not observed in NJ RAP. This decrease in SRM implies that there may be a critical temperature between 23 °C and 35 °C that, when reached,

starts to alter the physical characteristics of the asphalt binder coating the aggregates. Further studies are recommended to confirm this observation.

Cumulative plastic strain was calculated as an index using the M_r test data. Increased temperature caused the cumulative plastic strain and the strain rate to increase in all RAPs. No such effect was observed in the RCAs and natural aggregates with increasing temperature. NJ RAP had the highest strain rate, followed by TX RAP and then CO RAP. The majority of the increases in strain rate for RAP with temperature occurred within the first 1,000 cycles (conditioning phase) of the M_r test. Total cumulative plastic strains were overall high (> 7%) for RAPs at room temperature compared to other materials as was shown in previous studies, but increased temperature increased the rate at which the total plastic strain was achieved. Because of this trend, RAP compacted during the warmest time of the year could reduce total plastic strain after pavement is laid down. Further studies are recommended to evaluate if compacting RAP at elevated temperatures reduces subsequent total cumulative plastic strain. Plastic strain tests with higher cycles of loading at a constant deviatoric and confining stress would need to be completed to further evaluate this theory. The potential effects of temperature on hydraulic conductivity of RAP should also be evaluated because, when heated, void space in the RAP may decrease due to softening of the asphalt at elevated temperatures.

A procedure for evaluating the effect of wetting and drying of unbound aggregates was developed. 5, 10, and 30 wet/dry cycles were conducted on two RAPs, two RCAs, and two natural aggregates to evaluate the effects wetting and drying have on particle degradation. To evaluate particle degradation, Micro-Deval and

particle size distribution tests were completed on each specimen after the specified wet/dry cycle. No significant change that was outside of the coefficient of variation indicated by the standard in Micro-Deval loss was observed due to wet/dry cycles of any of the materials tested. Also, no significant change in particle size distribution was observed. However, increases in percent fines was observed with increasing wet/dry cycles for the two RCAs and two natural aggregates, but not change in fines content was seen for the two RAPs. Overall, RCA and RAP appear insensitive to wetting and drying.

1.7 TABLES

Table 1.1 Index Properties of Recycled Materials and Class 5 Aggregate

Material	States	D10 (mm)	D_{50} (mm)	C_u	C_c	G_s	AB (%)	AC (%)	w_{opt} (%)	γ_{dmax} (kN/m^3)	Gravel (%)	Fines (%)	USCS
Class 5 Aggregate	MN	0.08	1.0	21	1.4	2.6	-	-	8.9	20.1	22.9	9.5	GW-GM
Basalt	Senegal	0.10	7.0	125	6.6	2.9	0.5	-	4.2	22.0	58.0	7.8	GP
RCA	CA	0.31	4.8	22	1.4	2.3	5.0	-	10.4	19.9	50.6	2.3	GW
	TX	0.43	13.3	38	6.0	2.3	5.5	-	9.2	19.7	76.3	2.1	GW
	NJ	0.18	2.0	28	0.3	2.3	5.4	-	9.5	19.8	41.2	4.3	SP
RAP	TX	0.72	5.4	11	1.1	2.3	1.3	4.7	8.1	20.3	54.2	1.0	GW
	NJ	1.00	4.9	6	1.3	2.4	2.1	5.2	6.5	20.4	50.9	0.7	GW
	CO	0.35	2.2	9	0.7	2.2	3.0	5.9	5.7	20.7	31.7	0.7	SP

Note: AC=Asphalt Content, AB=Absorption, MN=Minnesota, CA=California, NJ=New Jersey, CO=Colorado, TX=Texas

Table 1.2 Quality Control of Class 5, Basalt, and RCA Specimen Preparation for Mr Test

	Temperature of Resilient Modulus Test	ω_{opt}	$\omega_{compacted}$	Percent ω Difference	ω Standard Deviation	Mass after Compaction Goal (kg)	Mass after Compaction (kg)	Percent Mass Difference	Mass after Compaction Standard Deviation	*95% g_{dmax} (kN/m^3)*	Dry Unit Weight of Compacted Material (kN/m^3)	Dry Unit Weight Difference	Standard Deviation
Class 5	7° C	8.90%	9.00%	0.10%	0.17%	11.79	12.65	7.29%	0.55%	19.1	20.47	7.17%	0.56%
	23° C	8.90%	8.90%	0.00%		11.79	12.6	6.87%		19.1	20.41	6.85%	
	35° C	8.90%	9.30%	0.40%		11.79	12.55	6.45%		19.1	20.25	6.03%	
	50° C	8.90%	8.80%	0.10%		11.79	12.5	6.02%		19.1	20.26	6.09%	
Basalt	7° C	4.20%	4.40%	0.20%	0.13%	13.59	13.65	0.44%	0.35%	23	23.06	0.27%	0.27%
	23° C	4.20%	4.60%	0.40%		13.59	13.7	0.81%		23	23.10	0.44%	
	35° C	4.20%	4.40%	0.20%		13.59	13.6	0.07%		23	22.98	0.10%	
	50° C	4.20%	4.30%	0.10%		13.59	13.7	0.81%		23	23.17	0.73%	
CA RCA	7° C	10.40%	10.84%	0.44%	0.19%	11.82	11.85	0.25%	0.38%	18.88	18.86	0.12%	0.27%
	23° C	10.40%	10.60%	0.20%		11.82	11.8	0.17%		18.88	18.82	0.33%	
	35° C	10.40%	10.10%	0.30%		11.82	11.7	1.02%		18.88	18.74	0.72%	
	50° C	10.40%	10.40%	0.00%		11.82	11.75	0.59%		18.88	18.77	0.57%	
TX RCA	7° C	9.20%	9.10%	0.10%	0.21%	11.56	11.6	0.35%	0.15%	18.68	18.75	0.39%	0.23%
	23° C	9.20%	9.60%	0.40%		11.56	11.55	0.09%		18.68	18.59	0.50%	
	35° C	9.20%	9.20%	0.00%		11.56	11.55	0.09%		18.68	18.66	0.13%	
	50° C	9.20%	8.80%	0.40%		11.56	11.6	0.35%		18.68	18.81	0.67%	
NJ RCA	7° C	9.50%	9.80%	0.30%	0.13%	11.65	11.6	0.43%	0.21%	18.76	18.63	0.67%	0.18%
	23° C	9.50%	9.80%	0.30%		11.65	11.6	0.43%		18.76	18.63	0.67%	
	35° C	9.50%	9.10%	0.40%		11.65	11.55	0.86%		18.76	18.67	0.47%	
	50° C	9.50%	9.40%	0.10%		11.65	11.6	0.43%		18.76	18.70	0.31%	

Table 1.3 Quality Control of RAP Specimen Preparation for M_r Test

	Temperature of Resilient Modulus Test	ω_{opt}	$\omega_{compacted}$	Percent ω Difference	ω Standard Deviation	Mass after Compaction Goal (kg)	Mass after Compaction (kg)	Percent Mass Difference	Mass after Compaction Standard Deviation	*95% g_{dmax} (kN/m^3)*	Dry Unit Weight of Compacted Material (kN/m^3)	Dry Unit Weight Difference	Standard Deviation
CO RAP	7° C	5.70%	5.90%	0.20%	0.05%	11.76	11.8	0.34%	0.15%	19.62	19.65	0.17%	0.12%
	23° C	5.70%	5.60%	0.10%		11.76	11.75	0.09%		19.62	19.63	0.03%	
	35° C	5.70%	5.60%	0.10%		11.76	11.75	0.09%		19.62	19.63	0.03%	
	50° C	5.70%	5.80%	0.10%		11.76	11.8	0.34%		19.62	19.67	0.26%	
NJ RAP	7° C	6.50%	6.30%	0.20%	0.10%	11.7	11.6	0.85%	0.41%	19.37	19.25	0.63%	0.34%
	23° C	6.50%	6.20%	0.30%		11.7	11.5	1.71%		19.37	19.10	1.40%	
	35° C	6.50%	6.10%	0.40%		11.7	11.55	1.28%		19.37	19.20	0.88%	
	50° C	6.50%	6.90%	0.40%		11.7	11.6	0.85%		19.37	19.14	1.19%	
TX RAP	7° C	8.00%	8.40%	0.40%	0.15%	11.8	11.65	1.27%	0.41%	19.27	18.96	1.63%	0.55%
	23° C	8.00%	7.80%	0.20%		11.8	11.65	1.27%		19.27	19.06	1.08%	
	35° C	8.00%	8.10%	0.10%		11.8	11.75	0.42%		19.27	19.17	0.51%	
	50° C	8.00%	7.60%	0.40%		11.8	11.7	0.85%		19.27	19.18	0.47%	

Note: ω_{opt} = Optimum moisture content; $\omega_{compacted}$ = Compacted moisture content;
ω Standard Deviation = Variability in percent moisture content difference; Std. Dev. = Standard Deviation

Table 1.4 Summary Resilient Modulus (SRM) at Varying Temperatures Calculated using both NCHRP and Power Models

		SMR (Mpa)							
		CA RCA	**TX RCA**	**NJ RCA**	**CO RAP**	**NJ RAP**	**TX RAP**	**Class 5**	**Basalt**
7 °C	Int NCHRP	199	211	169	200	261	459	123	157
	Int M & W	226	248	200	230	254	398	147	182
	Ext NCHRP	150	138	115	133	150	203	87	117
	Ext M & W	170	153	130	145	162	206	96	134
23 °C	Int NCHRP	245	188	163	228	290	369	123	180
	Int M & W	278	231	181	245	294	348	142	210
	Ext NCHRP	140	99	84	151	166	200	91	130
	Ext M & W	152	108	93	162	174	213	107	151
35 °C	Int NCHRP	215	180	154	208	234	371	141	168
	Int M & W	252	220	192	224	241	356	153	199
	Ext NCHRP	123	102	99	105	153	126	108	121
	Ext M & W	136	112	110	127	159	122	103	140
50 °C	Int NCHRP	197	193	188	177	NA	341	145	174
	Int M & W	207	233	223	202	NA	290	137	192
	Ext NCHRP	115	108	104	109	154	109	112	114
	Ext M & W	125	113	111	122	162	107	108	123

Note: Int = Internal LVDT recorded; Ext = External LVDT recorded

Table 1.5 SRM NCHRP Fitting Parameters for Natural Aggregate and RCA at Varying Temperatures

Material	Temperature	Internal						External						SRM_{int}/SRM_{ext}
		k_1	k_2	k_3	k_6	k_7	SRM (MPA)	k_1	k_2	k_3	k_6	k_7	SRM (MPA)	
Class 5	7 °C	21.0	3.6	-2.8	-206.9	3.0	123	0.4	5.2	-3.6	-450.1	5.8	87	1.41
	23 °C	0.7	4.2	-2.3	-291.8	2.6	123	6.8	3.9	-2.8	-251.5	3.5	91	1.35
	35 °C	0.003	5.14	-1.8	-405.3	1.0	141	1.3	2.4	0	-473.5	1.0	108	1.31
	50 °C	0.008	4.52	-0.7	-450.0	1.0	145	1.7	2.3	0	-473.5	1.0	112	1.29
Basalt	7 °C	23.2	2.9	-1.5	-168.8	2.1	157	101.5	2.1	-1.3	-109.6	2.0	117	1.34
	23 °C	0.003	6.6	-3.4	-515.1	4.5	180	8.7	4.0	-2.9	-273.9	4.1	130	1.38
	35 °C	1,031	1.1	-0.8	0.0	1.0	168	13.5	3.0	-1.7	-182.5	2.1	121	1.39
	50 °C	3.6	4.0	-2.5	-319.8	4.1	174	46.9	2.2	-1.0	-143.2	2.0	114	1.53
CA RCA	7 °C	6.5	3.5	-2.1	-248.1	2.2	199	12.5	4.1	-3.3	-368.7	5.3	150	1.33
	23 °C	0.7	5.4	-4.0	-406.2	4.4	245	1.2	4.4	-2.9	-471.2	5.8	140	1.75
	35 °C	6.0	3.6	-2.2	-202.9	1.7	215	24.9	2.9	-1.9	-220.2	3.0	123	1.75
	50 °C	0.006	4.7	-1.3	-478.4	1.1	197	111.7	1.7	-0.8	-101.4	1.2	115	1.71
TX RCA	7 °C	0.9	5.3	-3.8	-397.1	4.5	211	0.2	5.9	-4.3	-578.5	7.1	138	1.53
	23 °C	3.6	3.9	-2.4	-223.1	2.0	188	0.20	4.9	-3.0	-480.3	5.8	99	1.90
	35 °C	9.4	3.7	-2.6	-224.5	2.5	180	6.5	3.8	-2.6	-326.7	4.7	102	1.76
	50 °C	5.0	5.1	-4.1	-392.7	5.5	193	0.1	6.2	-4.4	-686.7	10.1	108	1.79
NJ RCA	7 °C	0.2	6.2	-4.6	-480.8	5.2	169	12.5	3.5	-2.5	-298.8	4.1	115	1.47
	23 °C	0.0002	5.9	-1.5	-480.1	1.0	163	15.0	2.8	-1.6	-212.5	2.9	84	1.94
	35 °C	74.6	2.9	-2.3	-148.9	2.5	154	0.9	4.3	-2.7	-412.9	4.8	99	1.56
	50 °C	0.1	6.5	-5.0	-481.2	5.2	188	9.6	5.1	-4.3	-586.6	11.1	104	1.81

Note: Due to rounding of fitting parameters for this table, SRM values calculated using the fitting parameters above will vary slightly from the actual SRM values reported above.

Table 1.6 SRM NCHRP Fitting Parameter for RAP at Varying Temperatures

Material	Temperature	Internal						External						SRM_{int}/SRM_{ext}
		k_1	k_2	k_3	k_6	k_7	SRM (MPA)	k_1	k_2	k_3	k_6	k_7	SRM (MPA)	
CO RAP	7 °C	7.8	3.6	-2.4	-242.5	2.4	200	0.4	4.6	-2.8	-517.0	5.8	133	1.50
	23 °C	0.01	4.6	-1.1	-476.0	1.0	228	12.6	3.1	-2.0	-326.2	3.8	151	1.51
	35 °C	3.5	2.9	-1.0	-267.1	1.0	208	2.0	2.7	-0.6	-349.7	2.4	105	1.98
	50 °C	13.5	2.7	-1.4	-225.6	1.7	177	0.01	4.4	-0.7	-479.3	1.0	114	1.55
NJ RAP	7 °C	11.1	3.3	-2.1	-271.9	2.3	261	1.9	4.1	-2.6	-441.9	5.1	150	1.74
	23 °C	4.8	3.5	-1.9	-255.5	1.8	290	9.2	3.0	-1.6	-369.1	4.5	166	1.75
	35 °C	0.4	3.1	0.0	-460.8	1.0	234	1,125.8	0.7	-0.4	0	1.1	153	1.53
	50 °C	NA	NA	NA	NA	NA	NA	0.10	3.7	0	-473.5	1.0	154	NA
TX RAP	7 °C	1.8	4.0	-2.3	-397.9	2.6	459	4.7	3.5	-2.1	-393.0	4.0	203	2.26
	23 °C	7.5	3.8	-2.7	-361.6	3.4	369	4.9	4.1	-2.9	-415.8	5.2	200	1.85
	35 °C	0.01	5.5	-0.8	-819.1	1.0	371	3.4	2.8	-0.7	-456.3	18.2	126	2.94
	50 °C	0.02	3.9	-0.9	-707.5	1.1	341	7.7	2.0	0.0	-322.3	1.0	109	2.53

Note: Due to rounding of fitting parameters for this table, SRM values calculated using the fitting parameters above will vary slightly from the actual SRM values reported above. Internal parameters for NJ RAP at 50 ℃ are not reported because the internal LVDTs maxed out during the conditioning phase due to the excessive plastic strain accumulation.

Table 1.7 SRM Power Model Fitting Parameters for Class 5, Basalt, and RCA at Varying Temperatures

Material	Temperature	Internal			External			SRM_{int}/SRM_{ext}
		k_1	k_2	SRM (MPa)	k_1	k_2	SRM (MPa)	
Class 5	7 °C	6,803	0.58	147	3,784	0.61	96	1.53
	23 °C	4,020	0.67	142	3,821	0.62	107	1.33
	35 °C	3,496	0.71	153	3,879	0.61	103	1.49
	50 °C	1,656	0.83	137	4,553	0.59	108	1.27
Basalt	7 °C	5,695	0.65	182	5,318	0.6	134	1.36
	23 °C	4,012	0.74	210	6,149	0.6	151	1.39
	35 °C	11,128	0.54	199	5,642	0.6	140	1.42
	50 °C	7,212	0.62	193	3,670	0.66	123	1.57
CA RCA	7 °C	21,074	0.44	226	16,574	0.44	170	1.33
	23 °C	21,074	0.48	278	11,827	0.48	152	1.83
	35 °C	20,000	0.47	252	8,849	0.51	136	1.85
	50 °C	18,160	0.46	207	8,645	0.5	125	1.66
TX RCA	7 °C	20,000	0.47	248	11,927	0.48	153	1.62
	23 °C	20,000	0.46	231	5,350	0.56	108	2.14
	35 °C	20,000	0.45	220	6,015	0.55	112	1.96
	50 °C	17,628	0.48	233	5,214	0.58	113	2.06
NJ RCA	7 °C	19,828	0.43	200	11,122	0.46	130	1.54
	23 °C	11,755	0.51	181	4,429	0.57	93	1.95
	35 °C	12,943	0.50	192	8,182	0.49	110	1.75
	50 °C	20,000	0.45	223	6,300	0.54	111	2.01

Note: Due to rounding of fitting parameters for this table, SRM values calculated using the fitting parameters above will vary slightly from the actual SRM values reported above.

Table 1.8 SRM Power Model Fitting Parameters for RAP at Varying Temperatures

Material	Temperature	Internal			External			SRM_{int}/SRM_{ext}
		k_1	k_2	SRM (MPa)	k_1	k_2	SRM (MPa)	
CO RAP	7 °C	21,074	0.45	230	12,118	0.46	145	1.59
	23 °C	21,074	0.46	245	17,138	0.42	162	1.51
	35 °C	21,074	0.44	224	5,245	0.56	107	2.09
	50 °C	17,195	0.46	202	5,077	0.60	122	1.66
NJ RAP	7 °C	22,148	0.46	254	14,528	0.45	162	1.57
	23 °C	23,221	0.48	294	14,475	0.47	174	1.69
	35 °C	8,467	0.63	241	11,071	0.50	159	1.52
	50 °C	NA	NA	NA	5,656	0.63	162	NA
TX RAP	7 °C	22,148	0.54	398	18,212	0.45	206	1.93
	23 °C	23221	0.51	348	17,138	0.47	213	1.63
	35 °C	24,168	0.50	356	3,687	0.66	122	2.92
	50 °C	25369	0.46	290	4290	0.60	107	2.71

Note: Due to rounding of fitting parameters for this table, SRM values calculated using the fitting parameters above will vary slightly from the actual SRM values reported above.

Table 1.9 Internal and External SRM Statistical Analysis on Replicate Specimens Prepared by Shedivy

		Internal LVDT Data				External LVDT Data			
Material	**M_r Tester**	**NCHRP SRM (MPa)**	**Average (MPa)**	**σ (MPa)**	**C_v**	**NCHRP SRM (Mpa)**	**Average (MPa)**	**σ (MPa)**	**C_v**
Class 5	Shedivy	123	154	36	23%	91	113	19	17%
	Shedivy	115				100			
	Shedivy	129				97			
Basalt	Shedivy	180	197	28	14%	131	130	8	7%
	Shedivy	192				121			
	Shedivy	187				135			
CA RCA	Shedivy	181	197	33	17%	121	123	17	14%
	Shedivy	246				140			
TX RCA	Shedivy	188	180	11	6%	99	115	22	19%
	Shedivy	172				130			

Note: Average is the mean, σ is the standard deviation, and C_v is the coefficient of variation

Table 1.10 Ratio of $SRM_{23\ °C}$ to $SRM_{35\ °C}$ or $SRM_{50\ °C}$

		CO RAP	NJ RAP	TX RAP	Average
23 °C-35 °C	Int	1.09	1.25	0.99	1.11
	Ext	1.45	1.07	1.64	1.39
23 °C-50 °C	Int	1.25	NA	1.35	1.30
	Ext	1.32	1.06	1.82	1.40

Table 1.11 1st Sequence (Conditioning Phase) Plastic Deformation and Plastic Strain at Varying Temperatures

		CA RCA	TX RCA	NJ RCA	CO RAP	NJ RAP	TX RAP	Class 5	Basalt
7° C	Int Deformation (mm)	0.3	0.2	0.3	0.6	0.9	0.4	0.99	0.6
	Int Plastic Strain (%)	0.20%	0.10%	0.20%	0.40%	0.60%	0.20%	0.70%	0.40%
	Ext Deformation (mm)	0.7	0.8	1.1	2.5	2.5	1.6	2.5	1.8
	Ext Plastic Strain (%)	0.20%	0.30%	0.40%	0.80%	0.80%	0.50%	0.80%	0.60%
23° C	Int Deformation (mm)	0.3	0.2	0.3	1.2	2.6	1.6	2.7	0.2
	Int Plastic Strain (%)	0.20%	0.10%	0.20%	0.80%	1.70%	1.10%	1.80%	0.10%
	Ext Deformation (mm)	1	0.9	1.2	3.4	5.9	4	5.8	1.4
	Ext Plastic Strain (%)	0.30%	0.30%	0.40%	1.10%	1.90%	1.30%	1.90%	0.50%
35° C	Int Deformation (mm)	0.3	0.3	0.4	2.2	6.8	3.8	1.8	0.4
	Int Plastic Strain (%)	0.20%	0.20%	0.30%	1.40%	4.50%	2.50%	1.20%	0.30%
	Ext Deformation (mm)	1.3	1.1	1.3	6.5	13.6	9	3.7	1.3
	Ext Plastic Strain (%)	0.40%	0.40%	0.40%	2.10%	4.50%	3.00%	1.20%	0.40%
50° C	Int Deformation (mm)	0.5	0.1	0.2	4.4	6.9	5.3	1.2	0.4
	Int Plastic Strain (%)	0.30%	0.10%	0.20%	2.90%	4.50%	3.50%	0.80%	0.30%
	Ext Deformation (mm)	1.2	0.4	0.9	10.4	21.7	11.1	2.9	1.3
	Ext Plastic Strain (%)	0.40%	0.10%	0.30%	3.40%	7.10%	3.60%	1.00%	0.40%

Note: Int = Internal LVDT recorded
Ext = External LVDT recorded

Table 1.12 2nd-31st Sequence Plastic Deformation and Plastic Stain at Varying Temperatures

		CA RCA	TX RCA	NJ RCA	CO RAP	NJ RAP	TX RAP	Class 5	Basalt
7° C	Int Deformation (mm)	3.2	3.2	5.8	4.5	7.6	2.7	9.3	3.9
	Int Plastic Strain (%)	2.10%	2.10%	3.80%	3%	5%	1.80%	6.10%	2.50%
	Ext Deformation (mm)	5.7	6.8	12.2	10.6	14.7	6.5	21.1	8.5
	Ext Plastic Strain (%)	1.90%	2.20%	4.00%	3.50%	4.80%	2.10%	6.90%	2.80%
23° C	Int Deformation (mm)	3	4.8	8.8	8.9	7.9	7.6	7.2	3.4
	Int Plastic Strain (%)	2%	3.20%	5.80%	5.80%	5.20%	5%	4.70%	2.20%
	Ext Deformation (mm)	5.8	9.4	16.8	18.9	16.7	13.8	18.1	8.2
	Ext Plastic Strain (%)	1.90%	3.10%	5.50%	6.20%	5.60%	4.50%	5.90%	2.70%
35° C	Int Deformation (mm)	3.6	4.9	8.5	8.2	2.6	5.6	8.4	4.2
	Int Plastic Strain (%)	2.40%	3.20%	5.60%	5.40%	1.70%	4.60%	5.50%	2.70%
	Ext Deformation (mm)	7.9	9.6	16.5	16.5	9.6	14	20.8	8.7
	Ext Plastic Strain (%)	2.60%	3.10%	5.40%	5.40%	3.10%	4.60%	6.80%	2.90%
50° C	Int Deformation (mm)	5.2	3.5	5.6	5.8	0	3.6	8.9	3.3
	Int Plastic Strain (%)	3.40%	2.30%	3.70%	3.80%	0.00%	2.40%	5.80%	2.20%
	Ext Deformation (mm)	9.3	7.6	10.2	12.3	0.7	6.6	21.7	8
	Ext Plastic Strain (%)	3.10%	2.50%	3.30%	4.00%	0.20%	2.20%	7.10%	2.60%

Note: Int = Internal LVDT recorded
Ext = External LVDT recorded

Table 1.13 Total Plastic Deformation and Plastic Stain at Varying Temperatures

		CA RCA	TX RCA	NJ RCA	CO RAP	NJ RAP	TX RAP	Class 5	Basalt
7° C	Int Deformation (mm)	3.5	3.4	6.1	5.1	8.5	3.1	10.29	4.5
	Int Plastic Strain (%)	2.3%	2.2%	4.0%	3.4%	5.6%	2.0%	6.8%	2.9%
	Ext Deformation (mm)	6.4	7.6	13.3	13.1	17.2	8.1	23.6	10.3
	Ext Plastic Strain (%)	2.1%	2.5%	4.4%	4.3%	5.6%	2.6%	7.7%	3.4%
23° C	Int Deformation (mm)	3.3	5	9.1	10.1	10.5	9.2	9.9	3.6
	Int Plastic Strain (%)	2.2%	3.3%	6.0%	6.6%	6.9%	6.1%	6.5%	2.3%
	Ext Deformation (mm)	6.8	10.3	18	22.3	22.6	17.8	23.9	9.6
	Ext Plastic Strain (%)	2.2%	3.4%	5.9%	7.3%	7.5%	5.8%	7.8%	3.2%
35° C	Int Deformation (mm)	3.9	5.2	8.9	10.4	9.4	9.4	10.2	4.6
	Int Plastic Strain (%)	2.6%	3.4%	5.9%	6.8%	6.2%	7.1%	6.7%	3.0%
	Ext Deformation (mm)	9.2	10.7	17.8	23	23.2	23	24.5	10
	Ext Plastic Strain (%)	3.0%	3.5%	5.8%	7.5%	7.6%	7.6%	8.0%	3.3%
50° C	Int Deformation (mm)	5.7	3.6	5.8	10.2	6.9	8.9	10.1	3.7
	Int Plastic Strain (%)	3.7%	2.4%	3.9%	6.7%	4.5%	5.9%	6.6%	2.5%
	Ext Deformation (mm)	10.5	8	11.1	22.7	22.4	17.7	24.6	9.3
	Ext Plastic Strain (%)	3.5%	2.6%	3.6%	7.4%	7.3%	5.8%	8.1%	3.0%

Note: Int = Internal LVDT recorded
Ext = External LVDT recorded

Table 1.14 Micro-Deval Results at Varying Wet/Dry Cycles

Material	30 Cycle	10 Cycle	5 Cycle
CA RCA	16%	16%	16%
TX RCA	21%	19%	17%
TX RAP	21%	21%	20%
NJ RAP	24%	22%	-
Basalt	8%	6%	7%
Class 5	11%	12%	12%

Note: NJ RAP 5 wet/dry cycle tests were not run due to lack of material

1.8 FIGURES

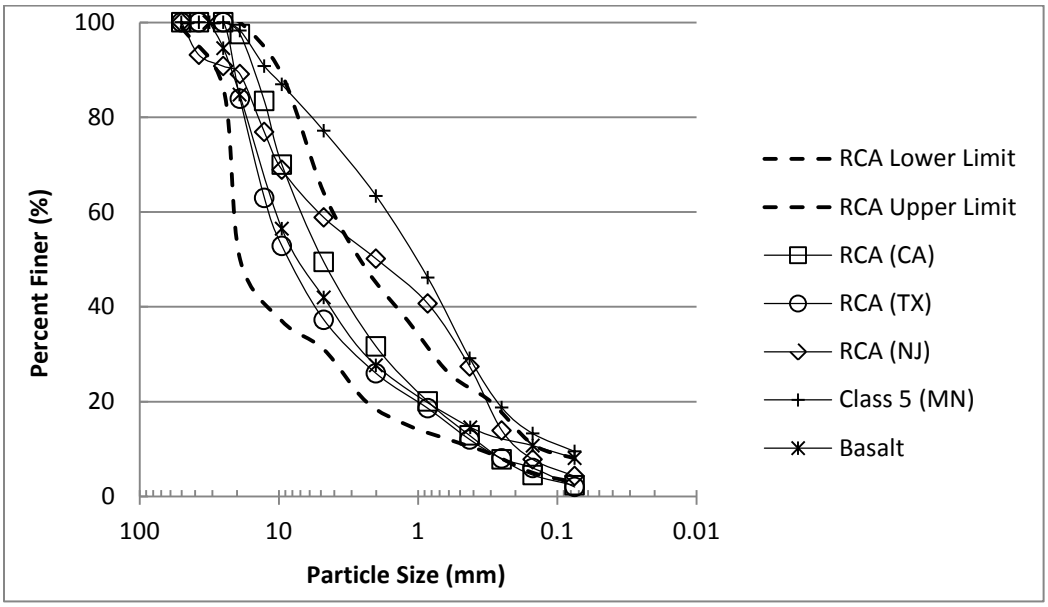

Figure 1.1a Particle Size Distribution for RCA, Basalt, and Class 5 Aggregate with Lower and Upper Limits of RCA from Literature

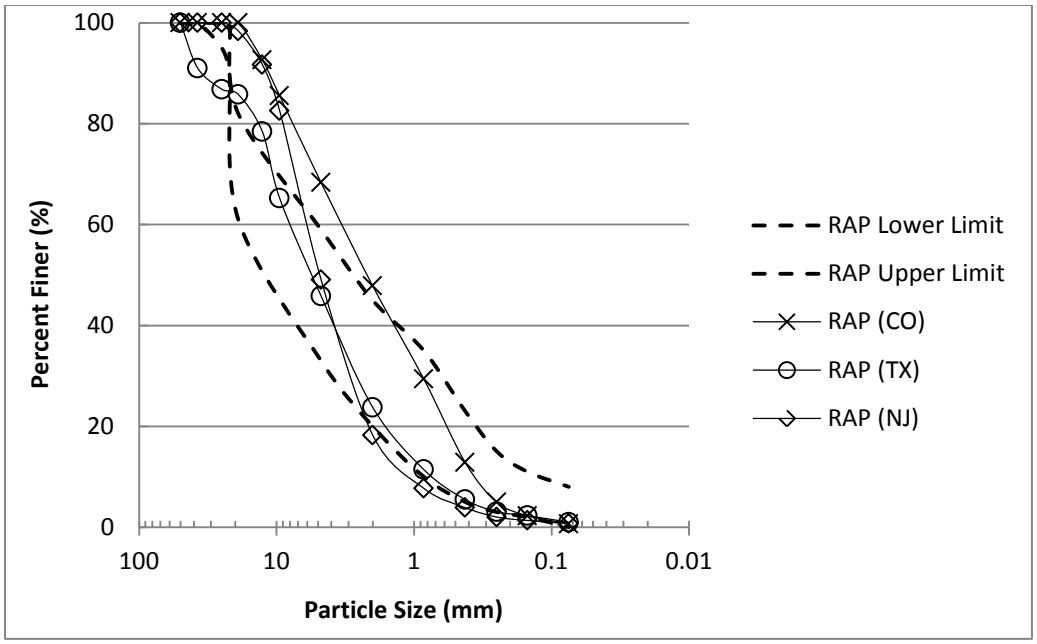

Figure 1.1b Particle Size Distribution for RAP with Lower and Upper Limits of RAP from Literature

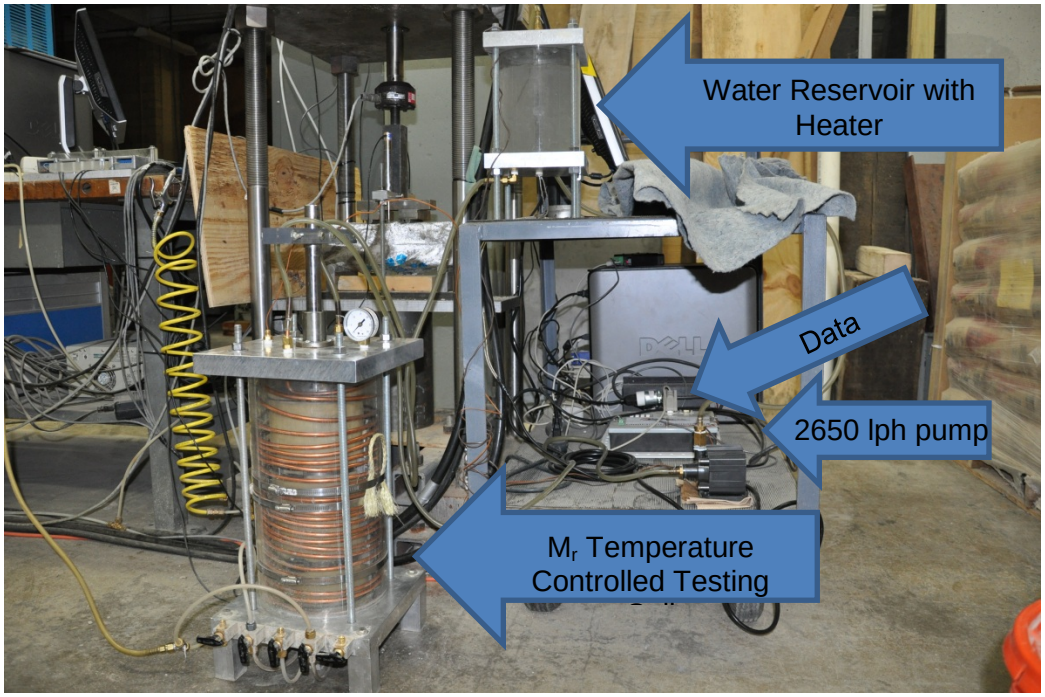

Figure 1.2a Resilient Modulus Testing Equipment with Heated Water

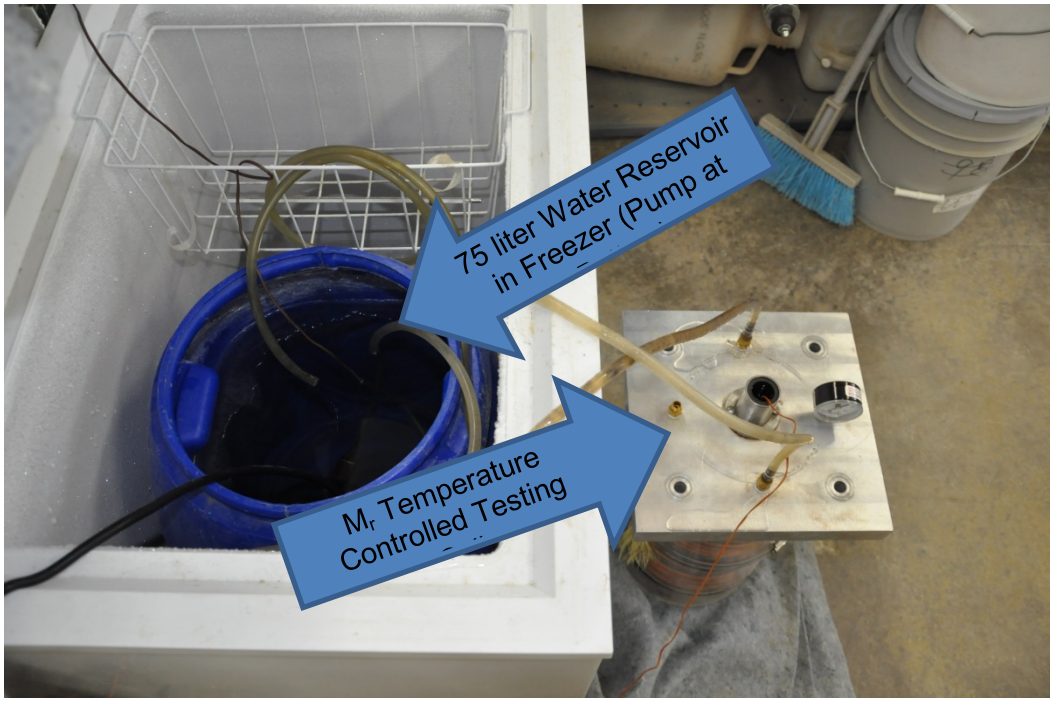

Figure 1.2b Resilient Modulus Testing Equipment with Chilled Water

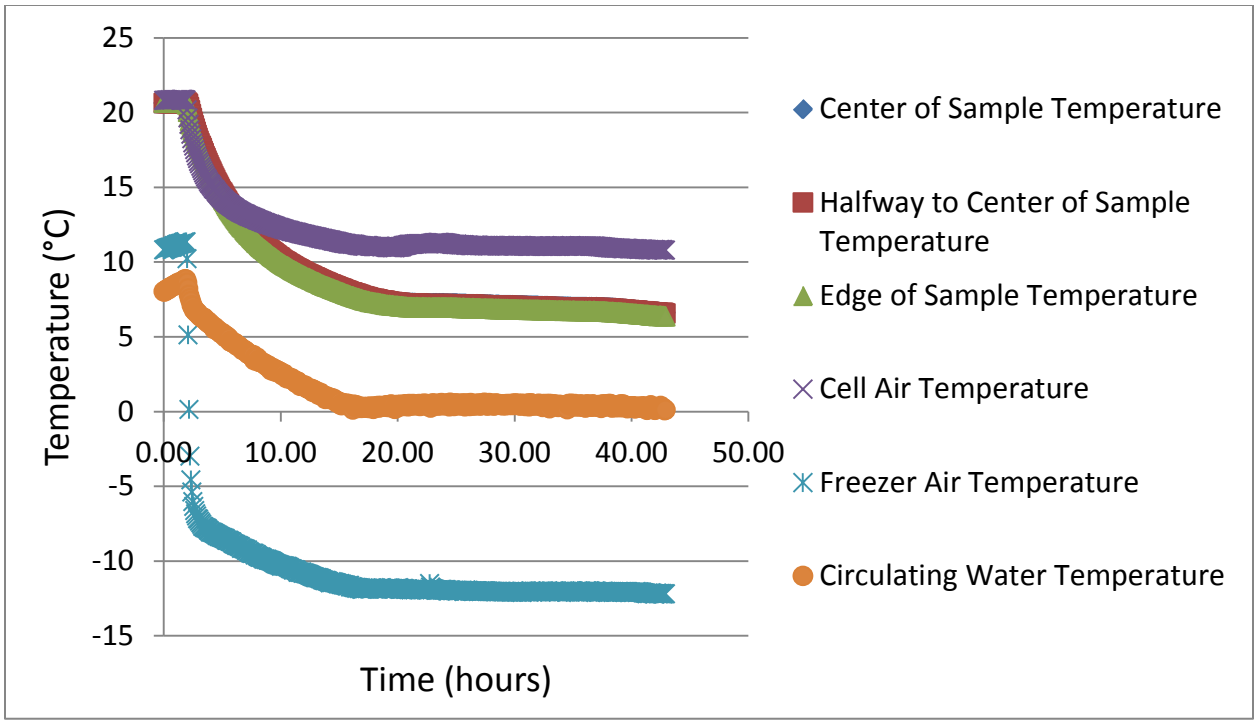

Figure 1.3a 7 °C Class 5 Temperature Calibration

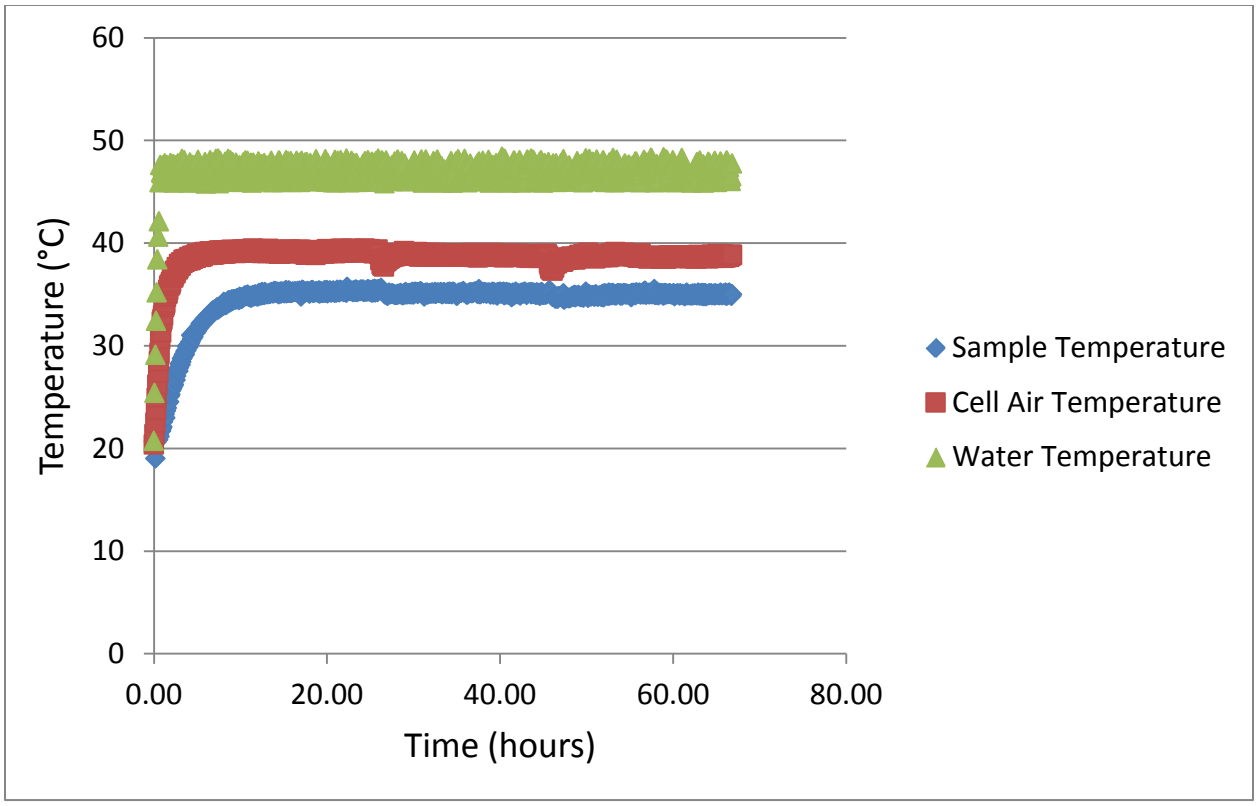

Figure 1.3b 35 °C Class 5 Temperature Calibration

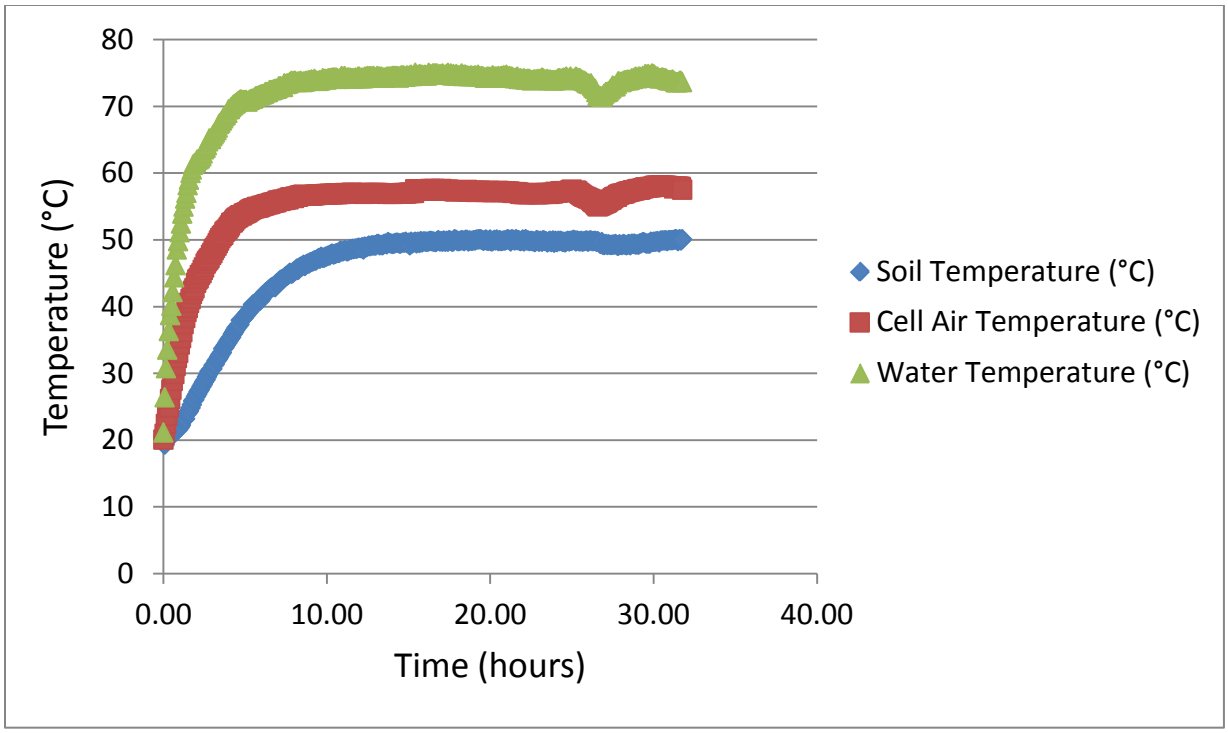

Figure 1.3c 50 °C Class 5 Temperature Calibration

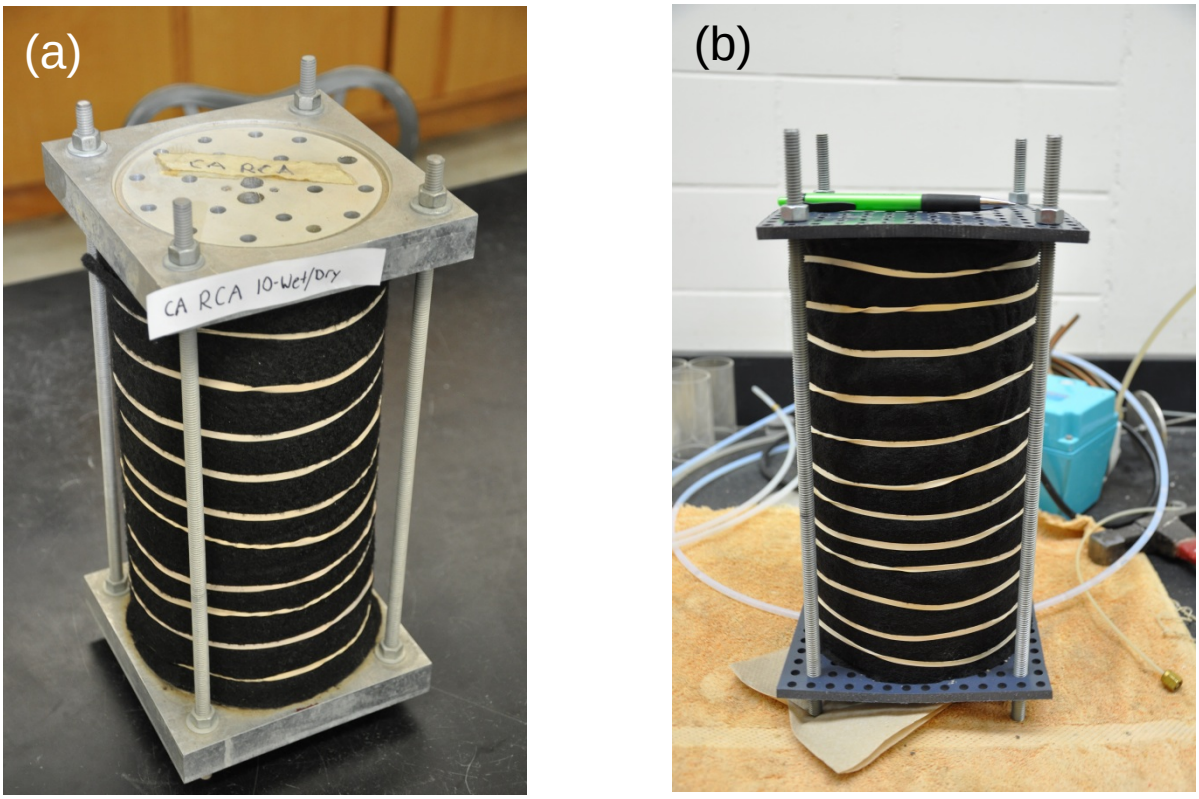

Figure 1.4 (a) Aluminum Wet/Dry Apparatus for RCA, Class 5, and Basalt Specimens; (b) PVC Wet/Dry Apparatus for RAP

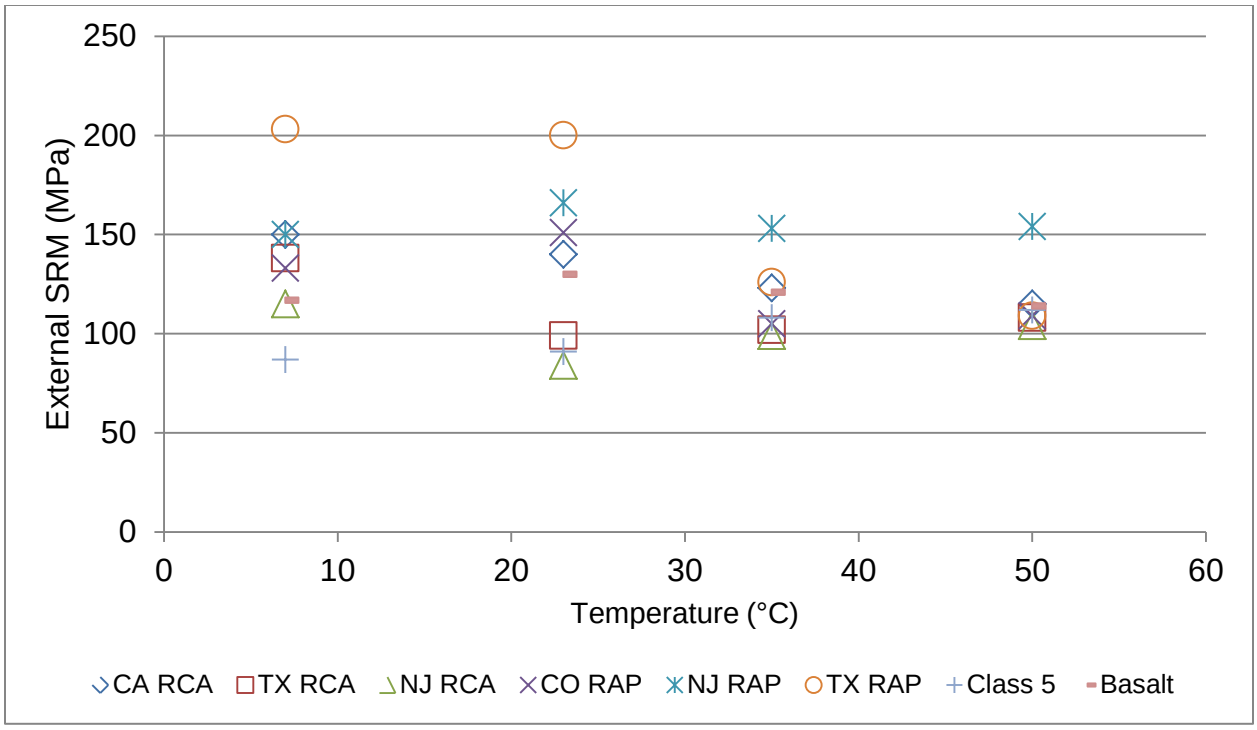

Figure 1.5a External LVDT Recorded NCHRP SRM Results at Varying Temperatures

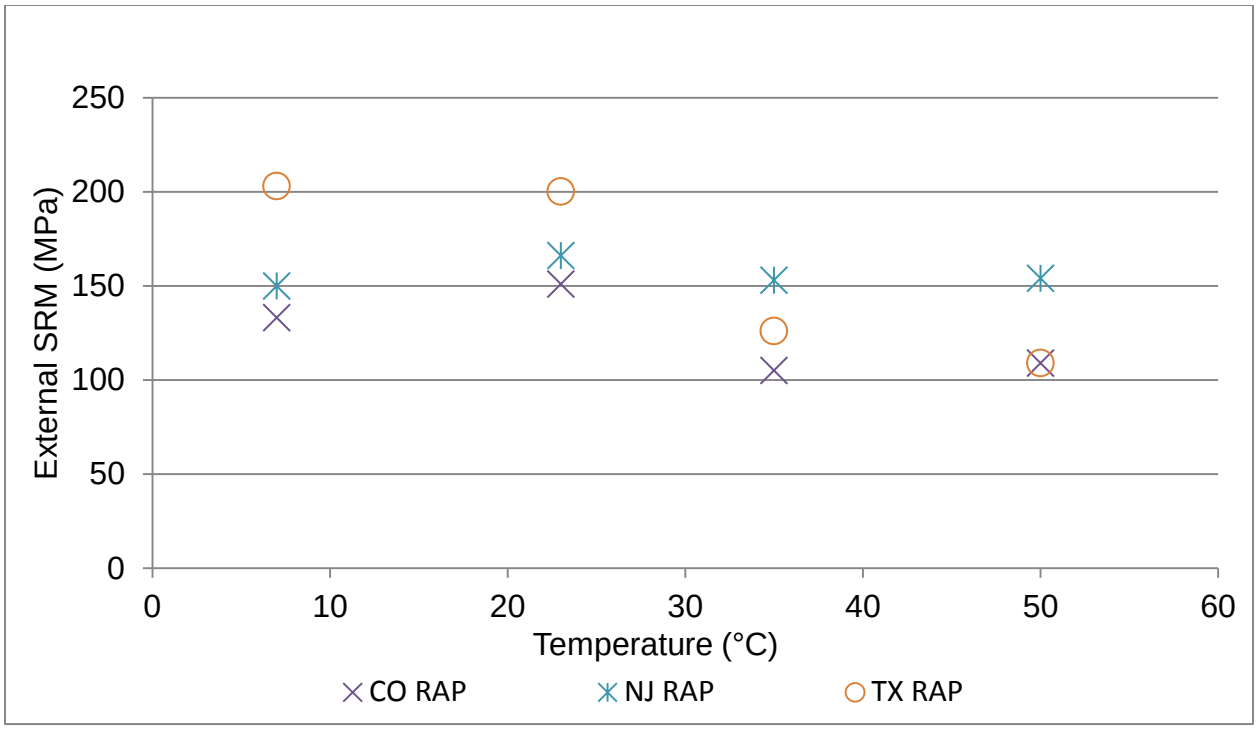

Figure 1.5b External LVDT Recorded NCHRP SRM Results of RAP at Varying Temperatures

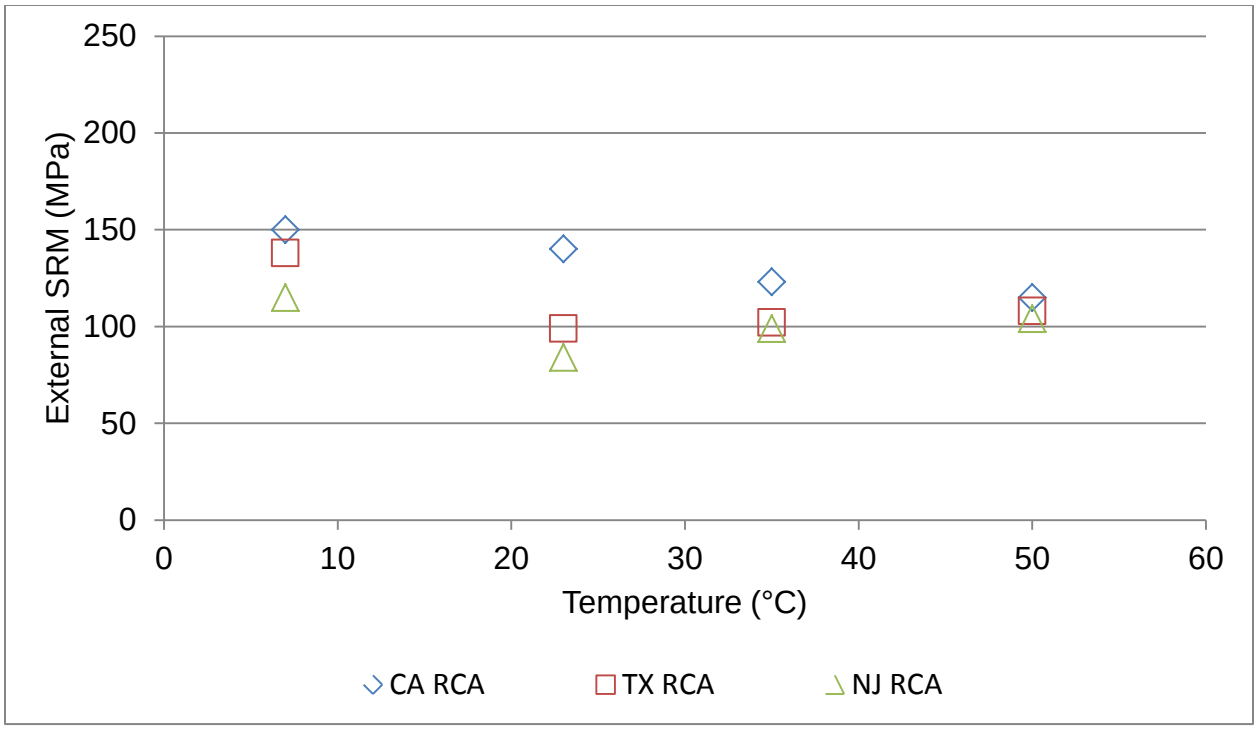

Figure 1.5c External LVDT Recorded NCHRP SRM Results of RCA at Varying Temperatures

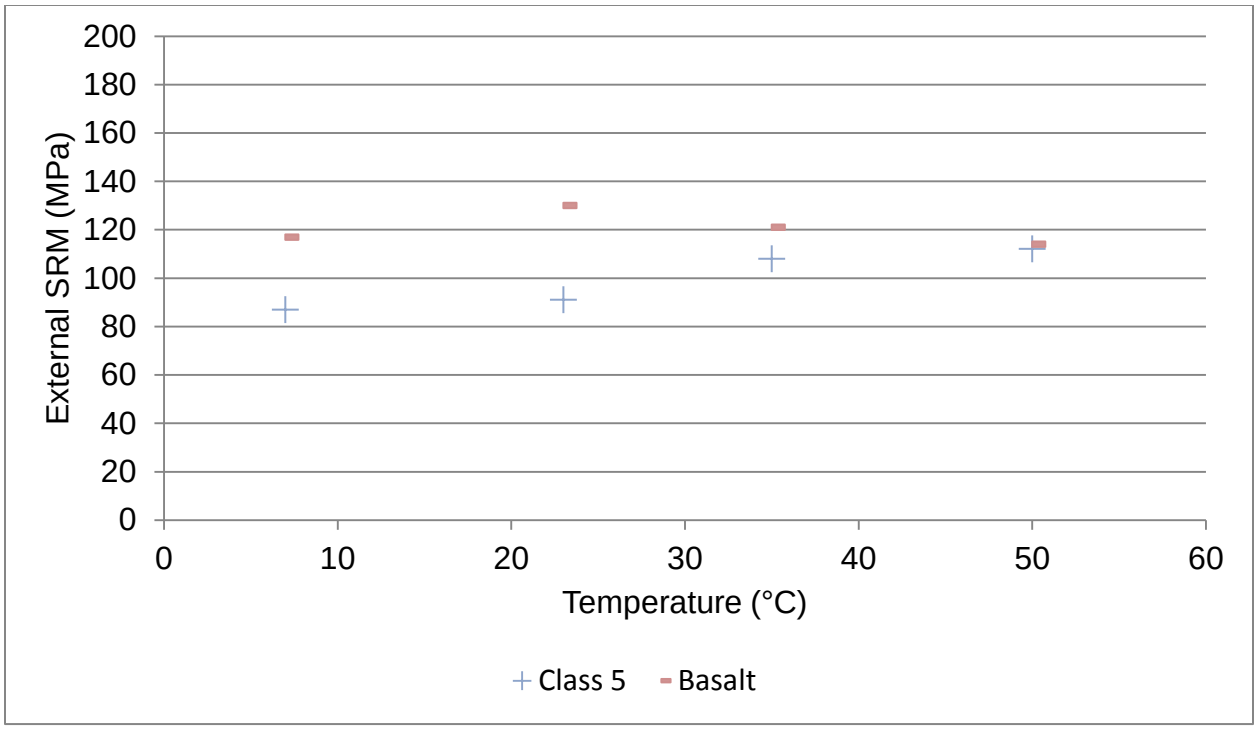

Figure 1.5d External LVDT Recorded NCHRP SRM Results of Natural Aggregate at Varying Temperatures

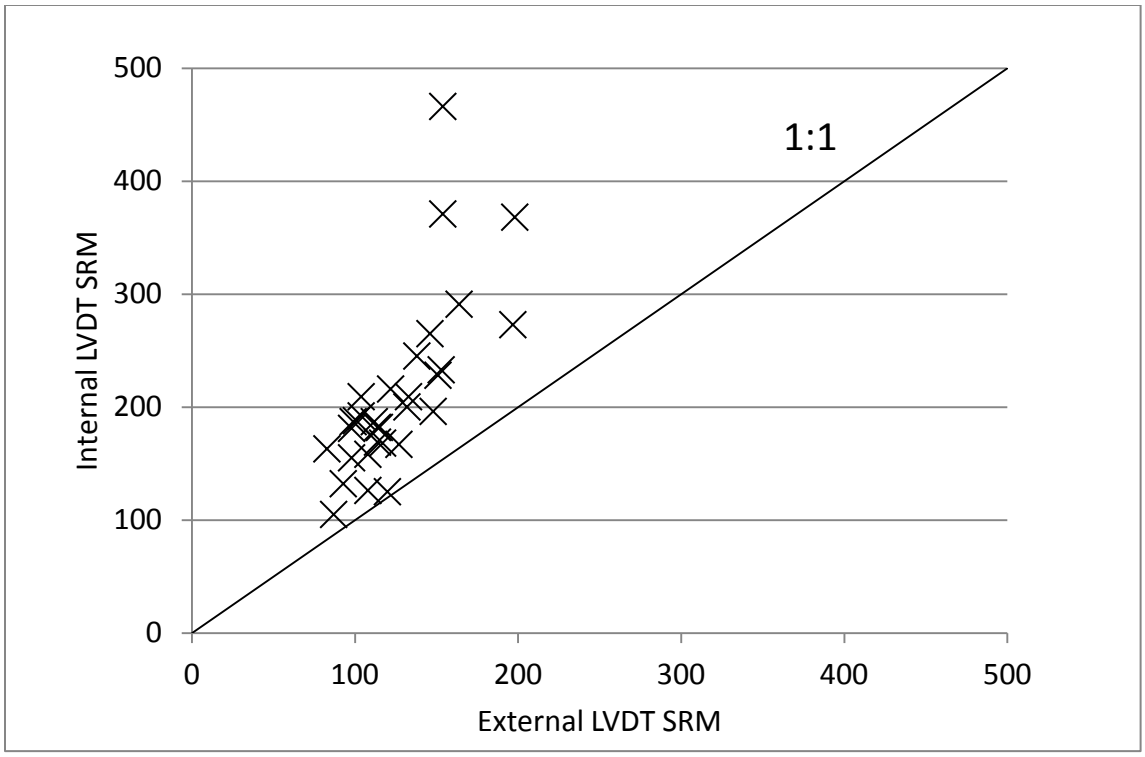

Figure 1.6a 1:1 Comparison of Internal SRM and External SRM (NCHRP Model) at 23 °C

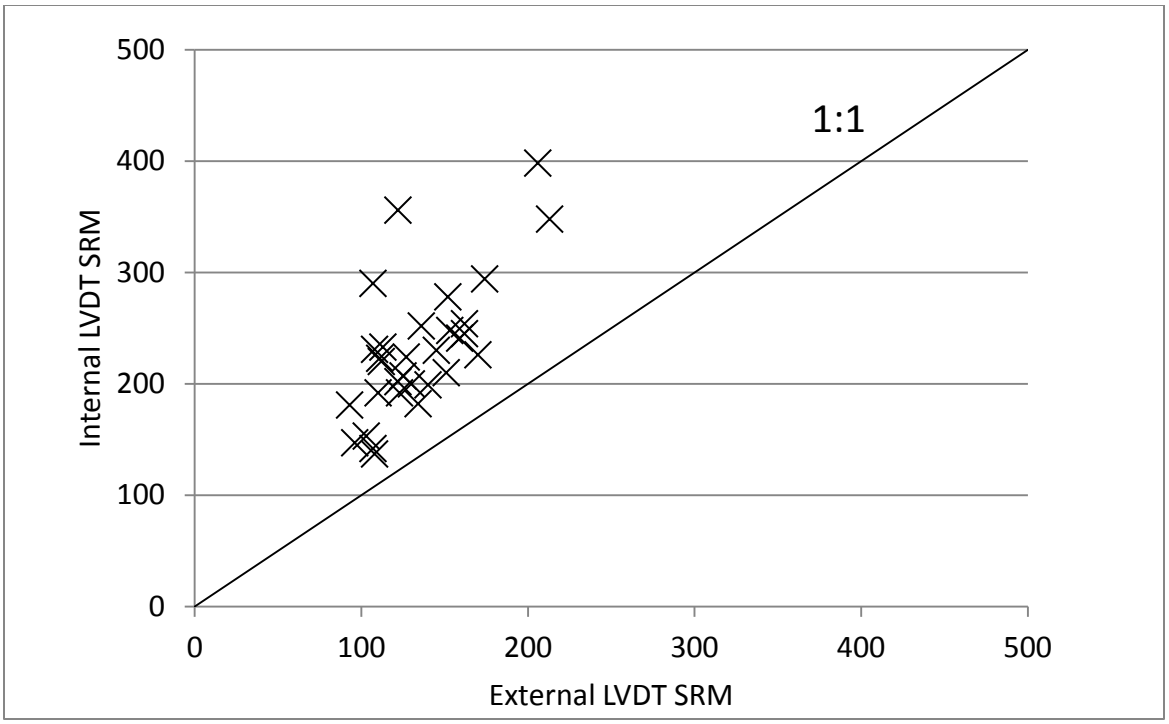

Figure 1.6b 1:1 Comparison of Internal SRM and External SRM (Power Model) at 23 °C

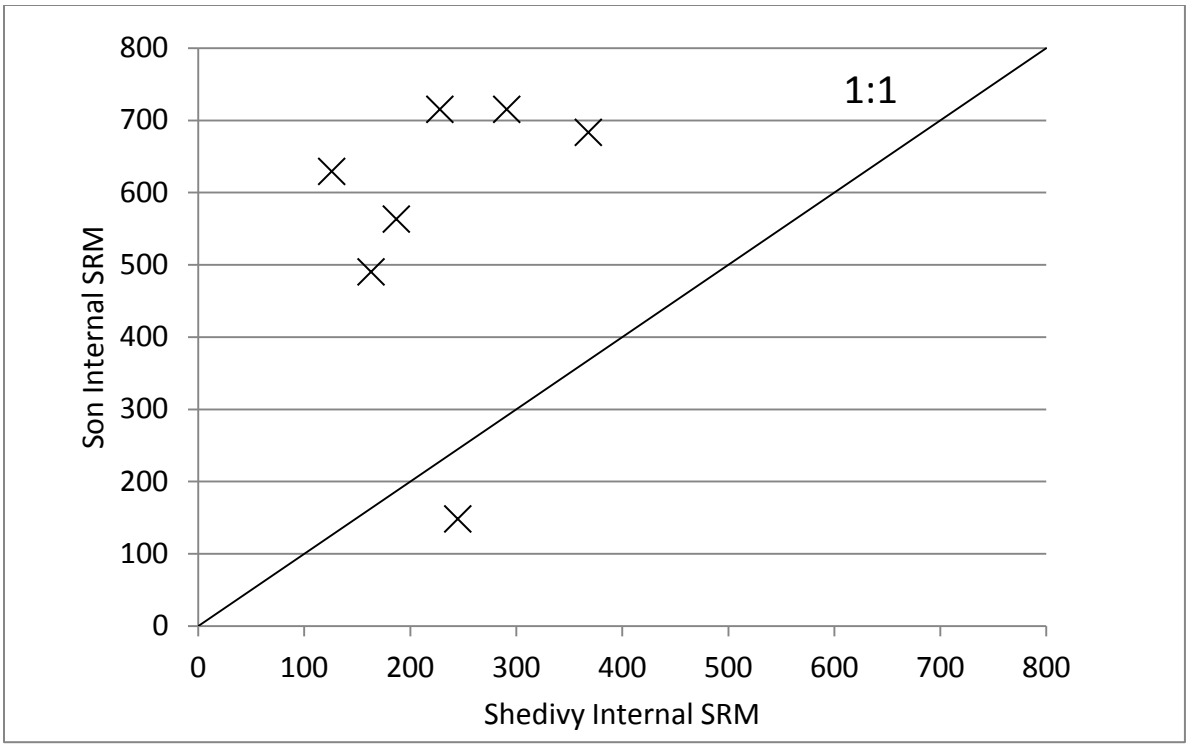

Figure 1.7a 1:1 Comparison of Shedivy's Internal SRM and Son's (2011) Internal SRM

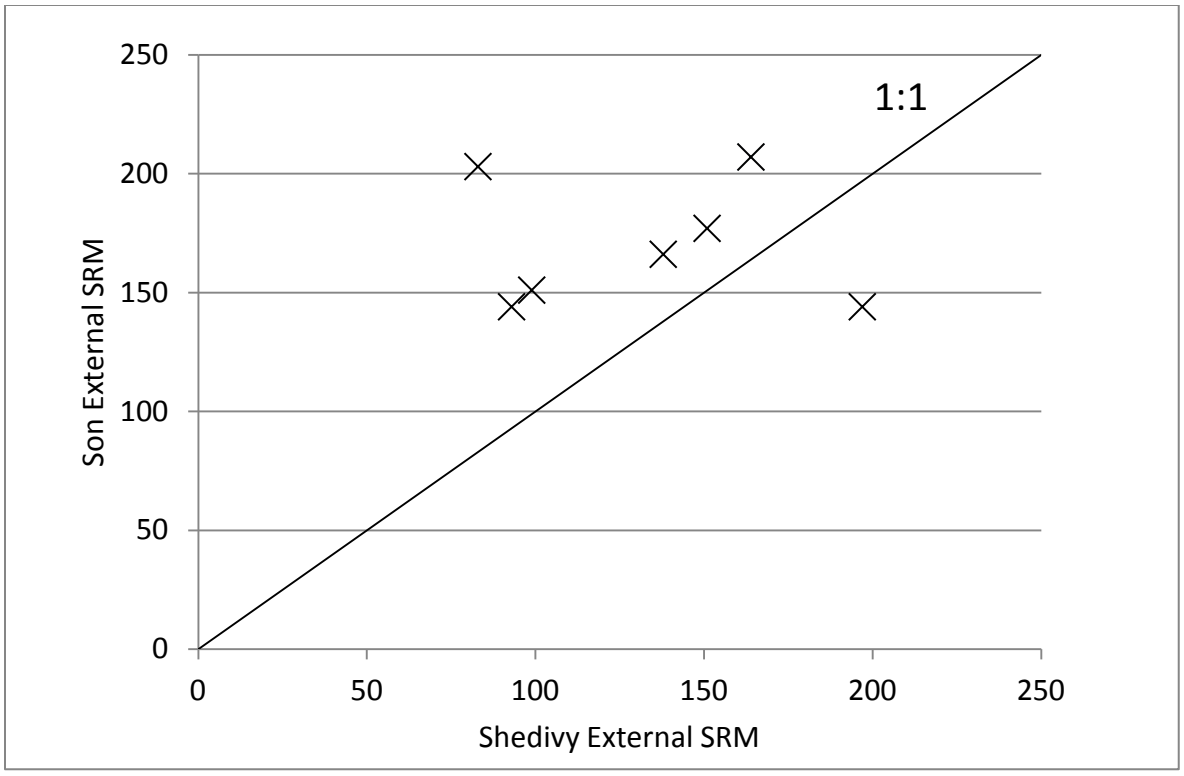

Figure 1.7b 1:1 Comparison of Shedivy's External SRM and Son's (2011) External SRM

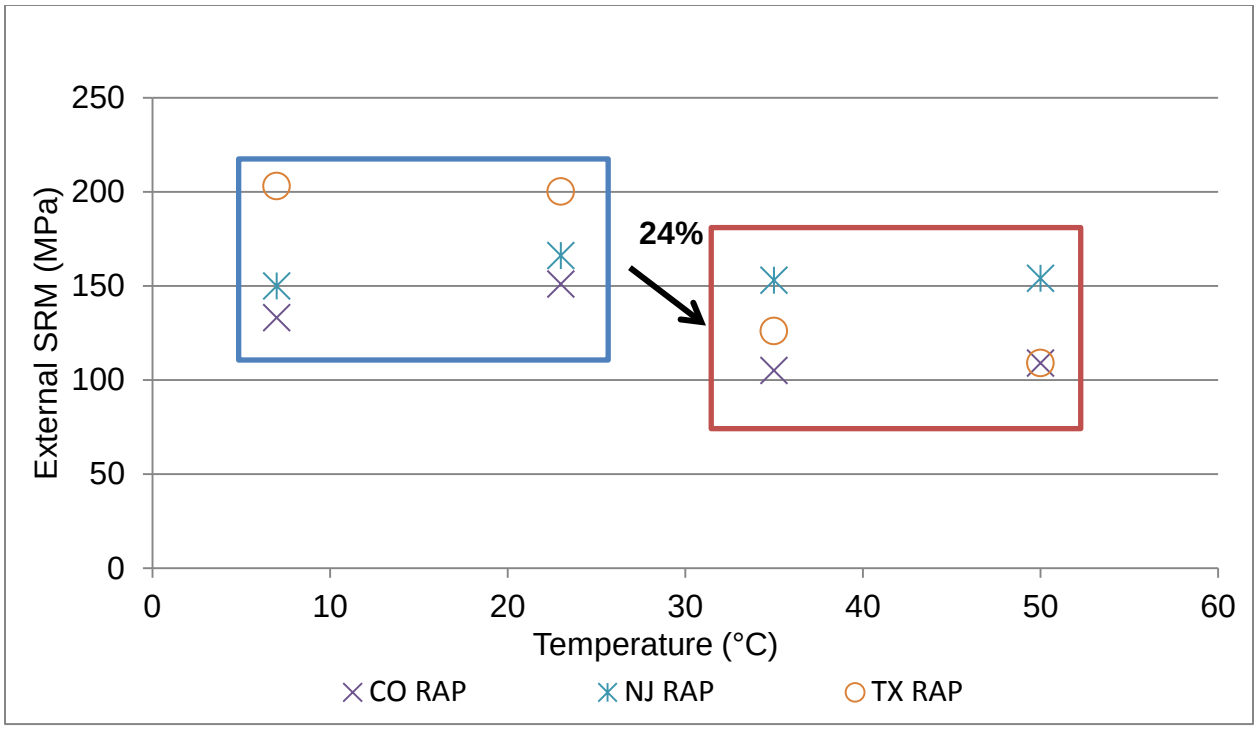

Figure 1.8a RAP Specimens Grouped Together for Statistical Analysis at Two Temperature Ranges (7 – 23 °C and 35 – 50 °C)

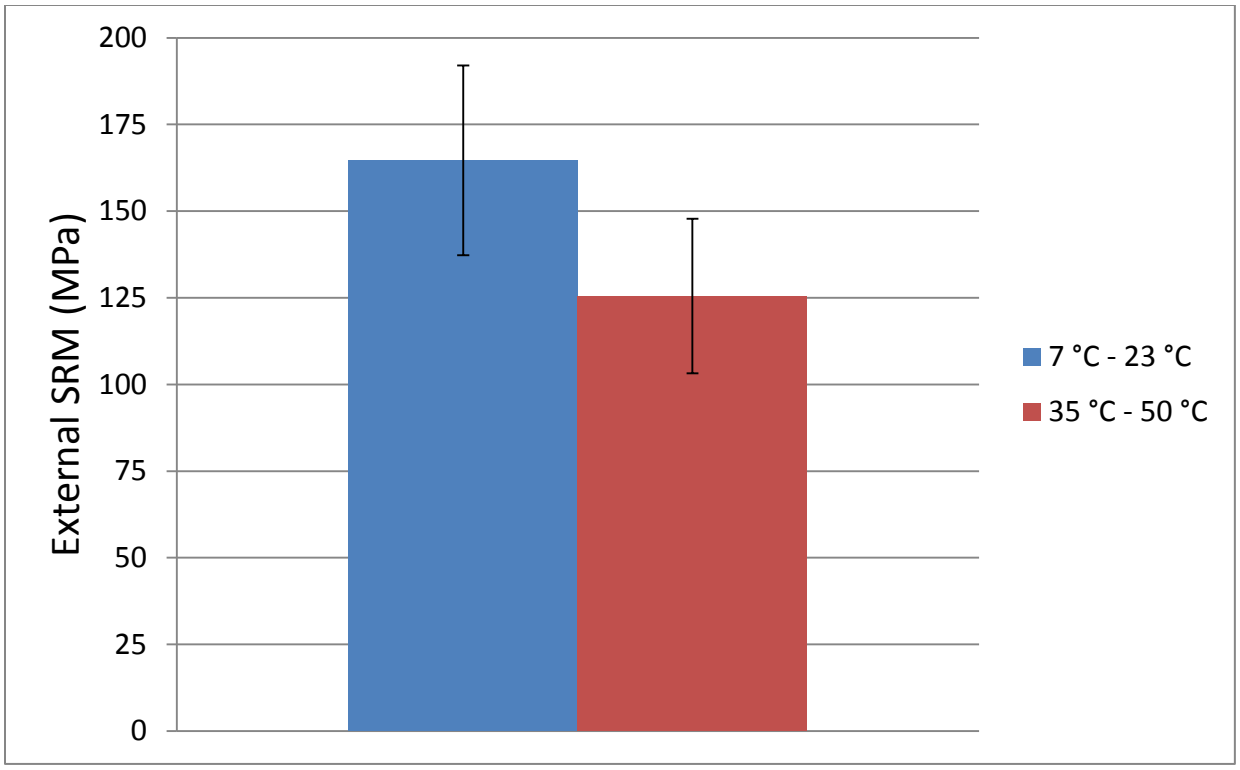

Figure 1.8b Average SRM for the 3 RAPs Tested at different Temperature Ranges with Standard Deviation Bars

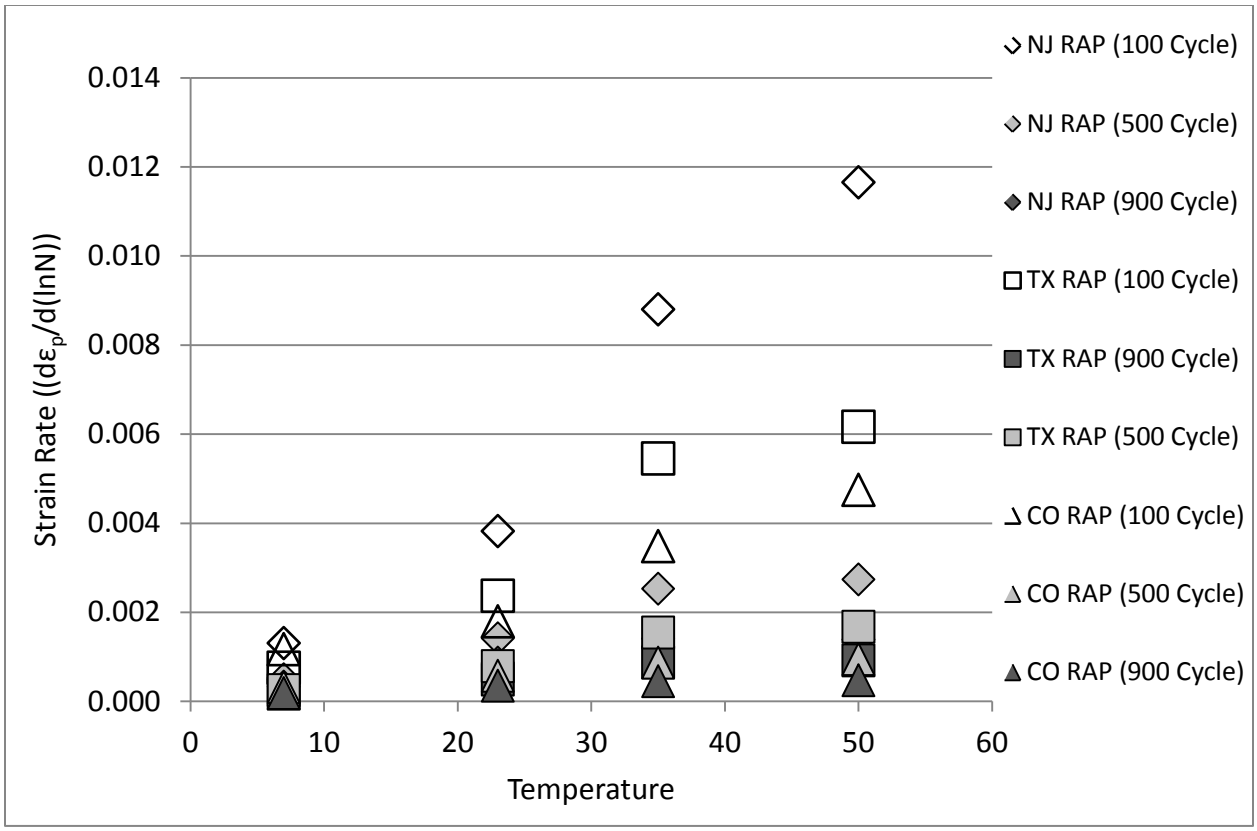

Figure 1.9a RAP Strain Rate at Varying Temperatures for 100, 500, and 900 Cycles of the 1st Sequence (Conditioning Phase)

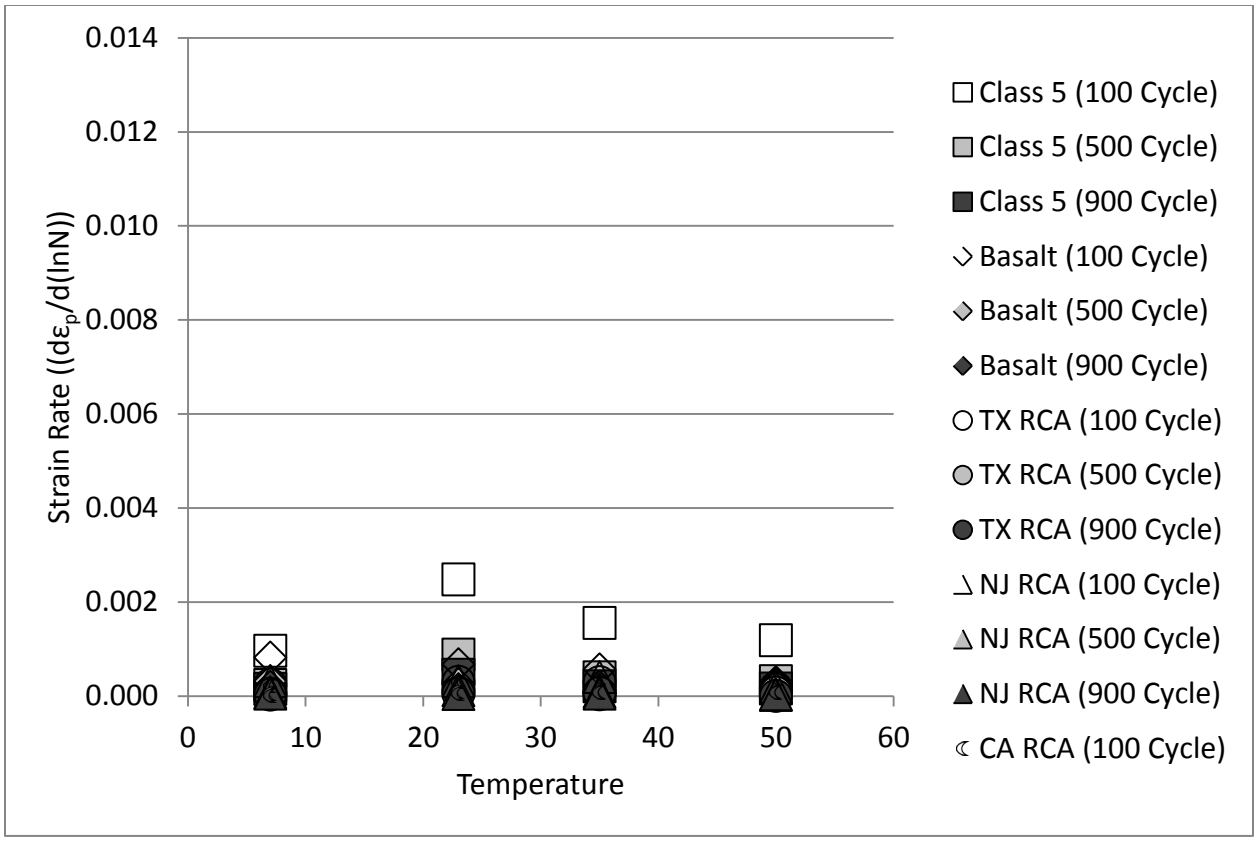

Figure 1.9b RCA and Natural Aggregate Strain Rate at Varying Temperatures for 100, 500, and 900 Cycles of the 1st Sequence (Conditioning Phase)

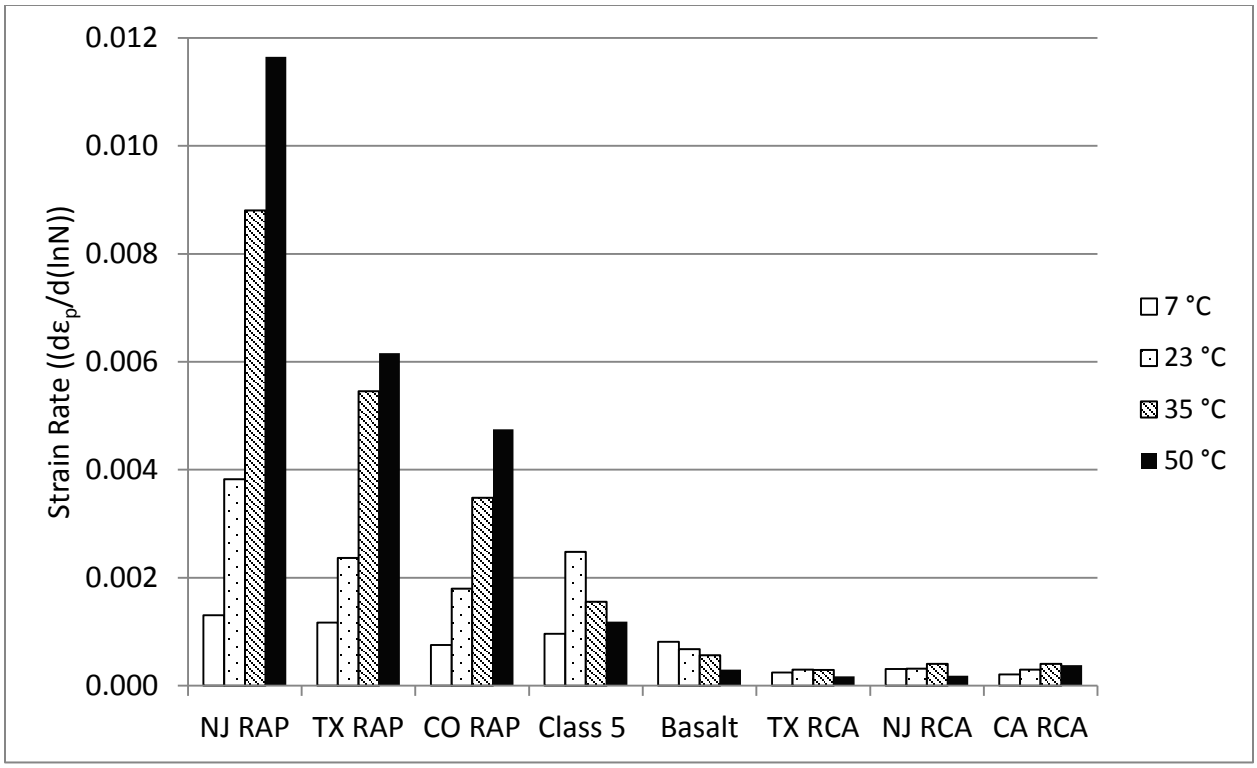

Figure 1.10 Strain Rates for Each Material at Varying Temperatures after the First 100 Cycles of the M_r Test

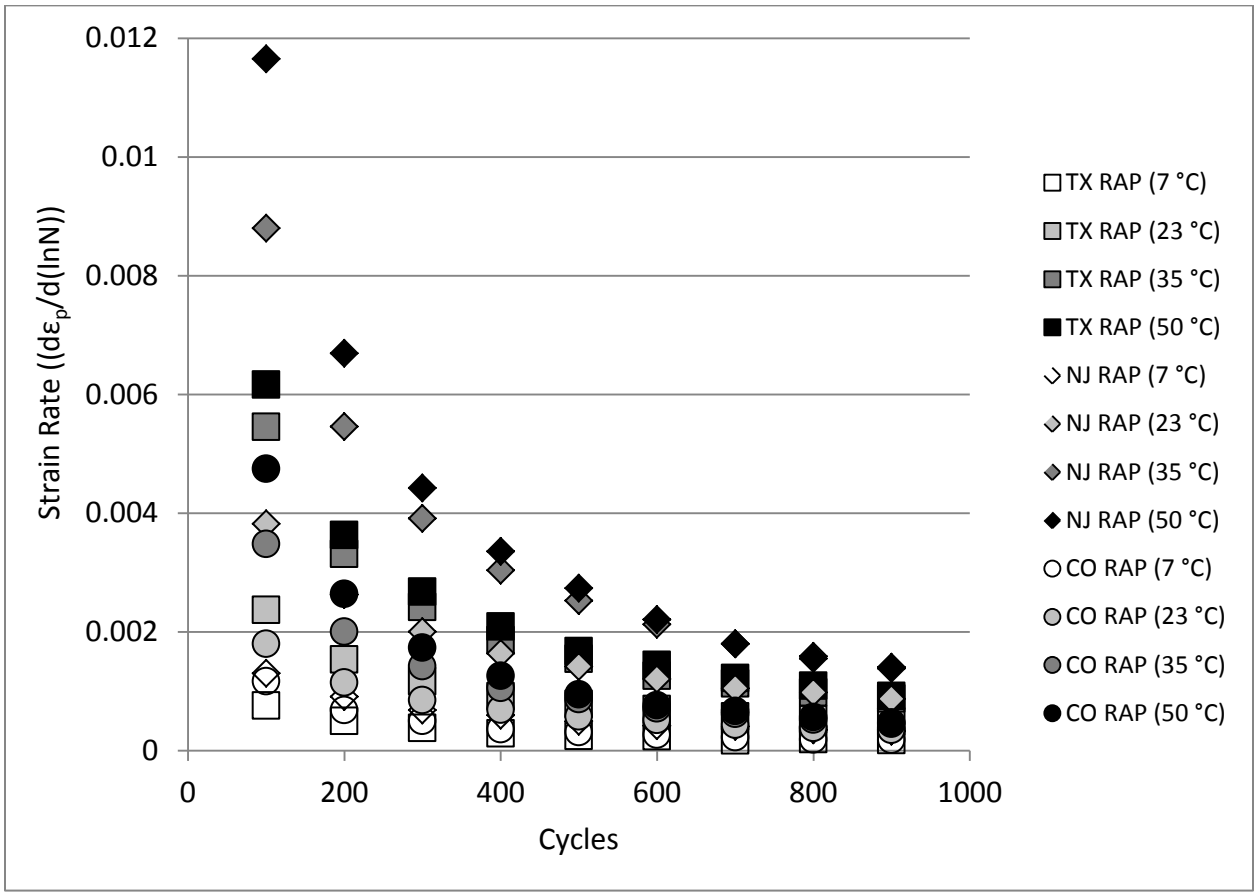

Figure 1.11a RAP Strain Rates at Varying Temperatures during the 1st Sequence (Conditioning Phase)

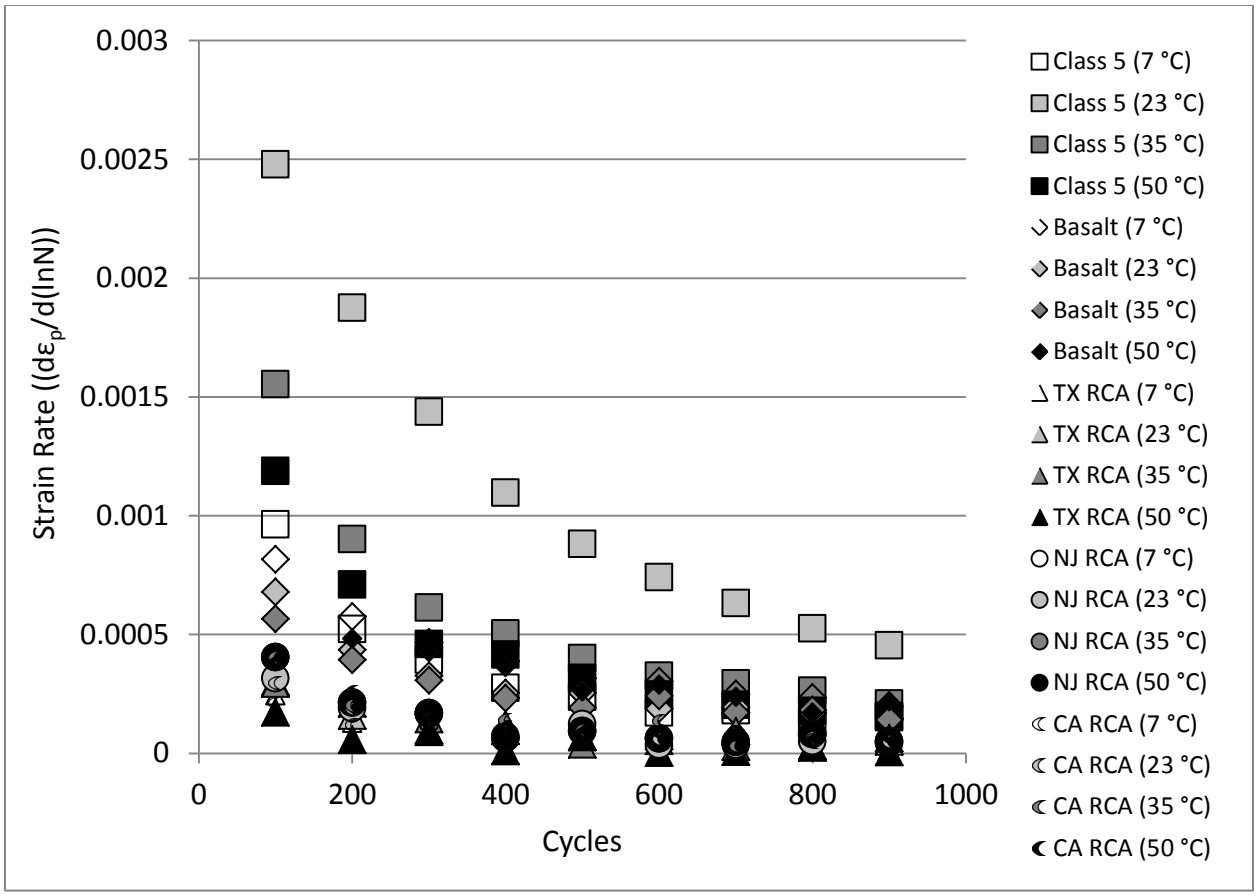

Figure 1.11b RCA and Natural Aggregate Strain Rates at Varying Temperatures during the 1st Sequence (Conditioning Phase)

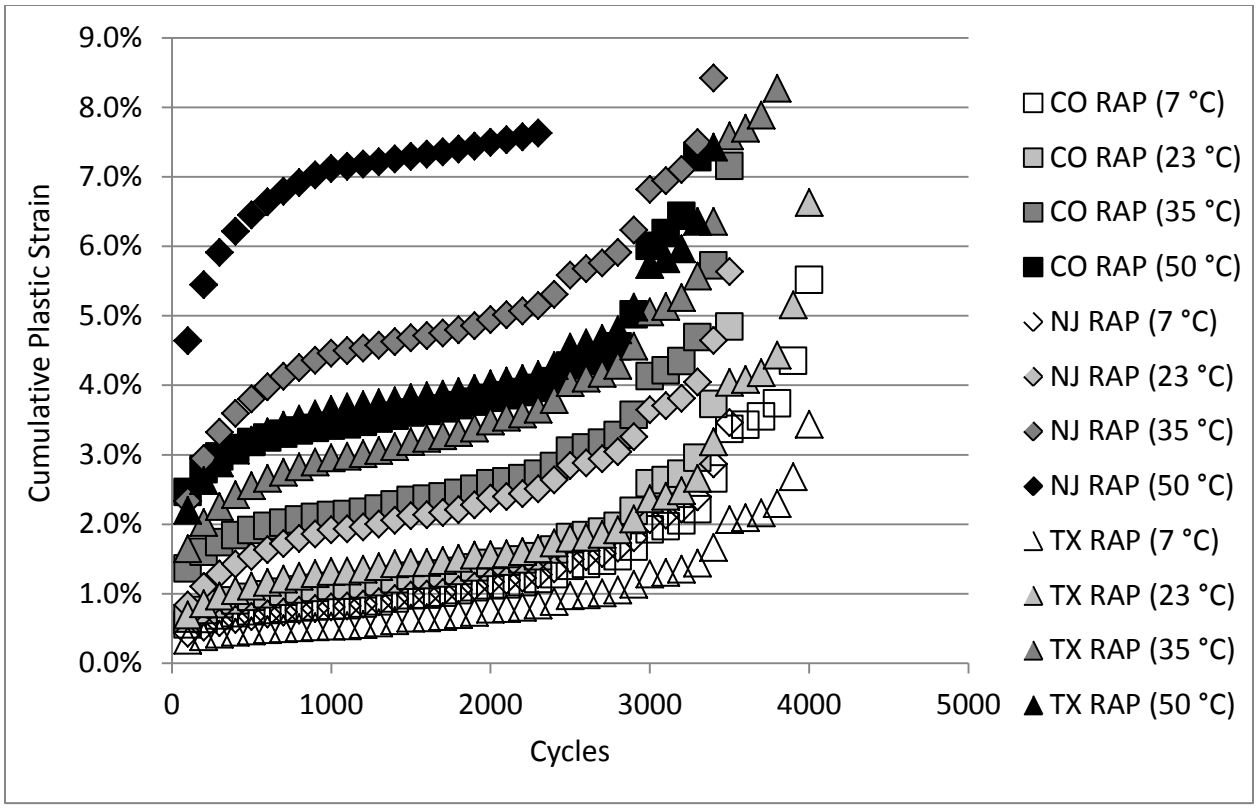

Figure 1.12a RAP Cumulative Plastic Strain throughout M_r Test at Varying Temperatures

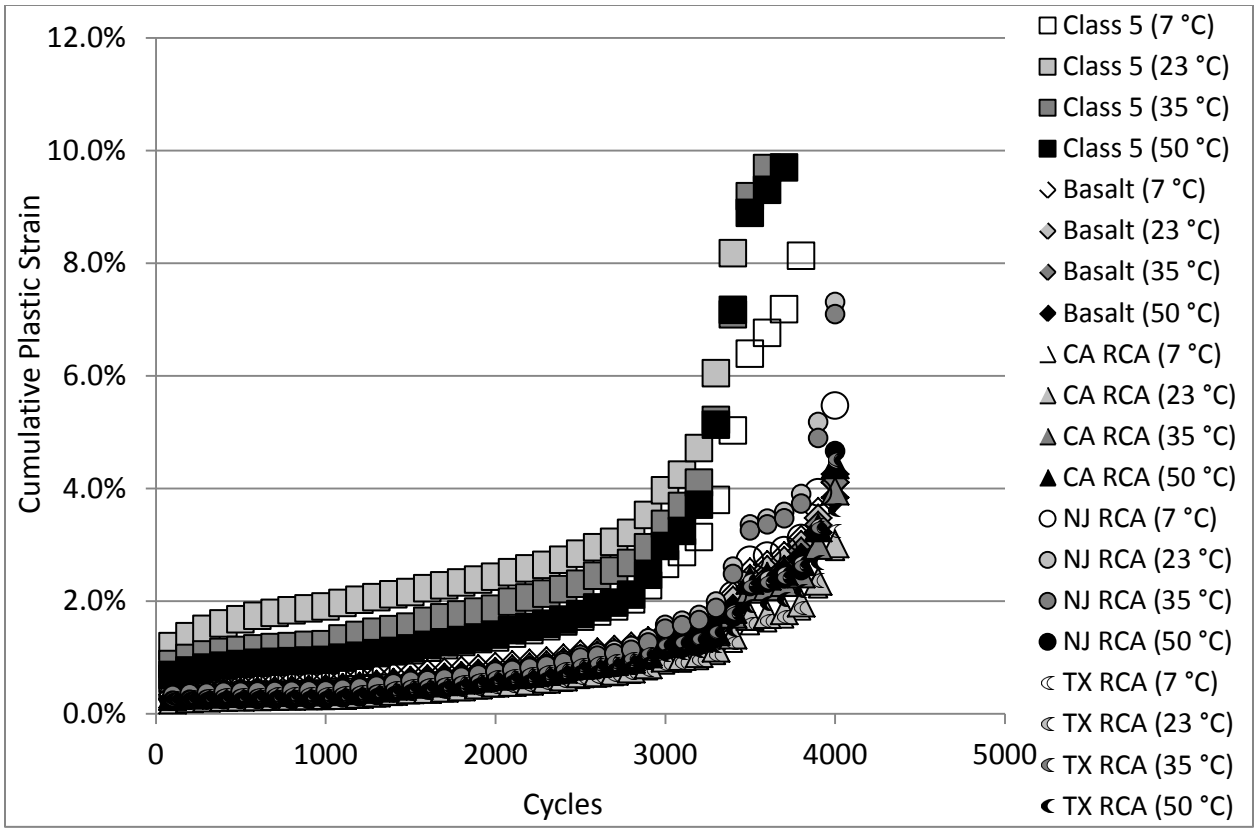

Figure 1.12b RCA and Natural Aggregate Cumulative Plastic Strain throughout M_r Test at Varying Temperatures

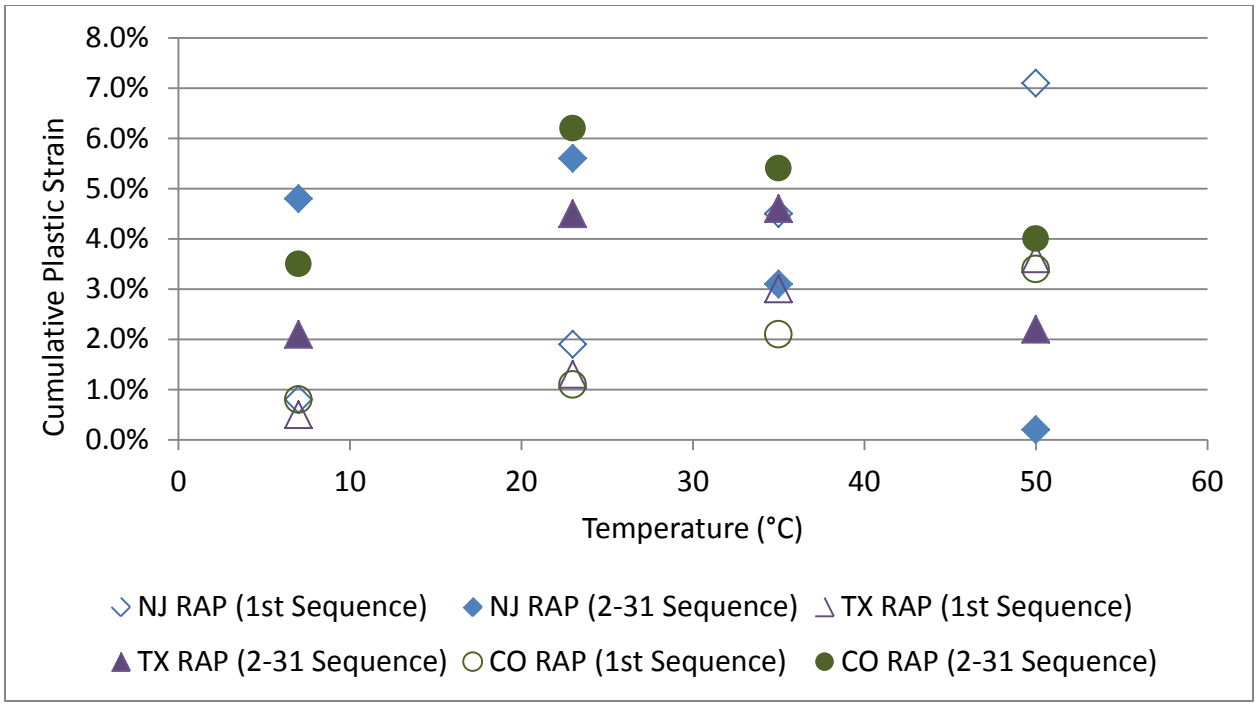

Figure 1.13 1st and 2nd-31st Sequence RAP Plastic Strain

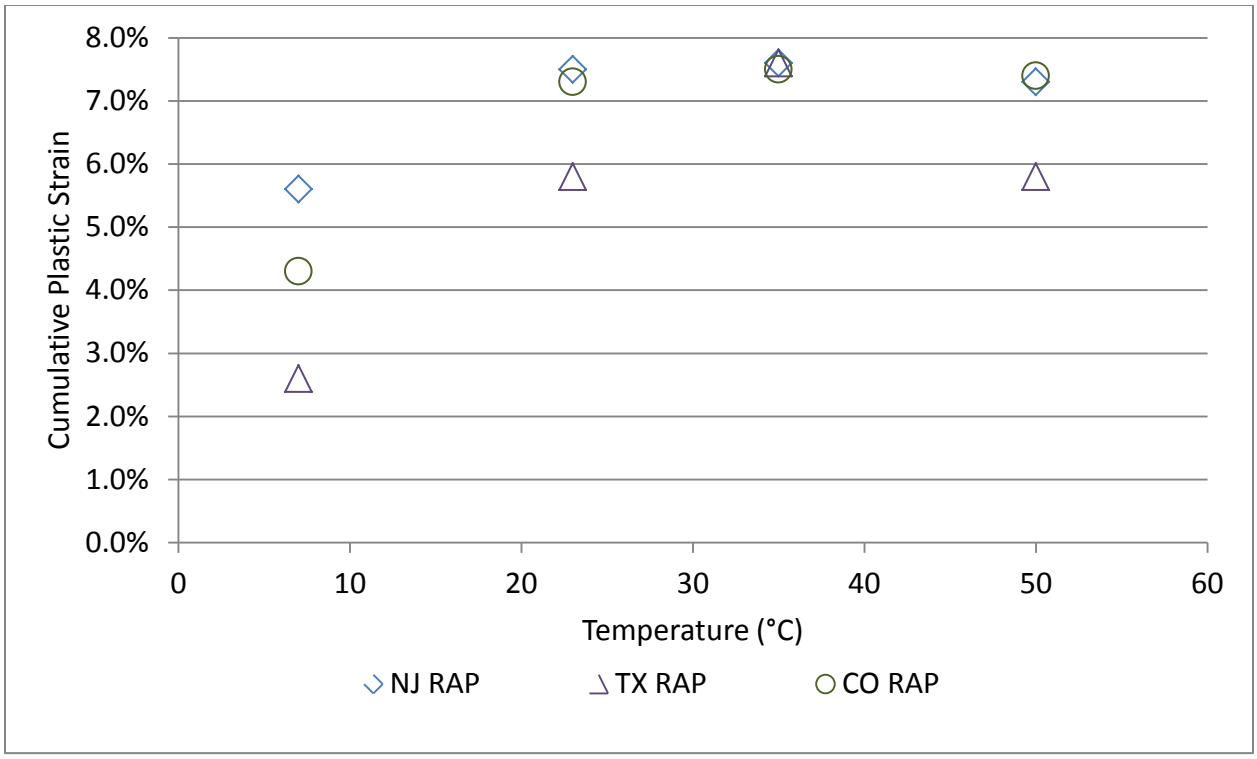

Figure 1.14 Total RAP Plastic Strain

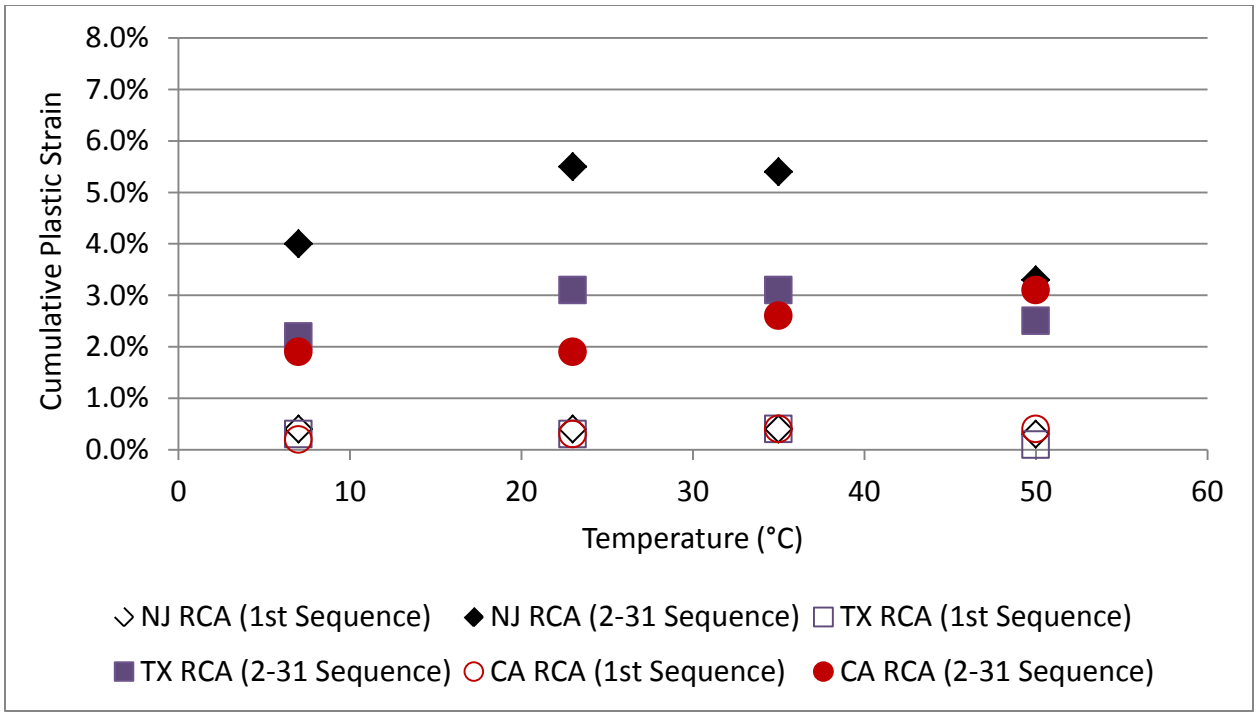

Figure 1.15 1st and 2nd-31st Sequence RCA Plastic Strain

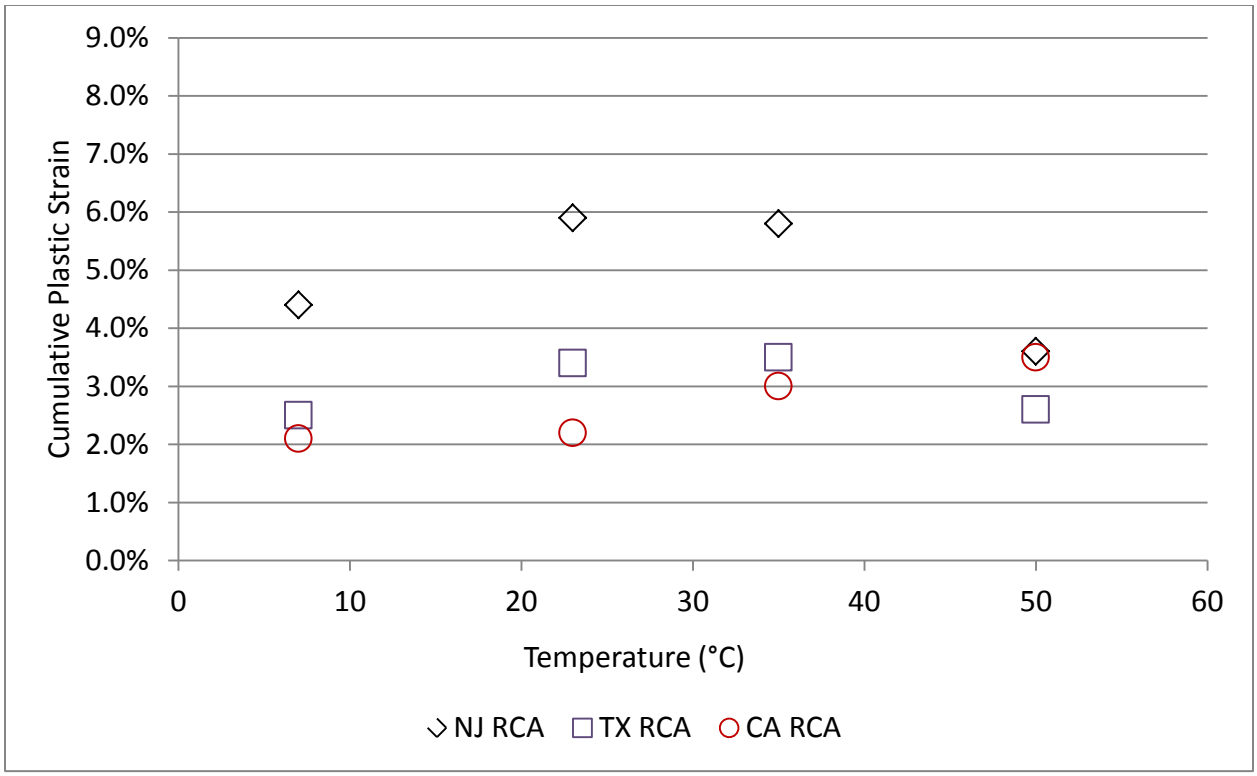

Figure 1.16 Total RCA Plastic Strain

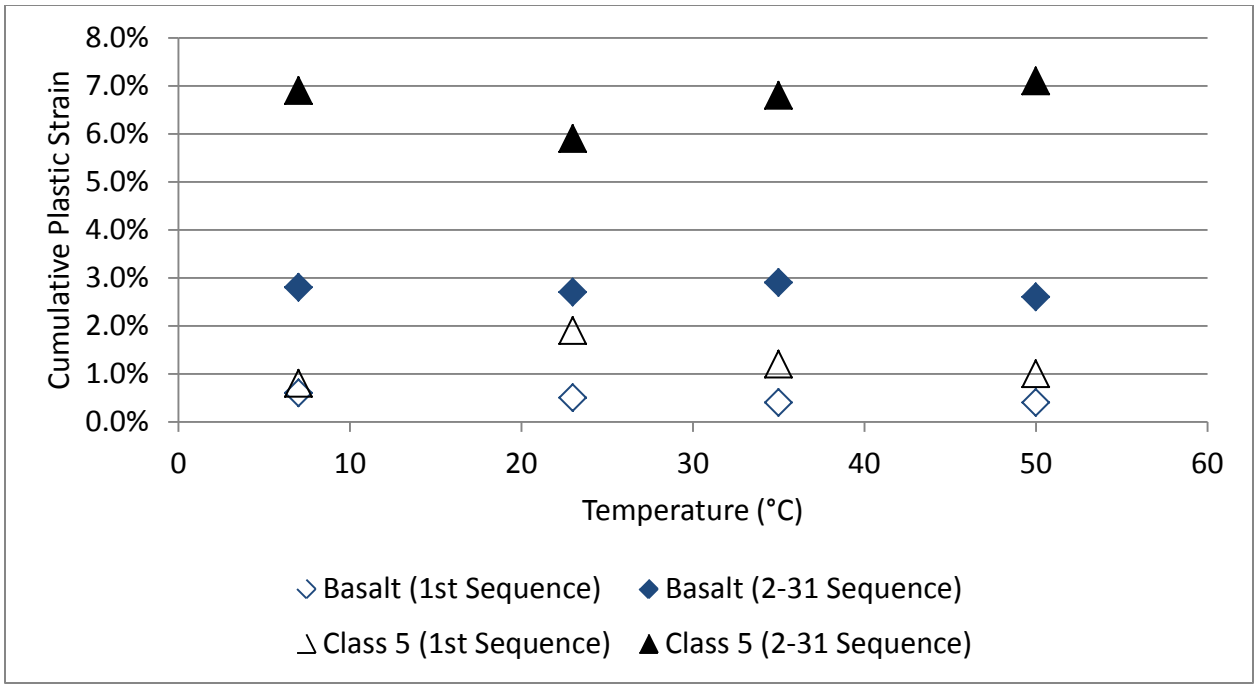

Figure 1.17 1st and 2nd-31st Natural Aggregate Plastic Strain

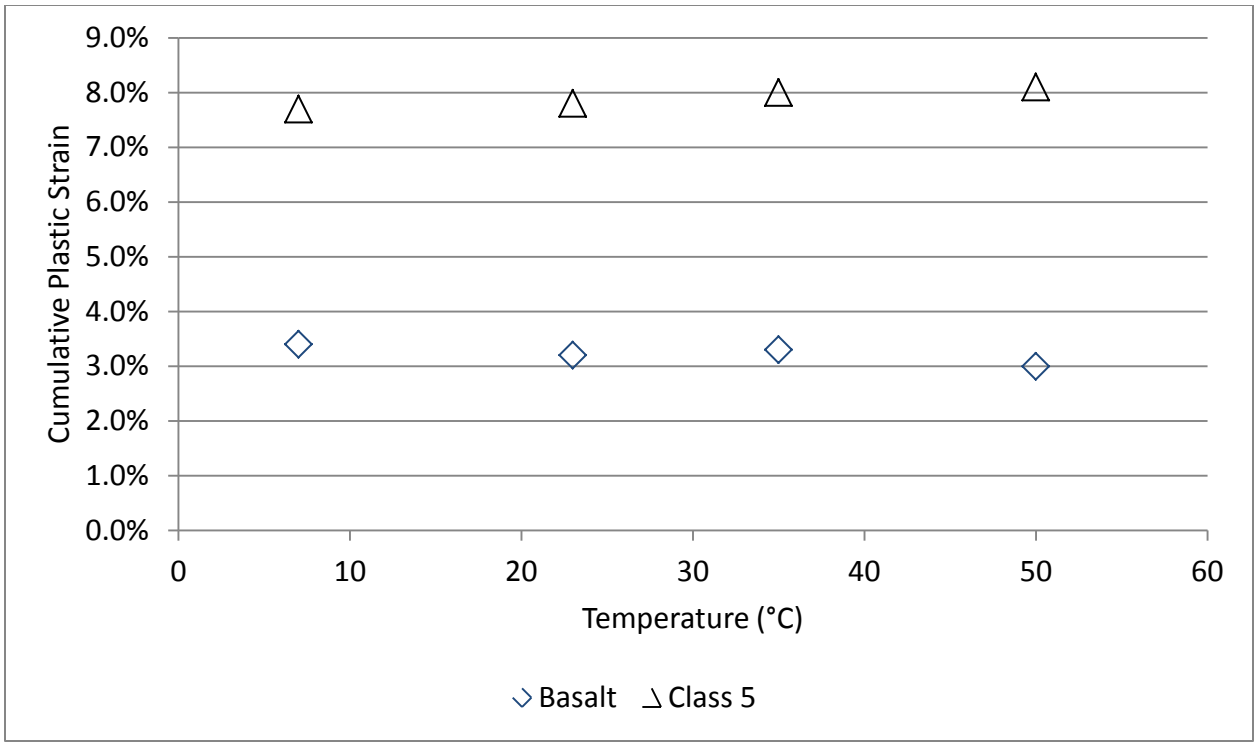

Figure 1.18 Total Natural Aggregate Plastic Strain

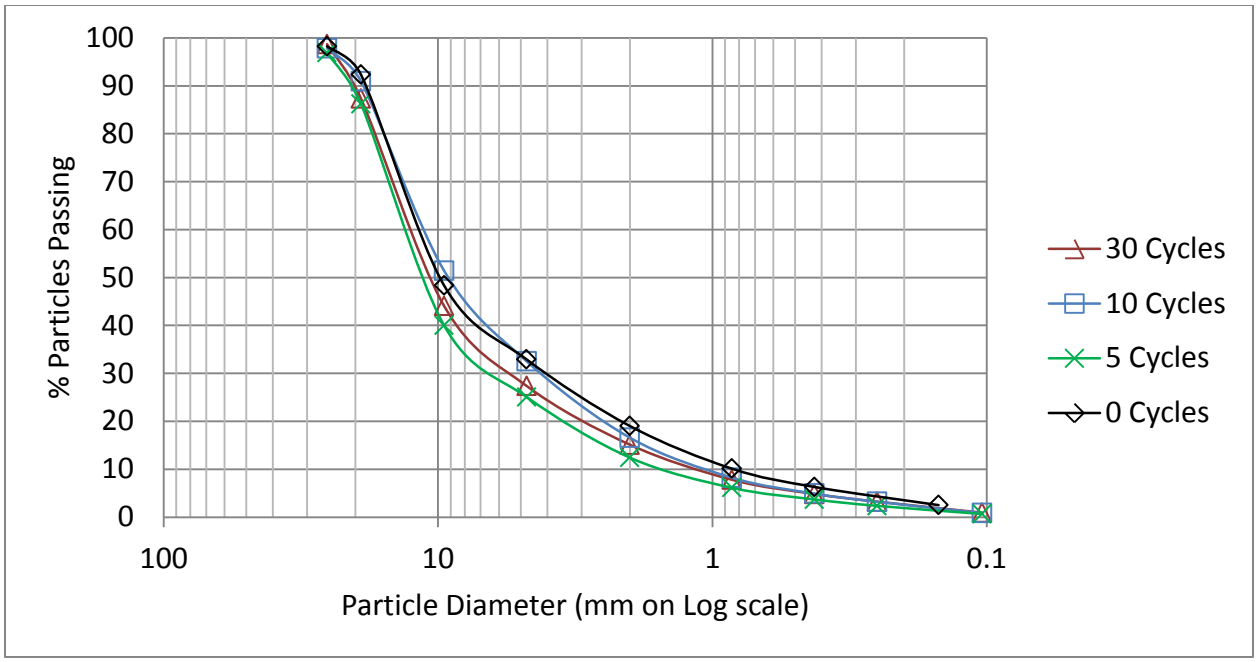

Figure 1.19 Basalt Wet/Dry Particle Size Distributions

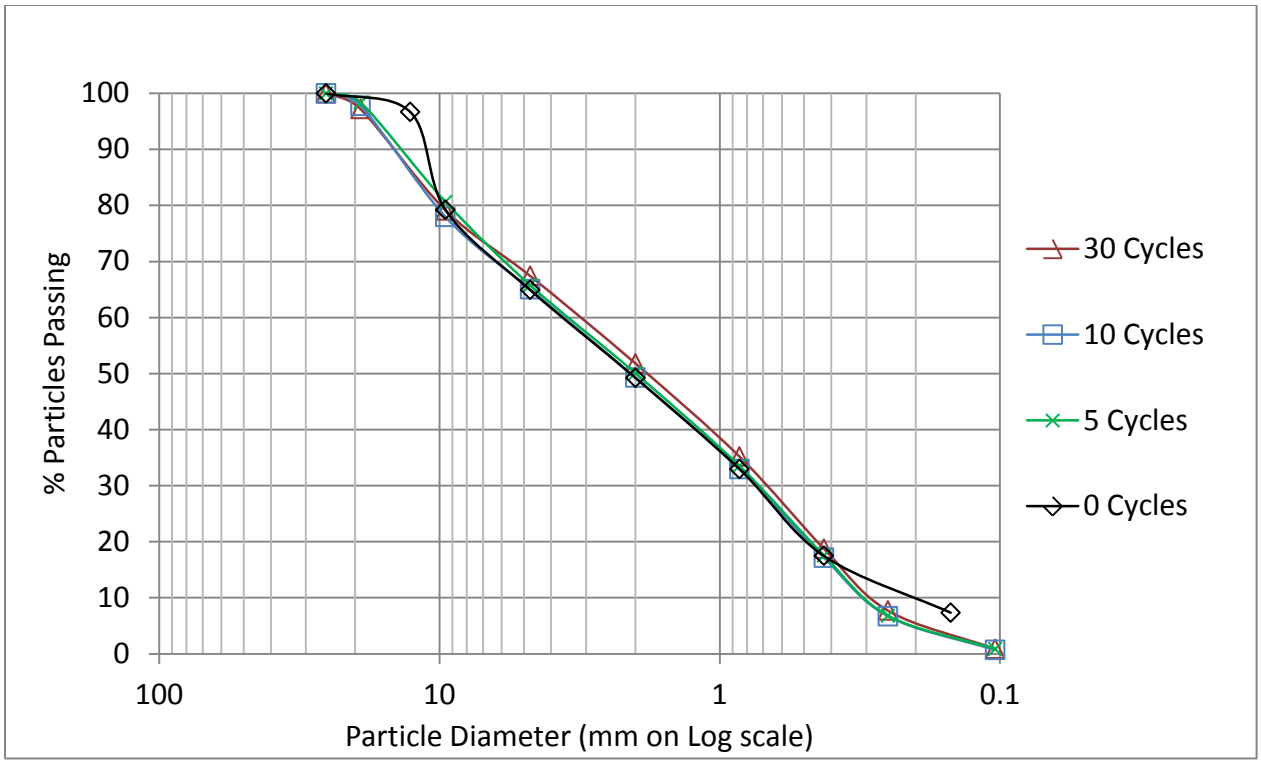

Figure 1.20 Class 5 Wet/Dry Particle Size Distributions

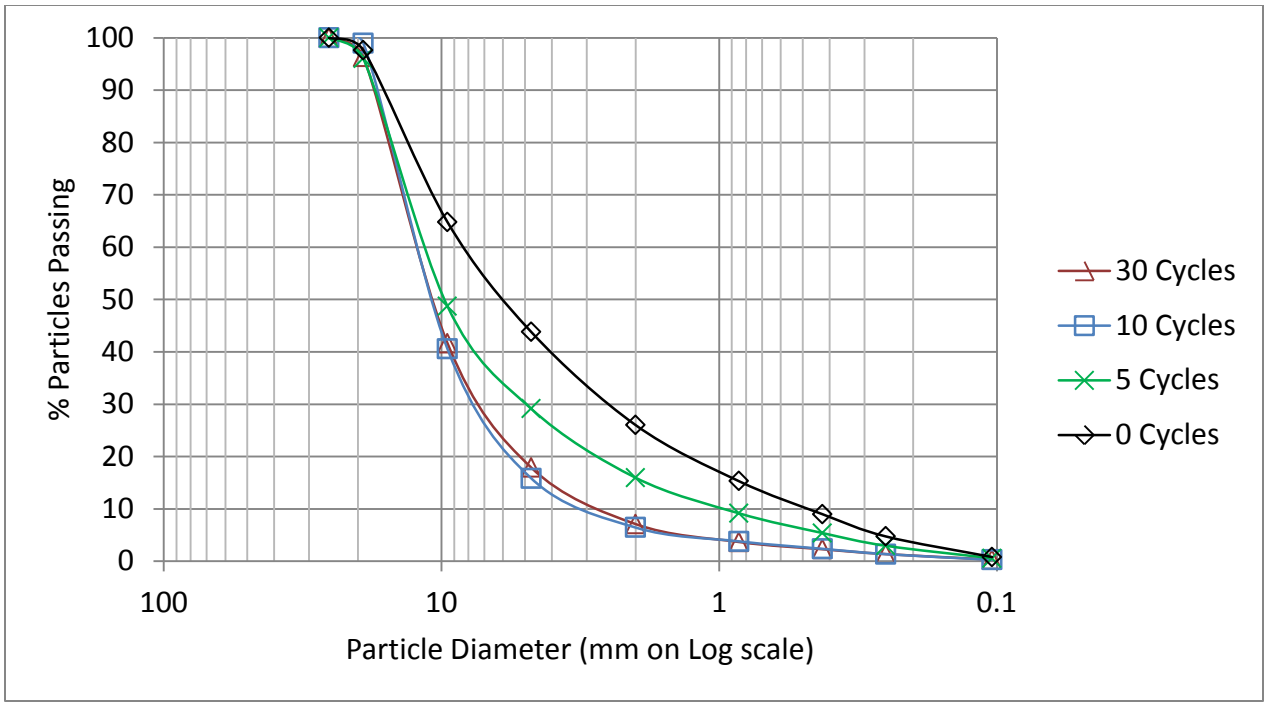

Figure 1.21 CA RCA Wet/Dry Particle Size Distribution

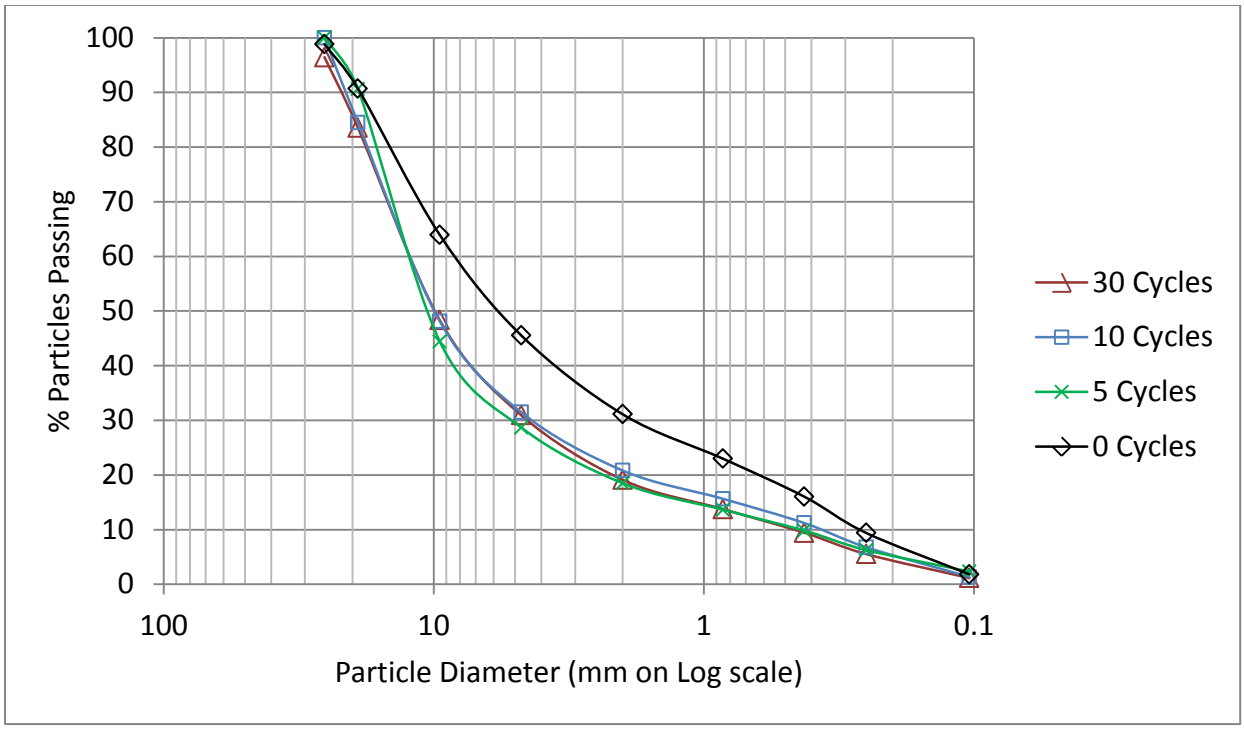

Figure 1.22 TX RCA Wet/Dry Particle Size Distributions

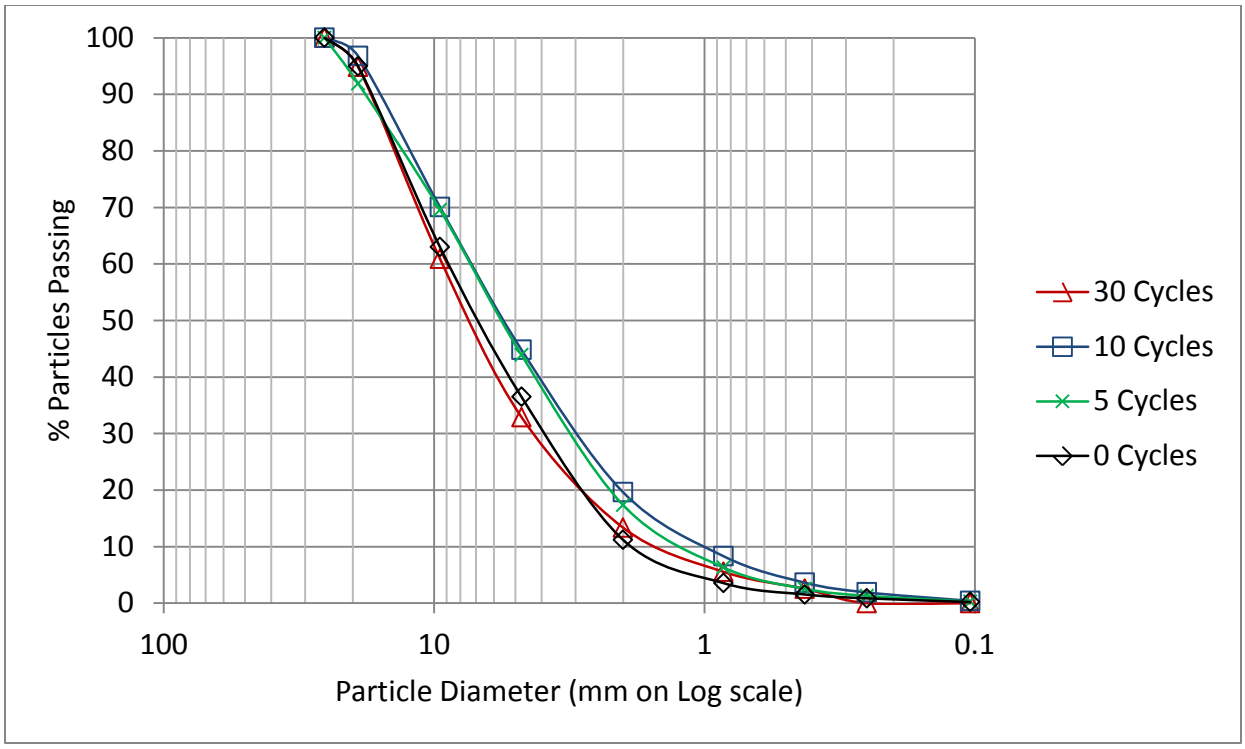

Figure 1.23 TX RAP Wet/Dry Particle Size Distributions

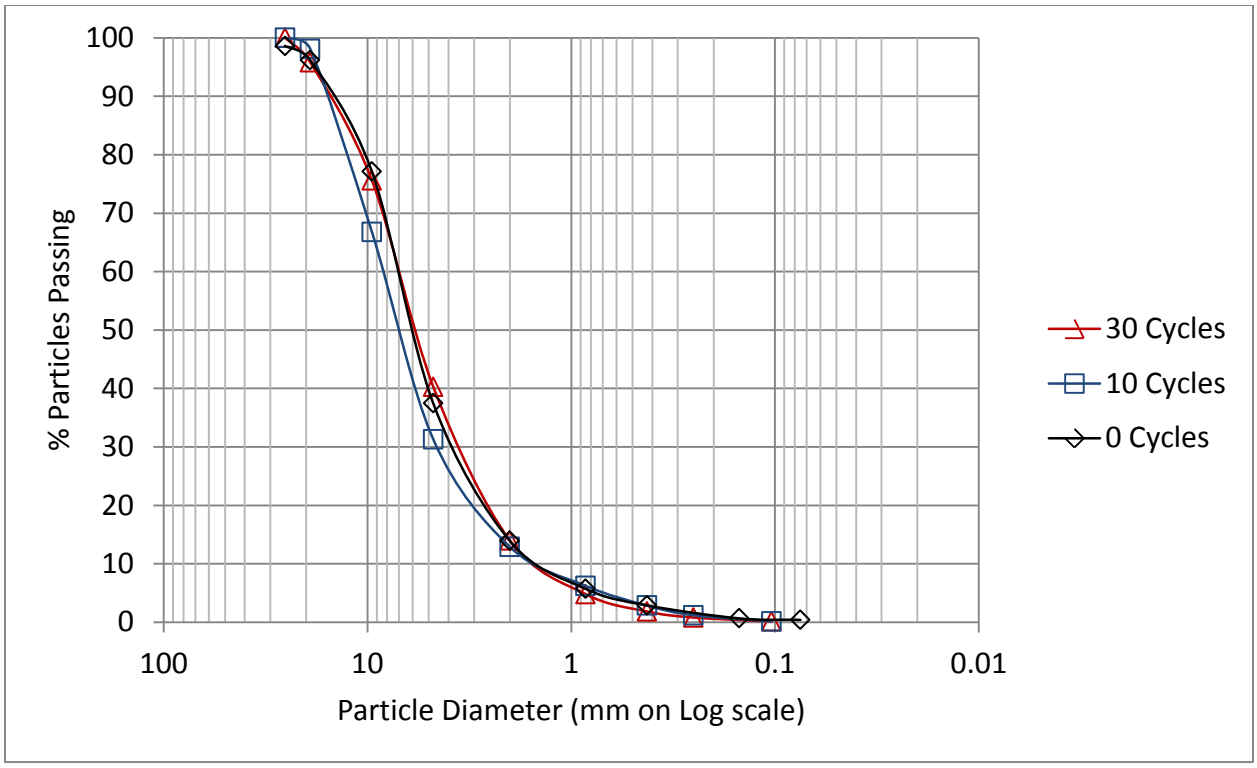

Figure 1.24 NJ RAP Wet/Dry Particle Size Distributions

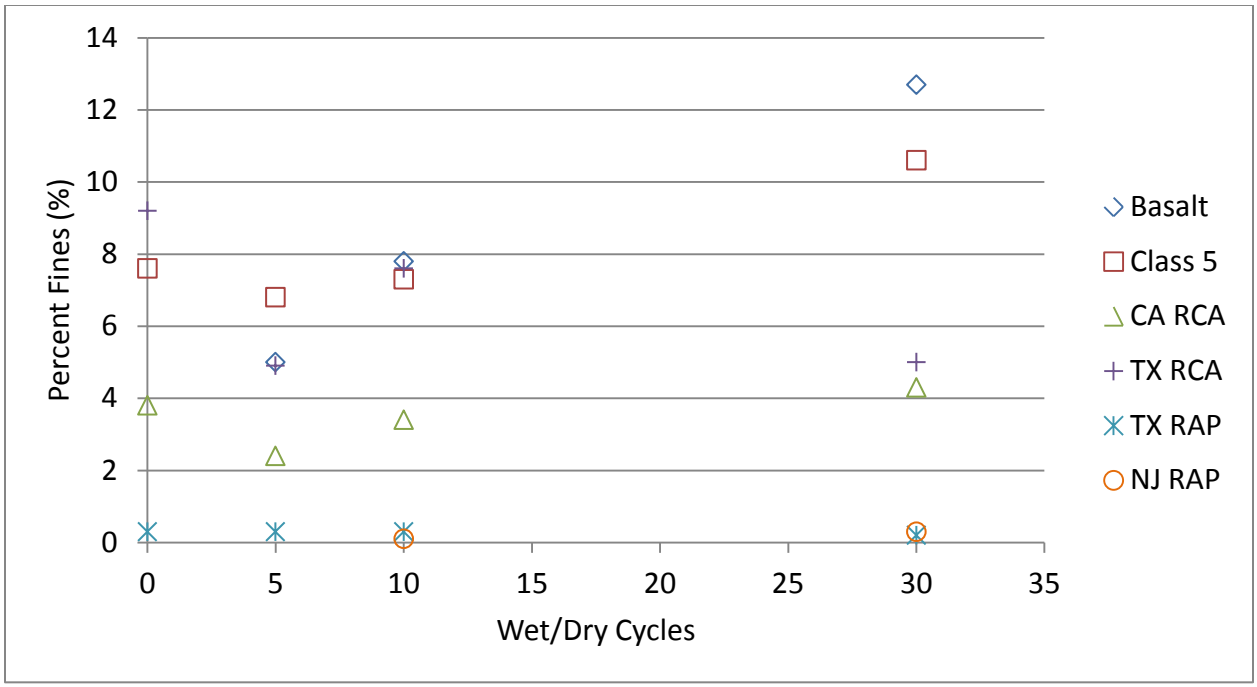

Figure 1.25 Percent Fines at Varying Wet/Dry Cycles

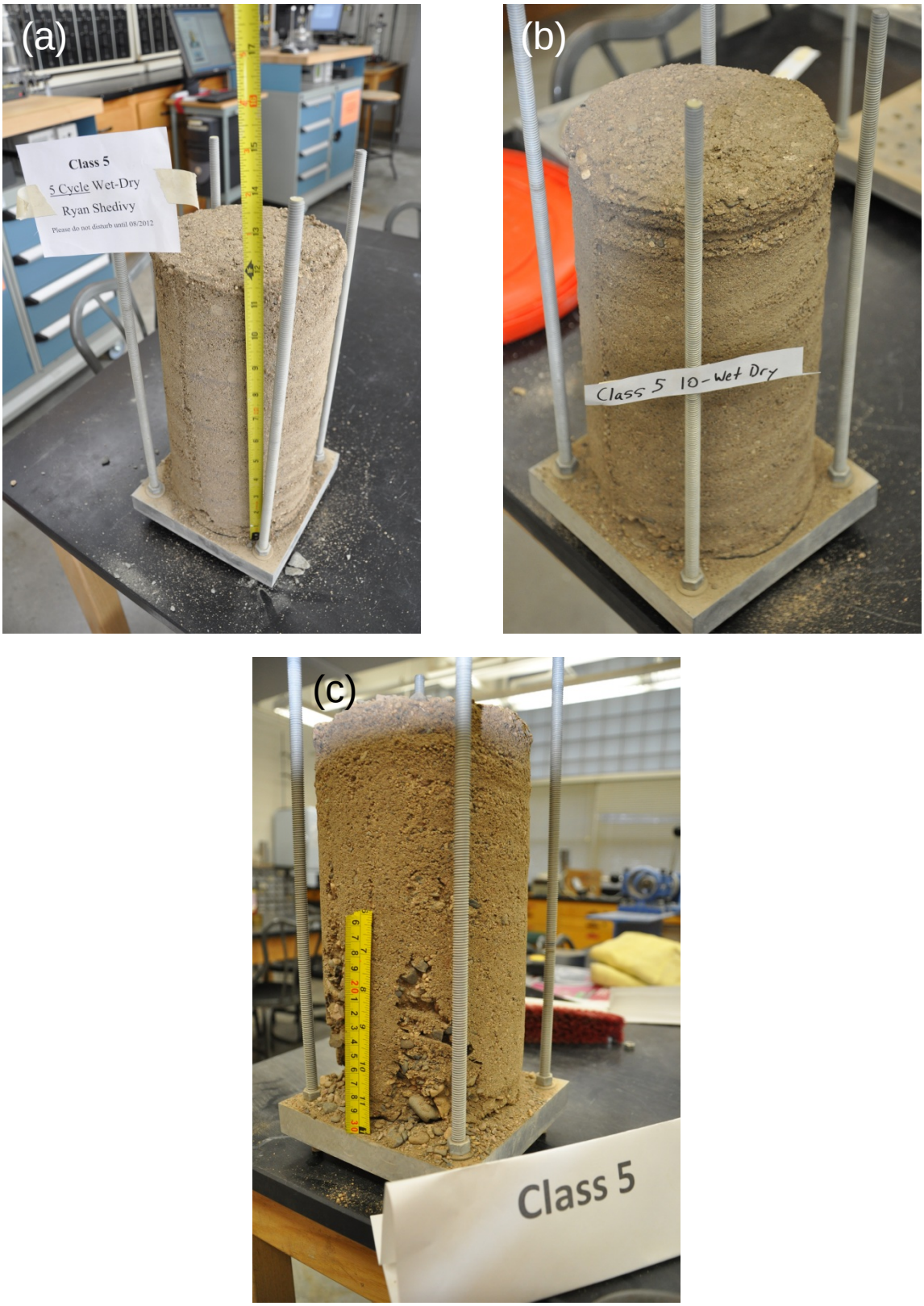

Figure 1.26 Class 5 after Wet/Dry Cycles: (a) 5 Cycles; (b) 10 Cycles; (c) 30 Cycles

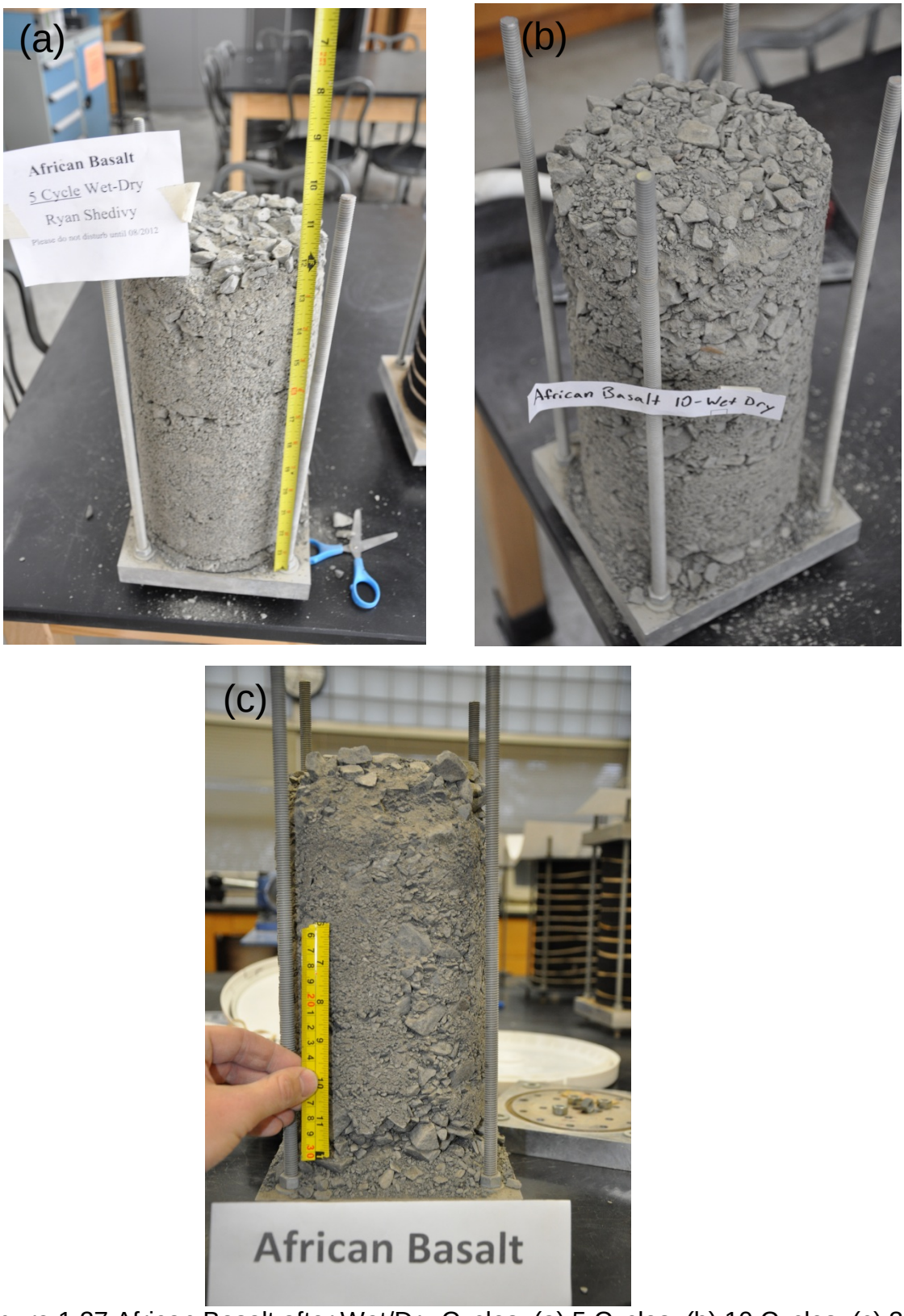

Figure 1.27 African Basalt after Wet/Dry Cycles: (a) 5 Cycles; (b) 10 Cycles; (c) 30 Cycles

Figure 1.28 CA RCA after Wet/Dry Cycles: (a) 5 Cycles; (b) 10 Cycles; (c) 30 Cycles

Figure 1.29 TX RCA after Wet/Dry Cycles: (a) 5 Cycles; (b) 10 Cycles; (c) 30 Cycles

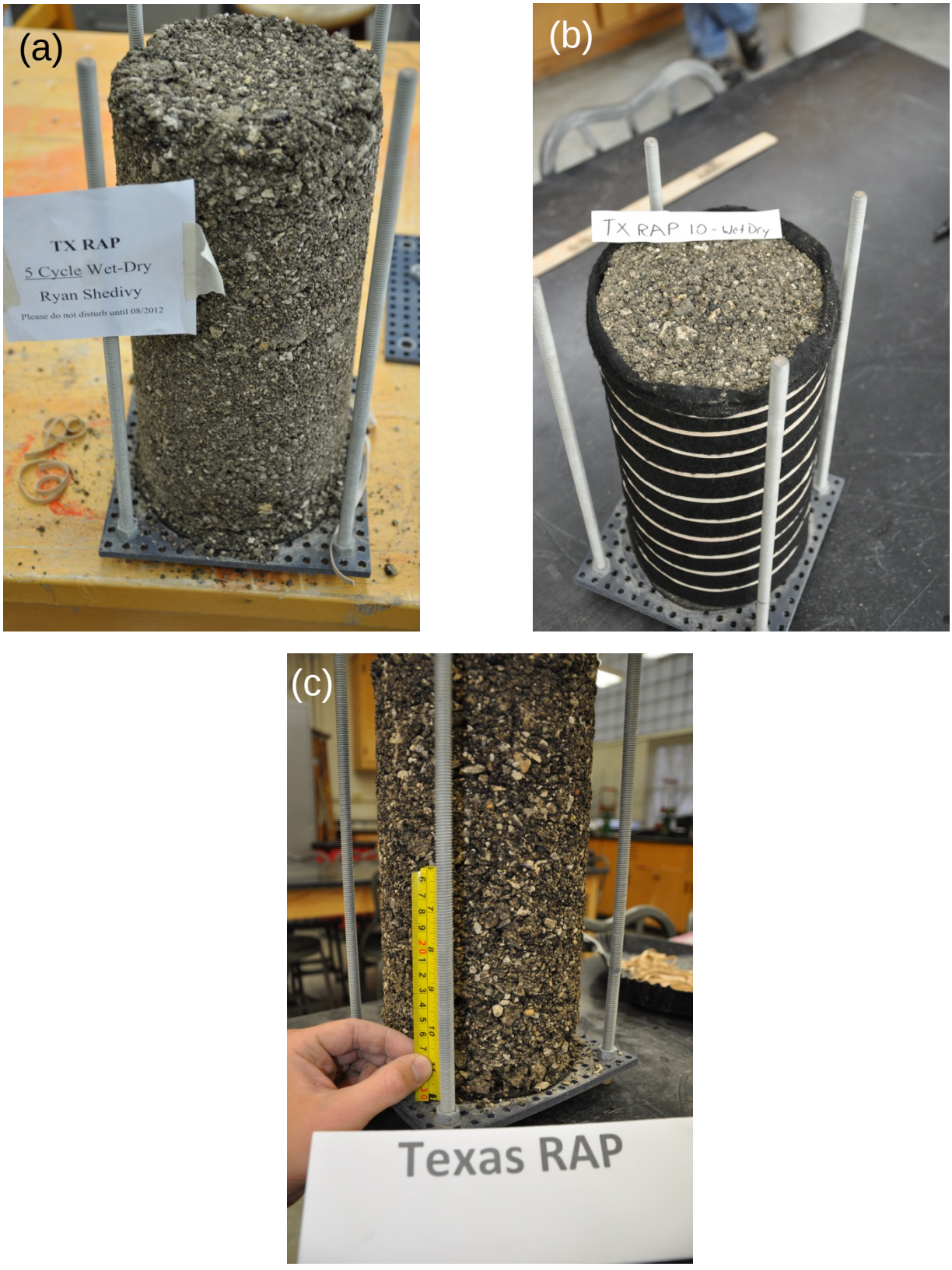

Figure 1.30 TX RAP after Wet/Dry Cycles: (a) 5 Cycles; (b) 10 Cycles; (c) 30 Cycles

Figure 1.31 NJ RAP after Wet/Dry Cycles: (a) 5 Cycles; (b) 10 Cycles; (c) 30 Cycles

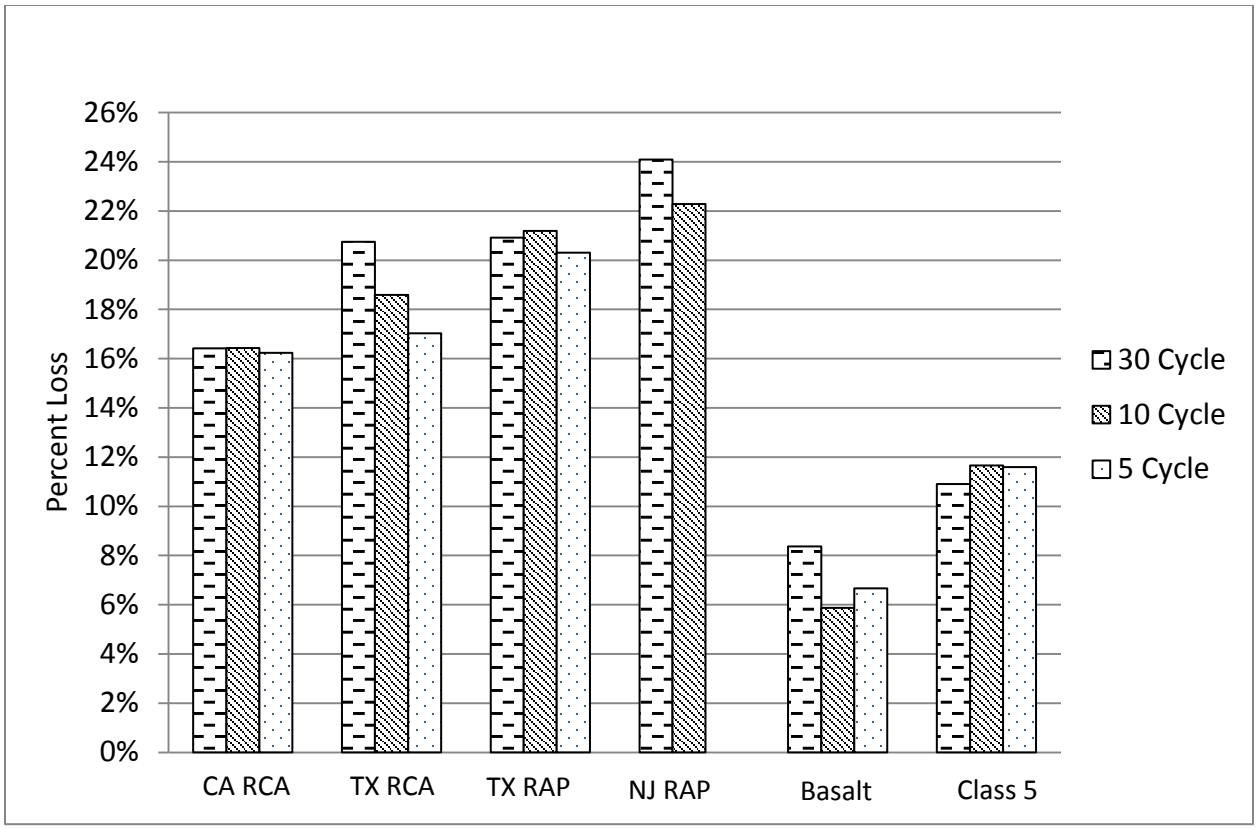

Figure 1.32 Wet/Dry Micro-Deval Results

2. The Effects of Recycled Clay Brick Content on the Compaction Properties and Resilient Modulus of Recycled Concrete Aggregate

2.1 INTRODUCTION

RCA and RAP/RPM may contain impurities that affect their mechanical properties and long-term performance. These impurities include soft bituminous materials such as crack sealants as well as pavement markings, metallic objects, recycled clay brick (RCB), and other potentially deleterious materials. A testing program was conducted to assess how impurity type and content affect the resilient modulus and plastic strain of RAP and RCA. This program was conducted in two parts. The first part of the testing program consisted of identifying the types and amounts of impurities present in RCA and RAP/RPM. This was accomplished by carefully segregating and identifying the components of each of the samples of RCA and RAP/RPM collected. Each component impurity was weighed and described. The second part of the testing program consisted of investigating the effects of RCB on compaction characteristics and resilient modulus when mixed with RCA.

RCB is a construction material most commonly used for facades. Clay is the main component of RCB, which is a very fine soil that is highly absorbent and can be hardened into brick when fired in a kiln. The use of RCB in tandem with RCA can benefit both cost and efficiency because of the operational difficulty of separating RCB from the RCA. The effects of RCB at various contents with RCA were evaluated because of the potential for brick to be mixed with RCA to be beneficially reused and because of the lack of literature on the subject. Brick is typically sorted from RCA at demolition sites and disposed of in landfills. The AASHTO (2002) standard for using

RCA as an unbound base course puts a limit on RCB percentage (5%); however, AASHTO allows higher percentages than 5% based on comparative structural testing (e.g., CBR, resilient modulus) that demonstrate that RCA with higher brick content is equivalent or better than RCA that complies with granular base specifications. Impurities other than RCB were not investigated past the first part of the testing program due to the lack of impurities present in all materials

2.2 BACKGROUND

2.2.1 Deleterious Materials (Impurities) in Recycled Materials

Kuo et al. (2002) reported that impurities (foreign material) present in RCA are one of the biggest concerns surrounding the use of this material in construction. Kuo et al. (2002) investigated the impurities in RCA made with limestone aggregate for a base course in flexible pavement. The amount of impurities was identified by means of visual inspection. Impurities were classified into categories including wood chips and paper, plastics, steel, asphalt, and RCB. Asphalt was found to be the most predominant type of impurity in the samples. The average impurity content was 3.67% by mass for RCA and 1.99% for limestone aggregates; both of these percentages were considered as negligible.

According to AASHTO Designation M 319-02, (2002), RCA for unbound base course shall be free of all materials that fall into the category of solid waste or hazardous material. Additionally, RCA should not contain more than 5% bituminous concrete material by mass and 5% brick by mass. No information or studies were provided for the basis of this limitation of materials other than the potential for properties

of the material to be affected. The 5% limit on RCB is most likely due to the clay nature and general notion that RCB is more susceptible to degradation and weathering than other building materials (e.g., concrete, rock, etc.). AASHTO (2002) also suggests that the engineer might select stockpiling as an approach to assist in qualitatively identifying the presence of deleterious materials. Stockpiling conditions of recycled material plays an important role in qualitatively assessing the uniformity of the material. Even though AASHTO (2002) defines mean percentages of impurities, AASHTO allows engineers to make some adjustments during construction on the amount of impurities allowed. However, visual examination of the material may not be helpful in determining the detrimental amount of wood chips or brick material in recycled material. Therefore, additional research or study will be important in establishing the acceptable amount of deleterious materials for recycled materials.

The Greenbook specification for construction materials (CMB) allows 3% brick by weight in RCA (Greenbook, 2009). The deleterious content should not comprise a detrimental quantity as defined in section 200-1.1. Various deleterious materials have different specific weights (i.e., wood chips are lighter than brick, plastic is lighter than small piece of wire meshes etc.). Wire mesh, plastic, and brick would be degraded less than sticks or pieces of wood, which would than leave voids in the base layer causing possible failures in the pavement. For concrete production, the amount of deleterious material is defined with many different specifications, but for unbound recycled base material, there are few specifications defining the effect of impurities.

Bozyurt (2011) found that, for the specific recycled materials tested in this study, RCA averaged approximately 1% impurities, while RAP had approximately 2%

impurities. Many of the impurities found in these recycled materials were wood chips, glass, geotextiles, steel, asphalt aggregate, and sea shells. The impurity content of each material reported in Bozyurt (2011) and this study is summarized in Table 2.1. Results from this study can also be found in Figure A.9 to Figure A.13 in the Appendix.

2.2.2 Recycled Clay Brick Mixed with Recycled Concrete Aggregate

The use of RCB as a natural aggregate substitute is not typically accepted in construction practices because of the lack of research pertaining to the beneficial reuse of RCB. The majority of research on RCB is on the mechanical properties of the material for use as a substitute for natural aggregate when used in concrete. Debieb and Kenai (2008) investigated using coarse, fine, and coarse/fine RCB as a substitute for natural aggregate in concrete mixes. Introducing RCB reduced bulk density and increased water absorption of the concrete when compared to natural aggregate. Densities of RCB before mixing with cement were also found to be lower (up to 17%) when compared to natural aggregate.

Yang et al. (2011) also evaluated the effects of substituting natural aggregate with RCA and RCB in concrete. Water absorption of the RCA and RCB were 4.2% and 10.2%, respectively, while that of natural aggregate was 1.4%. Particle densities for RCA and RCB were 24.71 kN/m^3 and 21.97 kN/m^3, which were lower than the natural aggregate (26.28 kN/m^3). Arulrajah et al. (2011) evaluated the potential use of RCB as an unbound subbase. They found similar values for RCB with absorption of 6.15% and density at 26.19 kN/m^3. The maximum dry density of the RCB after modified Proctor compaction was 19.82 kN/m^3 and the OMC was 10.7%. Arulrajah et al. (2011) also

evaluated permanent strain and resilient modulus of 100% RCB and reported satisfactory performance as a subbase at 98% maximum dry density and 65% OMC.

Poon and Chan (2006) reported that RCB mixed with RCA decreased the maximum dry density and increased the OMC of the mixture. The assumed reasoning for the decrease in maximum dry density was due to the reduced density of the RCB and irregular shape of the manually crushed RCB. California bearing ratio also decreased as RCB content increased. Cameron et al. (2012) investigated the effects of varying RCB content on two types of RCAs, one premixed at 20% RCB by mass and the other mixed at 10%, 20%, and 30% RCB. A decrease (< 80 MPa) in resilient modulus was observed with increased RCB content from 10% to 30% at approximately 90% OMC.

Arulrajah et al. (2011) also evaluated the effects of mechanical degradation and abrasion on RCB using the LA Abrasion test. The results showed a LA Abrasion loss of 36, higher than typical natural aggregate and RCA. 35 is the typical maximum percent loss adopted by state departments of transportation, suggesting the need to mix RCB with stronger aggregates such as RCA or natural aggregate.

2.3 MATERIALS

Sixteen recycled materials, one conventional base course, and one blended recycled/conventional material were used in the first part of this investigation, which evaluated the percentages of impurities present. Seven of the recycled materials were recycled asphalt pavement (RAP), six were recycled concrete aggregate (RCA), and two were recycled pavement material (RPM). The recycled materials used in this study were obtained from a wide geographical area, covering eight different states: California,

Colorado, Michigan, Minnesota, New Jersey, Ohio, Texas and Wisconsin (Figure 2.1). The materials were named according to the origin of the materials. The reference base course was a gravel meeting the Class 5 aggregate specification for base course in Minnesota per the Minnesota Department of Transportation (MnDOT). The Class 5 aggregate used in this study contains quartz, granite and carbonates (limestone and dolomite). The ratio of quartz/granite to carbonates is 2.1. The percentage of mineral type in Class 5 aggregate is 68% for quartz/granite and 32% for carbonates. Percent quartz/granite (aggregate and concrete) and percent carbonate of gravel (aggregate and concrete) of gravel are 43% and 20%, respectively. The blend (MN) was a mix of approximately equal parts (by mass) RCA from MnDOT (50%) and Class 5 aggregate (50%). The Class 5 aggregate was used as the control in this study.

The material from MnDOT was obtained during construction of roadway cells at the MnROAD test facility in Maplewood, Minnesota for investigation of the field behavior. The RAP was milled from the surface of roadway cells that were previously constructed at the MnROAD test facility. The RCA was obtained from a stockpile maintained by the Knife River Corporation at their pit located at 7979 State Highway 25 NE in Monticello, Minnesota.

The RAP from the Ohio Department of Transportation (ODOT) came from an existing asphalt pavement, processed through a portable plant, and stored in approximately 2268 Mg stockpiles. The Ohio RCA is from a 1.2-m-high barrier wall that existed between the north- and south-bound lanes of State Route 315 in downtown Columbus, Ohio. The broken-up concrete was taken from the project to a portable

processing plant, crushed, sized, and stockpiled. The material for this project came from stockpiles of approximately 9071 Mg. The RCA samples provided were 100% RCA.

The material received from the Colorado DOT was collected from over 500 demolition sites from curb, gutter, sidewalk, highways, high-rise buildings, and housing foundations. Although the concrete came from varied sources, the aggregates for the production of the concrete originated from rock in Colorado, most from quarries in Morrison and Golden and some aggregates were sourced from the Platte River.

The material provided by the New Jersey DOT (NJ DOT) is from stockpiles for demolition projects, primarily in New Jersey. The material in the stockpiles is in flux since NJ DOT constantly adds new loads and removes content for different purposes.

The RAP from California DOT is a combination of roadway millings and waste from an HMA plant (discharge from warm up and cleaning processes). The RCA is broken concrete rubble from the demolition of structures. Stockpiling in California is usually done three times a year. These stockpiles are not added to throughout their life-cycle. If stockpiled material is still unavailable during visits from subcontractors, new material is used to create a new stockpile.

The RCA sent by the Texas DOT is from a commercial source; therefore, the individual sources of aggregate or material characteristics included in the RCA are not known. The Texas RAP is from a highway project where the contractor milled the "binder" course after approximately 1.5 years of service. The RAP l from Michigan was provided by the Michigan DOT and is from highway reconstruction projects.

A summary of the grain characteristics and classifications for the seventeen materials is shown in Table 2.1. The materials used in this study are classified as non-

plastic per the Unified Soil Classification System (USCS). The Class 5 aggregate is classified as well-graded gravel (GW-GM) per USCS (ASTM D 2487) and A-1-b per the AASHTO Soil Classification System (ASTM D 3282). The blended RCA/Class 5 is classified as A-1-b according to ASTM D 3282 and as poorly graded sand (SP) according to ASTM D 2487. The samples of RCA range from an SP to a well-graded gravel (GW) classification via USCS and A-1-a or b for AASHTO. The various RAPs and RPMs classify as SP, SW, or GW, whereas their AASHTO classifications are A-1-a or b. All materials are coarse-grained granular materials with fines content less than 7% except Class 5 aggregate and one RCA (CO) sample.

The particle size distribution (PSD) curves were determined according to ASTM D 422. Samples were wet-sieved through a No. 200 (75-µm opening) sieve to separate the fine particles attached to the coarser aggregates. The PSDs for the RCA and the RAP/RPM samples are shown in Figure 2.2 and Figure 2.3 respectively, along with the upper and lower bounds from the literature.

The RCB was obtained from the demolition of the University of Wisconsin Credit Union's drive-through structure. The approximate age of the clay brick was 16 years. Brick and attached mortar were manually crushed using sledge hammers and then sieved to match the PSDs of each four RCAs used in the tests conducted. For the brick study, the RCAs from New Jersey, Minnesota, Texas, and Ohio were used.

2.4 METHODS

2.4.1 Resilient Modulus

The design of roadway pavement relies on proper characterization of the load-deformation response of the pavement layers (Tian et al. 1998). Base and subgrade deform when subjected to repeated loads from moving vehicular traffic. Resilient modulus (M_r) defines the nonlinear elastic response of pavement geomaterials, such as unbound aggregate base and subbase, under repeated traffic loading. The resilient behavior of unbound aggregate layers is affected by the stress state experienced because of wheel loading and the physical properties of aggregate (Pan et al. 2006). The M_r is a linear-elastic modulus obtained from dynamic loading, defined as the ratio of the cyclic deviator stress to the resilient (recoverable) strain, and is defined as:

$$M_r = \left({}^{\sigma_d}/_{\varepsilon_r} \right) \tag{2.1}$$

where ε_r is the recoverable elastic strain and σ_d is the applied deviator stress.

Design of pavements and rehabilitation of layered pavement systems use M_r as an essential parameter in the design process (Heydinger et al. 2007). The M_r is a key input in NCHRP 1-37 (mechanistic-based pavement design approach), which is being evaluated for adoption by numerous state highway agencies (Pan et al. 2006). The performance of pavement is dependent on the stiffness of the pavement structure under specified traffic loads and environmental conditions. Generally, a high M_r for a base course infers a stiffer base course layer, which increases pavement life. The resilient response of granular material is important for the load-carrying ability of the pavement and the permanent strain response, which characterize the long-term performance of the pavement and rutting phenomenon (Lekarp et al. 2000).

For base course, the summary resilient modulus (SRM) corresponds to the M_r at a bulk stress of 208 kPa, and octahedral shear stress of 48.6 kPa as suggested by Section 10.3.3.9 of NCHRP 1-28a. SRM is also used to determine the layer coefficient, which is a required input in the AASHTO pavement design equation (Tian et al. 1998).

2.4.2 Crushed Clay Brick Tests

To evaluate the effects of RCB on the resilient modulus and compaction properties, percentages of RCB to RCA were first determined. 10%, 20%, and 30% RCB by mass were used because these percentages have the possibility of being accidentally or purposely mixed in with RCA. These percentages also matched the percentages of the study completed by Cameron et al. (2012). The RCB was sieved through 25, 19, 9.5, 4.75, 2.36, and 0.425-mm sieves and matched to the PSD of the RCA it was mixed with. Once mixed, modified Proctor compaction tests were completed on the 30% RCB mixture per ASTM D422. Compaction tests were not completed on New Jersey RCA or at 10% and 20% RCB due to lack of RCA available.

For the resilient modulus tests, RCB/RCA specimens were compacted at OMC and 95% of maximum dry unit weight of the corresponding RCA the RCB was mixed with. The mixtures were compacted to the RCA's compaction characteristics to evaluate the effects associated with RCB unnoticeably being added to the RCA. The specimens were compacted in six lifts using a modified Proctor hammer into a 152-mm-diameter, 305-mm-high mold. Cyclic load triaxial tests were then completed according to NCHRP 1-28a on the RCB/RCA mixtures at 0%, 10%, 20%, and 30% RCB to determine the resilient modulus (M_r) and plastic strain of the material. Two interior and

two external linear variable differential transducers (LVDTs) were used to record the strain response of the loading on the specimens. The data was fitted using the Power fitting and NCHRP models shown as equation 2.2 and 2.3, respectively. Plastic strain was also calculated using both interior and exterior LVDT data from the triaxial test.

$$M_R = k_1 \times \theta^{k_2} \quad (2.2)$$

$$M_r = k_1 . p_a . \left(\frac{\theta - 3k_6}{p_a}\right)^{k_2} . \left(\frac{\tau_{oct}}{p_a} + k_7\right)^{k_3} \quad (2.3)$$

Where k_1, k_2, k_3, k_6, and k_7 are constants, p_a is atmospheric pressure (101.4 kPa), τ_{oct} is octahedral shear stress, and θ is bulk stress. Using the data collected, a summary resilient modulus (SRM) was determined at θ = 208 kPa and τ_{oct} = 48.6 kPa.

The Power function (Eq. 2.2) is a simple model widely used for granular material. The estimated SRM per the Power function model was compared to the measured modulus. Statistical analysis indicated that results from the Power function model are significant at a 95% confidence level, and the model represents the data reasonably well for RCA (R^2 = 0.85) and for RAP (R^2 = 0.90) (Bozyurt 2011).

2.5 RESULTS AND DISCUSSION

2.5.1 Compaction Characteristics of RCB/RCA Mixtures

Compaction tests conducted on TX RCA, MN RCA, and OH RCA with 30% RCB resulted in an increase in OMC and decrease in maximum dry unit weight when compared to the 0% RCB compaction tests (Table 2.3 and Figure 2.4a, b, and c). The

results for the RCA mixed with 30% RCB do not reflect parabolic curves as well as the 0% RCB material. The curves do not descend for any of the 30% RCB material, but stay very constant at OMC. This was caused by excessive drainage of water during compaction, reducing the moisture content in the middle of the compacted specimen and keeping a constant density. Regardless of the amount of water added to create a specimen above OMC, water is drained to the OMC of the material in the center of the compacted specimen. This could be viewed as a potential attribute of using RCB/RCA mixtures because the material cannot retain more than the optimum moisture content, so the hydraulic conductivity is quite high. This also could be viewed in the negative realm because of the increased OMC requiring more water to be added to achieve compaction requirements. Additional tests to determine the hydraulic conductivity of the mixture is recommended to further explain the compaction characteristics.

These compaction results are similar to the Poon and Chan (2006) results, which tested brick and RCA at 0%, 25%, and 50% brick. Similar conjectures can be made as Poon and Chan (2006) did as to the reasoning for this increase in OMC and decrease in maximum dry unit weight. Lower specific gravity of RCB compared to RCA can cause a decrease in maximum dry unit weight. The lower specific gravity in the RCB compared to the RCA is likely due to the increased air voids within the particles of RCB. This increased void space in RCB was also indicated by the RCB's 11.5% absorption, more than double the absorption of three of the four RCAs used. Higher absorption can also lead to the increase in OMC observed in compaction testing (Poon and Chan 2006).

2.5.2 Summary Resilient Modulus of RCB/RCA Mixtures

The SRM results fitted with the NCHRP and Power models for both the internal and external LVDTs are displayed in Table 2.4 and Figure 2.5a and Figure 2.5b. Table 2.5 and Table 2.6 display the fitting parameters for the NCHRP and Power models, respectively. Table 2.7 shows the coefficients of variations in SRM for the natural aggregates and RCAs, which were available in high enough quantities to allow for replicate M_r tests to be performed. TX RCA is the only recycled material used in this study, for which a coefficient of variation could be calculated. The coefficient of variation for TX RCA for external SRM is 19%, much higher than any changes in the data from 0% to 30% brick (< 7%), indicating that for TX RCA there is no impact on SRM with increasing brick content up to 30%. For the other three RCAs tested there was not enough material for replicates to be performed so a statistical analysis could not be performed to determine the extent of variation in SRM for replicates.

To evaluate the extent of variation for the remaining RCAs (NJ, OH, and MN) without the coefficient of variation, trends in external SRM were analyzed. For NJ RCA, the decrease in SRM from 0% RCB to 30% RCB was 7%. The SRM as reported for NJ RCA increased 12% from 0% to 10%, and then showed a gradual decreasing trend from 10% to 30% RCB. OH RCA's SRM decreased 20% from 0% RCB to 30% RCB and had an overall decreasing trend of SRM with increasing brick content. MN RCA decreased 3% from 0% RCB to 30% RCB. For all four RCAs tested, only one showed a noticeable (> 7%) decrease in SRM from 0% RCB to 30% RCB. All materials had similar, if not better, SRM than the natural aggregates tested in the first chapter of this thesis. With only one of the four RCAs having a noticeable change (SRM decrease of

20%) in SRM with increasing RCB content, there appears to be little effect of RCB content on the SRM of RCA up to 30% RCB.

The result of little trend in SRM with increasing RCB content up to 30% is similar to the results of the only previous study completed on resilient modulus of RCB/RCA mixtures by Cameron et al. (2012). Cameron et al. (2012) observed a marginal decrease (< 80 MPa) in resilient modulus with increased RCB content (0% to 30% RCB), which could be within the error for that specific test but no information is noted on error in the study. Cameron et al. (2012) used a different method (i.e., AUSTROADS method) that uses approximately 50,000 cycles, whereas the NCHRP method only uses about 4,000 cycles. In addition, the study completed by Cameron et al. (2012) was more focused towards evaluating resilient modulus of RCB/RCA mixtures at varying water content (60% to 100% OMC) than the SRM of RCB/RCA mixtures at OMC and found that lower (80% OMC) water contents was more favorable for stiffness of RCB/RCA blends. This finding was similar to the study by Arulrajah et al. (2011) which evaluated 25% RCB/75% RCA mixtures and found that 65% OMC was the highest water content RCB/RCA could be mixed at to be a viable material for road subbase applications. Arulrajah et al. (2011) used the same resilient modulus testing method as Cameron et al. (2012). This testing method change between this study and Arulrajah et al. (2011) and Cameron et al. (2012); and the lack of reporting SRM in the other two studies could both contribute to the different trend results observed. Both studies found that resilient modulus and permanent strain were marginal factors with RCB/RCA mixtures compared to moisture content and density changing the design.

The difference in material between this study and the studies by Arulrajah et al. (2011) and Cameron et al. (2012) may contribute to the difference in resilient modulus observed. This study used clay brick as the material tested, whereas neither Arulrajah nor Cameron state the type of brick used. A fly ash based brick or cement based brick could tremendously alter the physical characteristics of the RCB. The RCB used in this study had higher absorption values (11.5% compared to ~6.5%) than the RCB used in both Arulrajah et al. (2011) and Cameron et al. (2012). The particle dry unit weight of the RCB in this study was also lower (19.3 kN/m^3 compared to 26.2 kN/m^3) than that of Arulrajah et al (2011) (Cameron et al. 2012 did not report a dry unit weight of RCB alone). Both of these large differences in physical characteristics of the RCB between this study and the other two studies could explain the noticeable trend change in resilient modulus with increased RCB content.

2.5.3 Plastic Strain of RCB/RCA Mixtures

Plastic strains were calculated as an index using the data from the M_r tests and presented in Table 2.9 and Table 2.10 for the 1st load sequence and 2nd through 31st load sequences, respectively. There were no apparent trends in plastic strain observed from the data for the first sequence (conditioning phase) or last 30 sequences. All data suggests very little change in accumulation of plastic strain in all specimens regardless of RCB content, suggesting RCB has little impact on stiffness of RCA when mixed at or below 30% RCB. Cameron et al (2012) evaluated plastic strain and found that marginal (< 0.7%) changes were observed between 0% RCB and 30% RCB/RCA mixtures. It is recommended that tests designed specifically for plastic strain be completed if further analysis is wanted on plastic strain of the specific materials used in this study. The

resilient modulus test (NCHRP 1-28a) used in this study are not designed for calculating plastic strain accurately.

2.5.4 Weathering and Abrasion Resistance of RCB/RCA Mixtures

The results of the LA Abrasion tests conducted on MN RCA, Class 5, and RCB from literature can be seen in Table A.5. RCB appears to be less tough and less resistant to abrasion than both Class 5 and MN RCA. This is most likely due to the clay-based nature of the RCB, which depending on the source of the clay and the original firing temperature the clay brick was created at, could have lower bond strength than concrete and natural aggregates (Amrhein 1998). The variability in manufacturing of the clay brick directly impacts the weathering and strength of the RCB and the manufacturing specifications for the brick used in this study and Arulrajah et al. (2011) and Cameron et al. (2012) are unknown. Further weathering tests (i.e. freeze-thaw, wet/dry, and Micro-Deval) are recommended to determine the impact weathering has on RCB.

2.6 CONCLUSIONS

The amount of deleterious material present in RCA and RAP/RPM varied depending on source of the material. Generally, asphalt aggregate, aggregate with plastic fibers, and wood chips were the most predominant type of impurities for RCA. The average impurity content was 1% for RCAs obtained from different states (CO, OH, TX, MN, CA, MI, WI, and NJ). Geotextiles and pavement markings were the predominant type of impurities for RAP/RPM. The average impurity amount was 2% for all RAP/RPM samples from different states (CO, OH, TX, MN, CA, MI, WI, and NJ).

Due to the general lack of deleterious materials found in recycled materials, possibility for beneficial reuse and lack of research on its use, brick was chosen to be investigated further using resilient modulus at 0%, 10%, 20%, and 30% by mass with RCA. Brick acquired from a demolition site was crushed and sieved to match particle size distributions of each of the four RCAs it was mixed with. The four RCAs used were NJ, OH, MN, and TX. Compaction tests were completed at 0% and 30% RCB on all RCA materials except NJ RCA because of lack of material available. When 30% RCB compaction characteristics were compared to 0% RCB, OMC increased while maximum dry unit weight decreased. This was attributed to RCB having higher absorption and lower specific gravity and dry unit weight than RCA. The compaction curves for the 30% RCB mixtures did not decrease in maximum dry unit weight above OMC because water drained out of the molds not allowing for a water content above OMC to be achieved. This lack of decrease was observed in all three RCB/RCA mixtures tested at 30% RCB.

Resilient modulus tests were completed on the four RCA samples at 0%, 10%, 20%, and 30% RCB content. Each specimen was compacted at OMC and 95% of maximum dry density of the RCA it was compacted with. No apparent trends in SRM were observed at any RCB content for three of the four RCAs. OH RCA exhibited a 20% decrease in SRM from 0% to 30% RCB, but without a coefficient of variation to determine the error for replicate RCA tests it is hard to assess this trend. All RCAs tested at 30% RCB had similar, if not higher, SRM than natural aggregate tested for comparison. This lack of decreasing trend was not seen by previous studies, but difference in materials tested and methods used to test for resilient modulus could

contribute to this difference in results. Further testing at higher RCB content is recommended to determine an exact limit to the amount of RCB that can be added to RCA or other aggregates for beneficial reuse. It is also recommended that further testing be completed to evaluate the hydraulic conductivity, effects of weathering (i.e., freeze-thaw and wet-dry), and abrasion resistance (i.e., micro-deval) of the RCB/RCA mixtures.

2.7 TABLES

Table 2.1Index Properties for Recycled Materials and Class 5 Aggregate

Material	States	D_{10} (mm)	D_{30} (mm)	D_{50} (mm)	D_{60} (mm)	C_u	C_c	G_s	Dry Unit Weight (kN/m^3)	Absorption (%)	Asphalt Content (%)	Impurities (%)	Gravel (%)	Sand (%)	Fines (%)	USCS	AASHTO
Class 5	MN	0.1	0.4	1.0	1.7	21	1.4	2.57	25.11	_	_	0.25	22.9	67.6	9.5	GW-GM	A-1-b
Blend	MN	0.2	0.6	1.5	2.8	13	0.5	_		_	_	0.36	32.7	63.8	3.4	SP	A-1-b
RCA	MN	0.1	0.4	1.0	1.7	21	1.4	2.39	23.34	5.0	_	0.87	31.8	64.9	3.3	SW	A-1-a
	MI	0.4	4.1	9.7	12.3	35	3.9	2.37	23.16	5.4	_	0.35	68.5	28.3	3.2	GP	A-1-a
	CO	0.1	0.6	2.8	4.9	66	1.1	2.28	22.3	5.8	_	0.26	40.9	46.3	12.8	SC	A-1-b
	CA	0.3	1.7	4.8	6.8	22	1.4	2.32	22.74	5.0	_	0.26	50.6	47.1	2.3	GW	A-1-a
	TX	0.4	6.5	13.3	16.3	38	6.0	2.27	22.22	5.5	_	0.86	76.3	21.6	2.1	GW	A-1-a
	OH	0.2	1.2	3.4	5.3	34	1.7	2.24	21.95	6.5	_	0.16	43.2	49.5	7.3	SW-SM	A-1-a
	NJ	0.2	0.5	2.0	5.1	28	0.3	2.31	22.64	5.4	_	1.67	41.2	54.6	4.3	SP	A-1-b
RAP	MN	0.3	0.7	1.6	2.3	7	0.7	2.41	23.54	1.8	7.1	0.06	26.3	71.2	2.5	SP	A-1-a
	CO	0.4	0.9	2.2	3.3	9	0.7	2.23	21.8	3.0	5.9	0.09	31.7	67.7	0.7	SP	A-1-a
	CA	0.3	1.3	3.0	4.2	13	1.2	2.56	18.31	2.0	5.7	0.33	36.8	61.4	1.8	SW	A-1-a
	TX	0.7	2.5	5.4	7.9	11	1.1	2.34	22.86	1.3	4.7	0.05	41.0	44.9	1.0	SW	A-1-a
	OH	0.5	1.6	2.9	3.8	7	1.3	2.43	23.73	0.6	6.2	0.06	32.1	66.2	1.7	SW	A-1-a
	NJ	1.0	2.8	4.9	5.9	6	1.3	2.37	23.17	2.1	5.2	0.48	50.9	48.4	0.7	GW	A-1-a
	WI	0.6	1.4	2.7	3.6	6	0.9	2.37	23.22	1.5	6.2	0.08	30.9	68.5	0.5	SP	A-1-b
RPM	NJ	0.5	2.1	5.8	8.7	18	1.0	2.35	23.42	2.6	4.3	0.04	55.7	43.6	0.6	GW	A-1-b
	MI	0.4	1.7	4.6	6.5	17	1.1	2.39	23.00	1.7	5.3	0.13	49.3	50.4	0.4	SW	A-1-b
RCB	WI	NA	NA	NA	NA	NA	NA	2.20	19.33	11.5	_	NA	NA	NA	NA	NA	NA

C_u = coefficient of uniformity, C_c = coefficient of curvature, G_s= Specific Gravity, AC= Asphalt Content, Abs=Absorption, Note: Particle size analysis conducted following ASTM D 422, G_s determined by ASTM D 854, Absorption of coarse aggregate were determined by ASTM C127-07, USCS classification determined by ASTM D 2487, AASHTO classification determined by ASTM D 3282, asphalt content determined by ASTM D 6307

Table 2.2 Quality Control of Specimen Preparation

	Brick Content of Material	ω_{opt}	$\omega_{compacted}$	Percent ω Difference	Std. Dev. (Percent ω Difference)	Mass after Compaction Goal (kg)	Mass after Compaction (kg)	Percent Mass Difference	Std. Dev. (Percent Mass Difference)	*95% Dry Unit Weight (kN/m^3)*	Dry Unit Weight of Compacted Material (kN/m^3)	Dry Unit Weight Difference	Std. Dev. (Dry Unit Weight Difference)
MN RCA	0%	11.20%	11.70%	0.50%	0.10%	11.68	11.6	0.68%	0.57%	18.53	18.32	1.15%	0.23%
	10%	11.20%	11.50%	0.30%		11.68	11.85	1.46%		18.53	18.75	1.16%	
	20%	11.20%	11.60%	0.40%		11.68	11.9	1.88%		18.53	18.81	1.50%	
	30%	11.20%	11.50%	0.30%		11.68	11.9	1.88%		18.53	18.82	1.59%	
TX RCA	0%	9.20%	9.60%	0.40%	0.10%	11.56	11.55	0.09%	0.22%	18.68	18.59	0.50%	0.26%
	10%	9.20%	9.50%	0.30%		11.56	11.5	0.52%		18.68	18.52	0.84%	
	20%	9.20%	9.00%	0.20%		11.56	11.5	0.52%		18.68	18.61	0.38%	
	30%	9.20%	9.60%	0.40%		11.56	11.5	0.52%		18.68	18.51	0.93%	
NJ RCA	0%	9.50%	9.80%	0.30%	0.06%	11.65	11.6	0.43%	0.73%	18.76	18.63	0.67%	0.50%
	10%	9.50%	9.30%	0.20%		11.65	11.45	1.72%		18.76	18.48	1.51%	
	20%	9.50%	9.70%	0.20%		11.65	11.5	1.29%		18.76	18.49	1.44%	
	30%	9.50%	9.20%	0.30%		11.65	11.4	2.15%		18.76	18.41	1.85%	
OH RCA	0%	11.80%	12.10%	0.30%	0.05%	11.66	11.55	0.94%	0.54%	18.39	18.17	1.18%	0.57%
	10%	11.80%	12.10%	0.30%		11.66	11.45	1.80%		18.39	18.02	2.04%	
	20%	11.80%	12.10%	0.30%		11.66	11.45	1.80%		18.39	18.02	2.04%	
	30%	11.80%	12.20%	0.40%		11.66	11.4	2.23%		18.39	17.92	2.55%	

Note: ω_{opt} = Optimum moisture content; $\omega_{compacted}$ = Compacted moisture content; ω Standard Deviation = Variability in percent moisture content difference ; Std. Dev. = Standard Deviation

Table 2.3 Maximum Dry Unit Weight and Optimum Moisture Content Changes with Varying Brick Content

Material	**Percent Brick**	**Max Dry Unit Weight (KN/m^3)**	**ω_{opt}**
TX RCA	0	19.7	9.20%
	30	18.44	11.70%
MN RCA	0	19.5	11.20%
	30	18.6	11.80%
OH RCA	0	19.8	11.80%
	30	17.52	12.40%

Table 2.4 External and Internal LVDT Summary Resilient Modulus Values at Varying Brick Content Calculated using NCHRP and Power Function Models

		SRM (MPa)			
		OH RCA	**TX RCA**	**NJ RCA**	**MN RCA**
0% Brick	Int NCHRP	233	172	157	134
	Int Power	254	197	200	176
	Ext NCHRP	149	130	85	109
	Ext Power	166	142	130	128
10% Brick	Int NCHRP	188	197	178	166
	Int Power	217	237	208	200
	Ext NCHRP	141	125	130	115
	Ext Power	162	139	152	132
20% Brick	Int NCHRP	173	233	170	147
	Int Power	201	277	199	171
	Ext NCHRP	111	127	123	97
	Ext Power	128	145	140	107
30% Brick	Int NCHRP	156	168	162	112
	Int Power	166	200	193	133
	Ext NCHRP	122	123	106	107
	Ext Power	142	145	120	125

Note: Bulk Stress = 208 kPa, Octahedral Stress = 48.6 kPa

Table 2.5 NCHRP Fitting Parameters and Summary Resilient Modulus (SRM) Values

Material	Brick %	Internal						External						SRM_{int}/SRM_{ext}
		k_1	k_2	k_3	k_6	k_7	SRM (MPA)	k_1	k_2	k_3	k_6	k_7	SRM (MPA)	
OH RCA	0	3.9	3.3	-1.5	-205.8	1.1	233	1.8	4.3	-2.8	-377.1	4.0	149	1.56
	10	4.9	3.7	-2.2	-241.0	2.2	188	9.6	3.4	-2.1	-253.6	2.9	141	1.33
	20	0.4	6.7	-5.5	-565.1	7.1	173	16.7	2.9	-1.7	-189.5	2.2	111	1.56
	30	0.1	4.3	-1.9	-418.7	2.1	156	8.5	3.9	-2.9	-286.1	3.8	122	1.28
TX RCA	0	2.6	3.2	-1.2	-229.1	1	172	3.7	3.7	-2.3	-381.3	4.8	130	1.32
	10	5.0	3.7	-2.3	-230.5	2.2	197	4.4	3.9	-2.6	-321.8	4.2	125	1.58
	20	2.0	4.1	-2.5	-290.3	2.5	233	13.9	2.7	-1.4	-192.9	1.7	127	1.83
	30	0.3	5.9	-4.2	-416.4	5.3	168	13.1	3.1	-1.9	-199.5	2.2	123	1.37
NJ RCA	0	0.1	7.1	-5.5	-531.6	6.2	157	1.5	3.5	-1.7	-319.4	3.3	85	1.85
	10	0.4	5.0	-3.2	-395.0	3.8	178	23.6	3.4	-2.6	-242.8	3.4	130	1.37
	20	5.0	3.8	-2.5	-271.4	2.9	170	12.0	3.6	-2.7	-295.4	4.0	123	1.38
	30	0.003	7.6	-5.2	-586.8	5.7	162	19.7	2.7	-1.5	-196.4	2.4	106	1.53
MN RCA	0	824.0	1.29	-1.2	0.0	1.0	134	7.3	3.9	-2.8	-256.4	3.4	109	1.23
	10	6.0	4.6	-3.7	-302.9	4.1	166	6.3	4.2	-3.2	-324.8	4.5	115	1.44
	20	22.3	3.8	-3.0	-245.7	3.7	147	6.5	3.3	-2.4	-296.3	4.2	97	1.52
	30	284	1.6	-0.9	-32.9	1.0	112	10.7	3.8	-2.8	-257.9	3.7	107	1.05

Note: Due to rounding of fitting parameters for this table, SRM values calculated using the fitting parameters above will vary slightly from the actual SRM values reported above.

Table 2.6 Power Model Fitting Parameters and SRM Values

Material	Brick %	Internal			External			SRM_{int}/SRM_{ext}
		k_1	k_2	SRM (MPA)	k_1	k_2	SRM (MPA)	
OH RCA	0	20,000.00	0.48	254	16,064.50	0.44	166	1.53
	10	20,146.20	0.44	217	12,438.70	0.48	162	1.34
	20	20,000.00	0.43	201	7,601.40	0.53	128	1.57
	30	12,951.30	0.48	166	11,000.20	0.48	142	1.17
TX RCA	0	15,201.60	0.48	197	10,334.30	0.49	142	1.39
	10	17,887.80	0.48	237	7,868.20	0.54	139	1.71
	20	28,302.00	0.43	277	11,745.00	0.47	145	1.91
	30	7,208.50	0.62	200	10,279.90	0.5	145	1.38
NJ RCA	0	11,755.20	0.51	181	4,429.00	0.57	93	1.95
	10	18,648.40	0.45	208	13,870.90	0.45	152	1.37
	20	17,344.40	0.46	199	11,596.80	0.47	140	1.42
	30	16,098.30	0.47	193	7,471.40	0.52	120	1.61
MN RCA	0	14,631.30	0.47	176	7,311.30	0.54	128	1.38
	10	14,335.60	0.49	200	9,489.20	0.49	132	1.52
	20	10,533.70	0.52	171	5,048.90	0.57	107	1.60
	30	4,995.50	0.61	133	7,348.70	0.53	125	1.06

Note: Due to rounding of fitting parameters for this table, SRM values calculated using the fitting parameters above will vary slightly from the actual SRM values reported above.

Table 2.7 Internal and External SRM Statistical Analysis on Replicate Specimens Prepared by Shedivy

		Internal LVDT Data				External LVDT Data			
Material	**M_r Tester**	**NCHRP SRM (MPa)**	**Average (MPa)**	**σ (MPa)**	**C_v**	**NCHRP SRM (Mpa)**	**Average (MPa)**	**σ (MPa)**	**C_v**
Class 5	Shedivy	123	154	36	23%	91	113	19	17%
	Shedivy	115				100			
	Shedivy	129				97			
Basalt	Shedivy	180	197	28	14%	131	130	8	7%
	Shedivy	192				121			
	Shedivy	187				135			
CA RCA	Shedivy	181	197	33	17%	121	123	17	14%
	Shedivy	246				140			
TX RCA	Shedivy	188	180	11	6%	99	115	22	19%
	Shedivy	172				130			

Note: Average is the mean, σ is the standard deviation, and C_v is the coefficient of variation

Table 2.8 1st Load Sequence Deformation and Plastic Strain

		1st Load Sequence Deformation and Plastic Strain			
		OH RCA	**TX RCA**	**NJ RCA**	**MN RCA**
0% Brick	Int Deformation (mm)	0.2	0.2	0.3	0.7
	Int Plastic Strain (%)	0.10%	0.10%	0.20%	0.40%
	Ext Deformation (mm)	0.7	0.9	1.2	1.7
	Ext Plastic Strain (%)	0.30%	0.30%	0.40%	0.60%
10% Brick	Int Deformation (mm)	0.1	0.2	0.2	0.4
	Int Plastic Strain (%)	0.10%	0.10%	0.10%	0.30%
	Ext Deformation (mm)	0.6	2.3	1.1	1.3
	Ext Plastic Strain (%)	0.20%	0.80%	0.40%	0.40%
20% Brick	Int Deformation (mm)	0.3	0.1	0.2	0.4
	Int Plastic Strain (%)	0.20%	0.10%	0.20%	0.30%
	Ext Deformation (mm)	1	1	0.9	1.7
	Ext Plastic Strain (%)	0.30%	0.30%	0.30%	0.60%
30% Brick	Int Deformation (mm)	0.2	0.3	0.2	0.5
	Int Plastic Strain (%)	0.10%	0.20%	0.10%	0.30%
	Ext Deformation (mm)	1	1	1.3	1.5
	Ext Plastic Strain (%)	0.30%	0.30%	0.40%	0.50%

Table 2.9 2nd-31st Load Sequence Deformation and Plastic Strain

		2nd-31st Load Sequence Deformation and Plastic Strain			
		OH RCA	**TX RCA**	**NJ RCA**	**MN RCA**
0% Brick	Int Deformation (mm)	2.1	2.9	8.8	9.3
	Int Plastic Strain (%)	1.40%	1.90%	5.80%	6.10%
	Ext Deformation (mm)	4.6	5.6	16.8	16.1
	Ext Plastic Strain (%)	1.50%	1.80%	5.50%	5.30%
10% Brick	Int Deformation (mm)	1.4	1.4	3.8	6.9
	Int Plastic Strain (%)	0.90%	0.90%	2.50%	4.50%
	Ext Deformation (mm)	3.5	4.8	7.3	13
	Ext Plastic Strain (%)	1.20%	1.60%	2.40%	4.30%
20% Brick	Int Deformation (mm)	2.4	1.6	3.1	5.6
	Int Plastic Strain (%)	1.60%	1.10%	2.00%	3.70%
	Ext Deformation (mm)	5	5	6.5	10.3
	Ext Plastic Strain (%)	1.70%	1.65%	2.10%	3.40%
30% Brick	Int Deformation (mm)	2.9	1.8	3	4.2
	Int Plastic Strain (%)	1.90%	1.20%	2.00%	2.80%
	Ext Deformation (mm)	5.4	4.1	5.9	8.3
	Ext Plastic Strain (%)	1.80%	1.40%	2.00%	2.70%

2.8 FIGURES

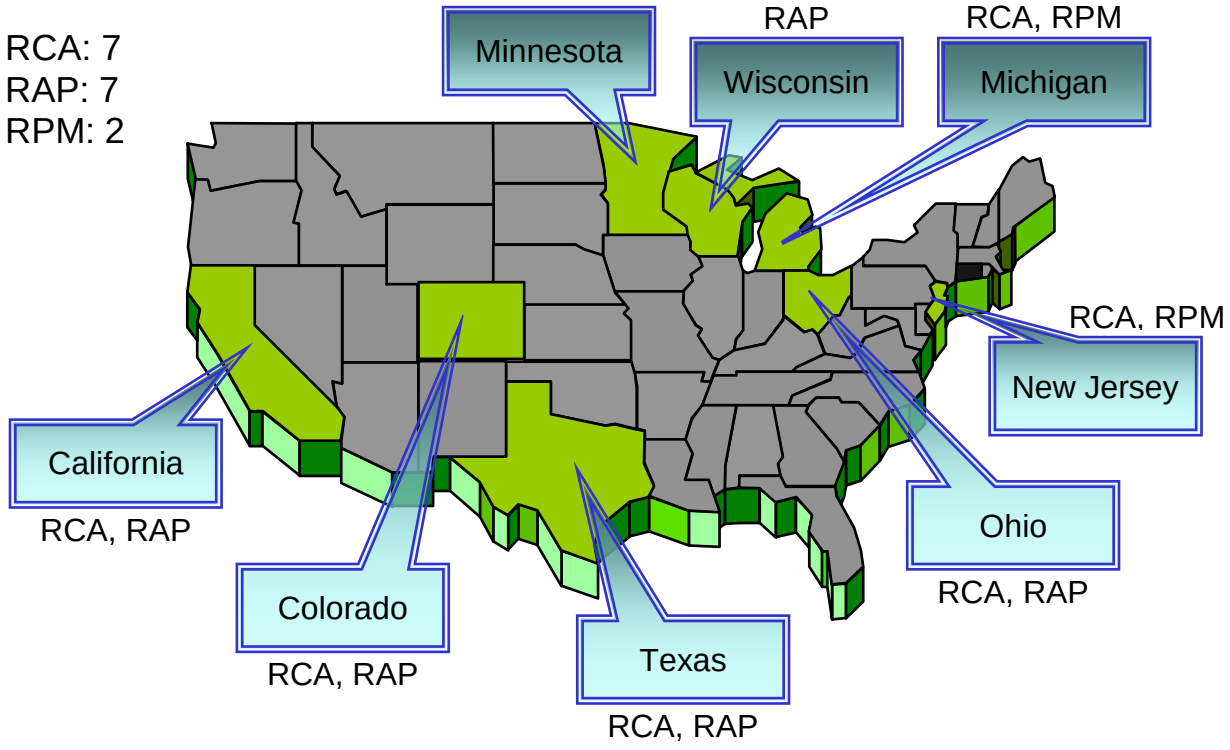

Figure 2.1 Locations of Recycled Material used in this Study

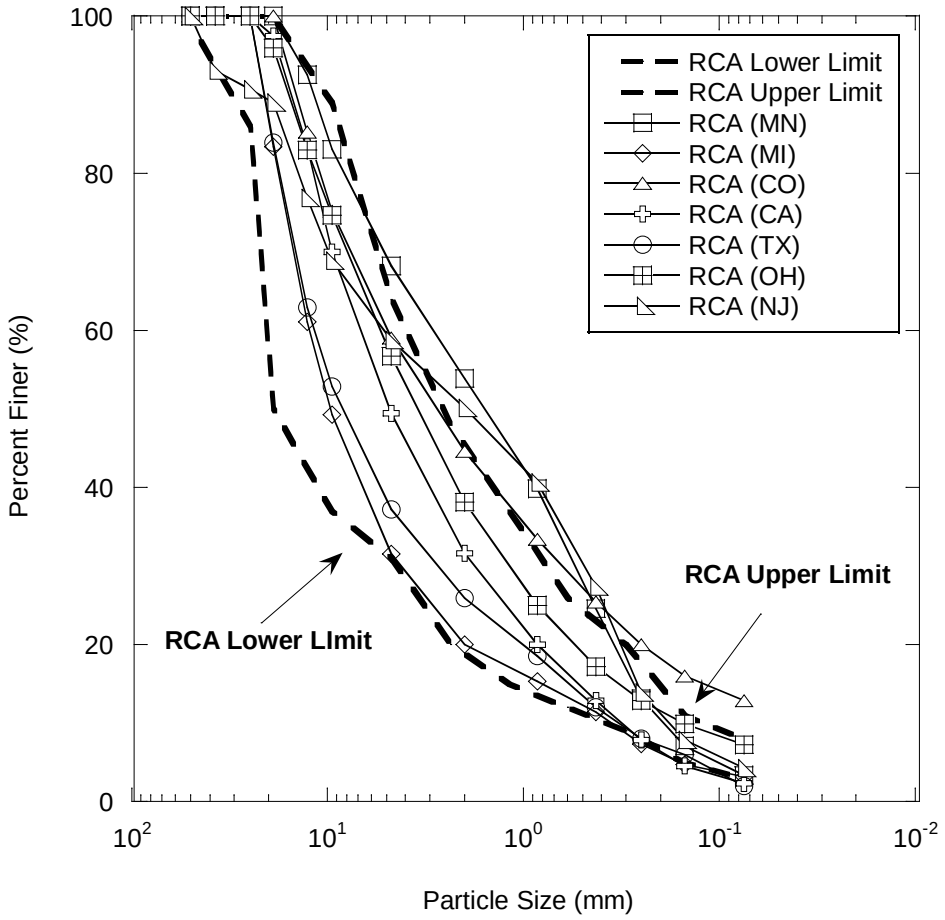

Figure 2.2 Particle Size Distribution for RCA and RCAs reported Lower and Upper Limits from Literature

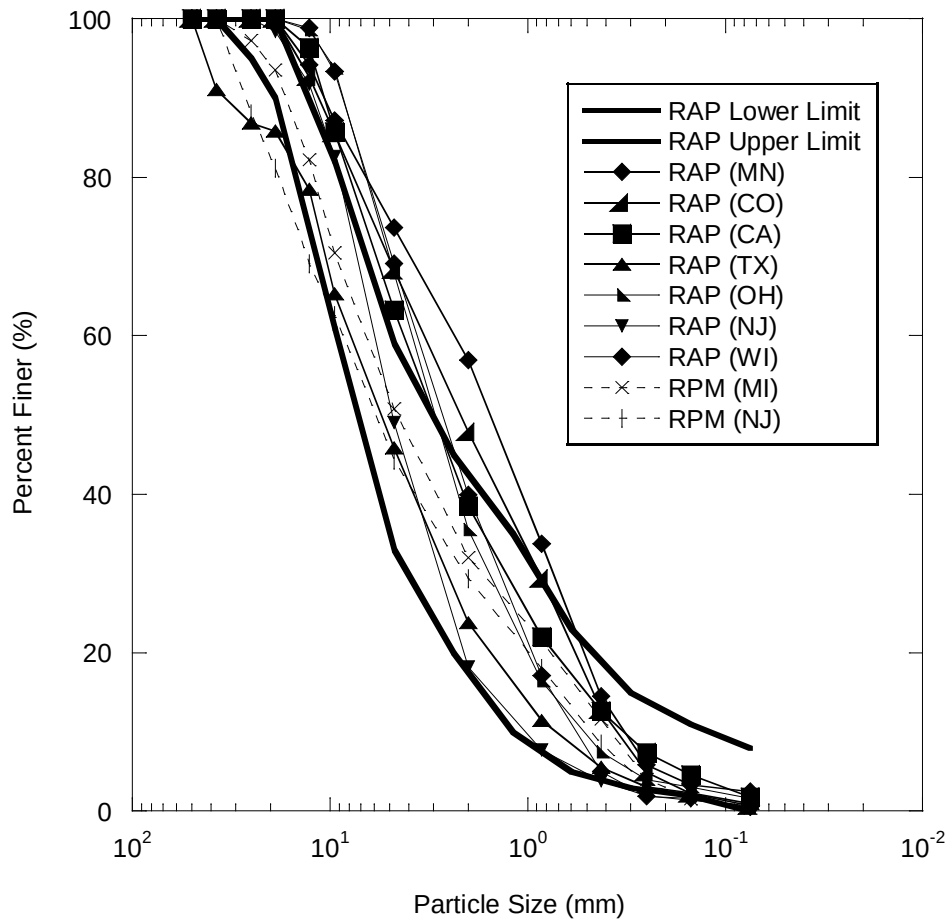

Figure 2.3 Particle Size Distribution for RAP/RPM and RAPs reported Lower and Upper Limits from Literature

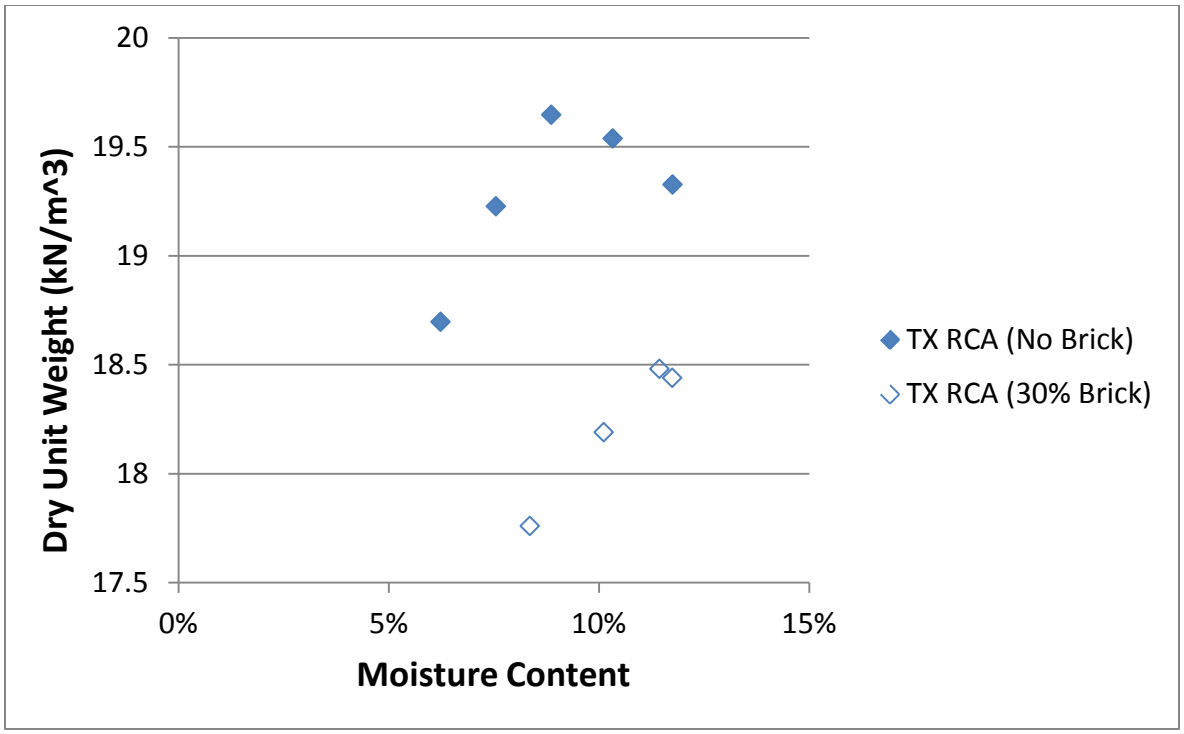

Figure 2.4a TX RCA Compaction Data at 0% Brick and 30% Brick

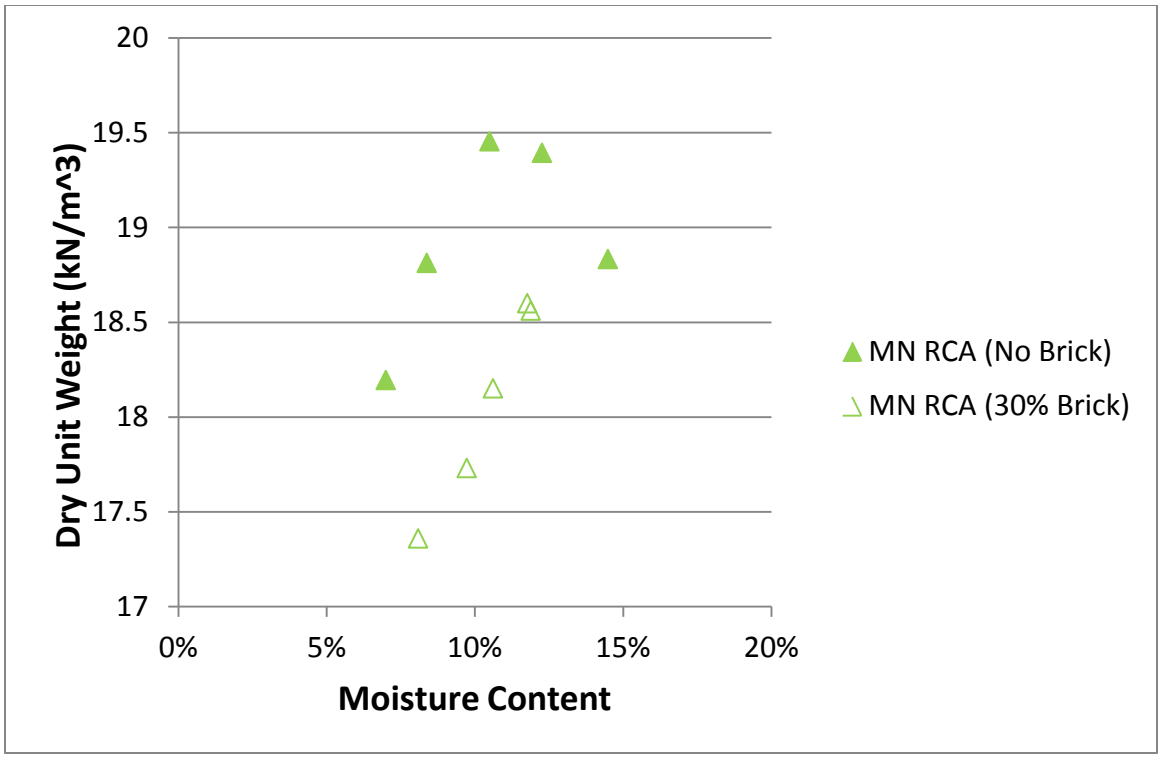

Figure 2.4b MN RCA Compaction Data at 0% Brick and 30% Brick

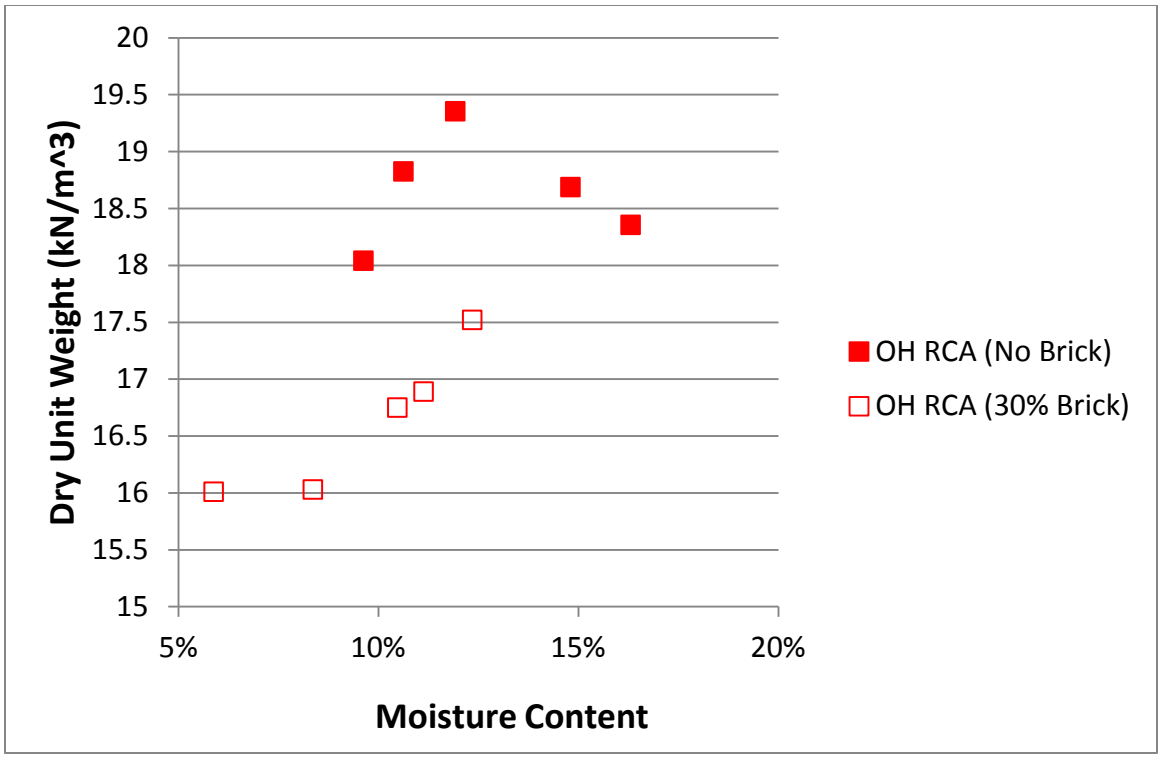

Figure 2.4C OH RCA Compaction Data at 0% Brick and 30% Brick

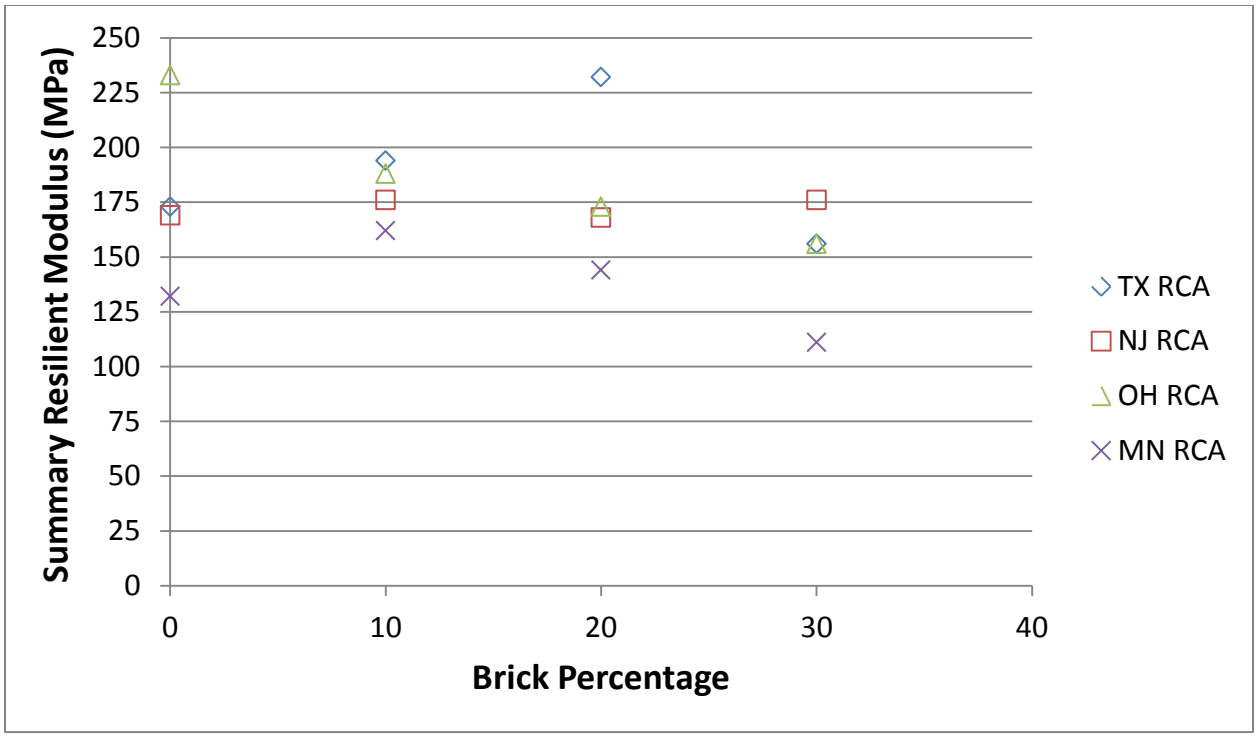

Figure 2.5a Internal LVDT Recorded SRM (NCHRP) at Varying Brick Contents

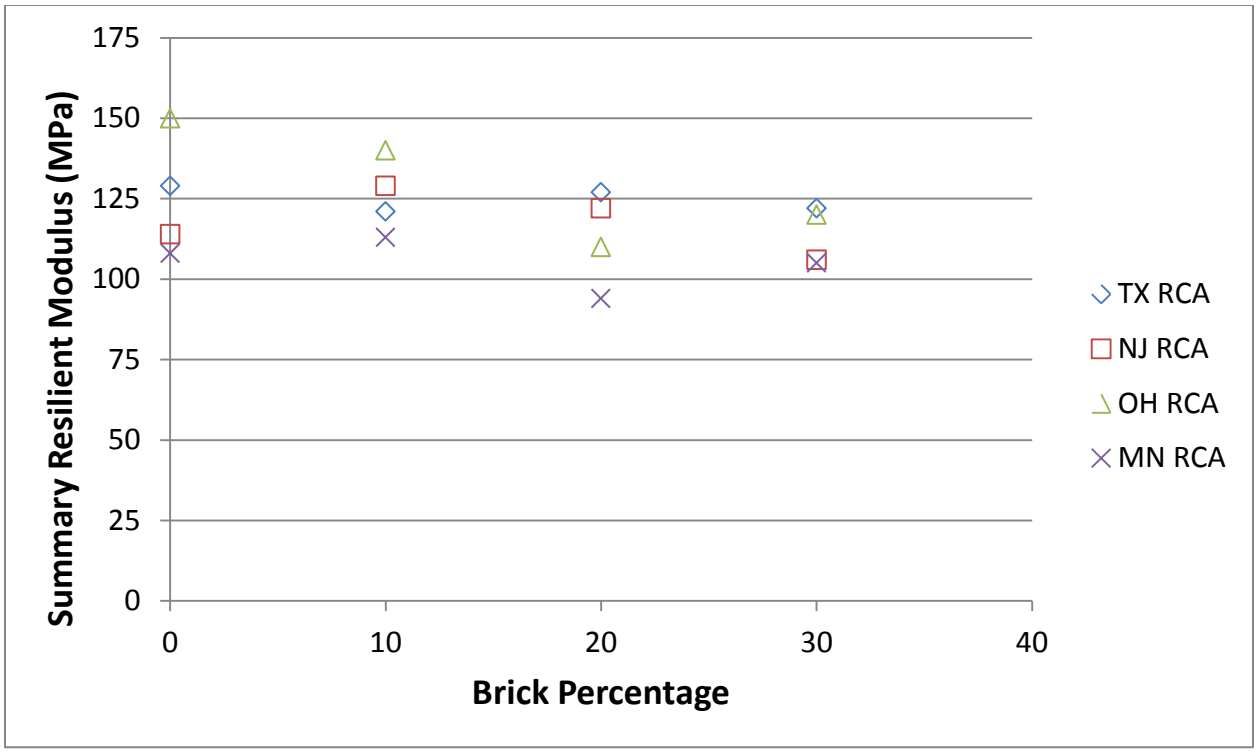

Figure 2.5b External LVDT Recorded SRM (NCHRP) at Varying Brick Content

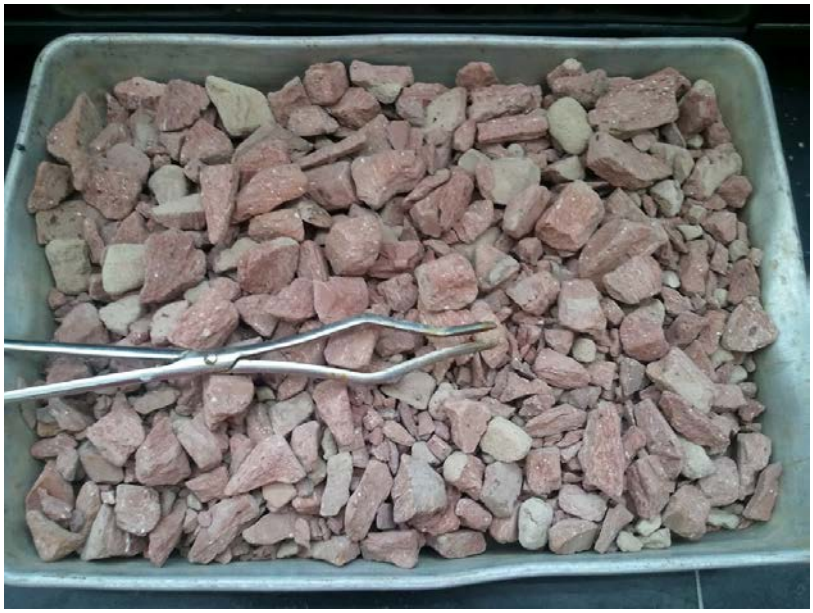

Figure 2.6 Crushing Brick and Final Product

Figure 2.7 0%, 10%, 20%, and 30% RCB with MN RCA at OMC

Figure 2.8 10%, 20%, and 30% RCB with NJ RCA at OMC

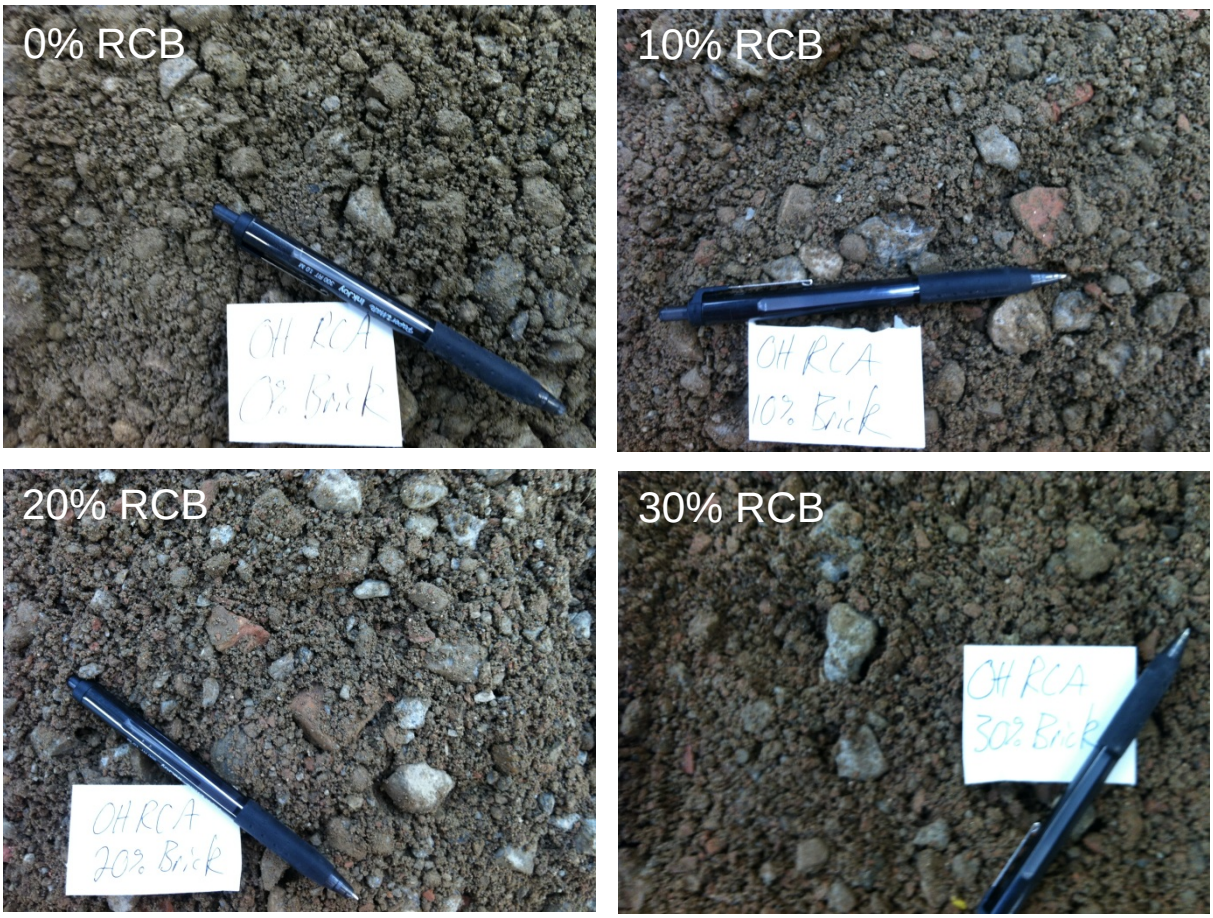

Figure 2.9 0%, 10%, 20%, and 30% RCB with OH RCA at OMC

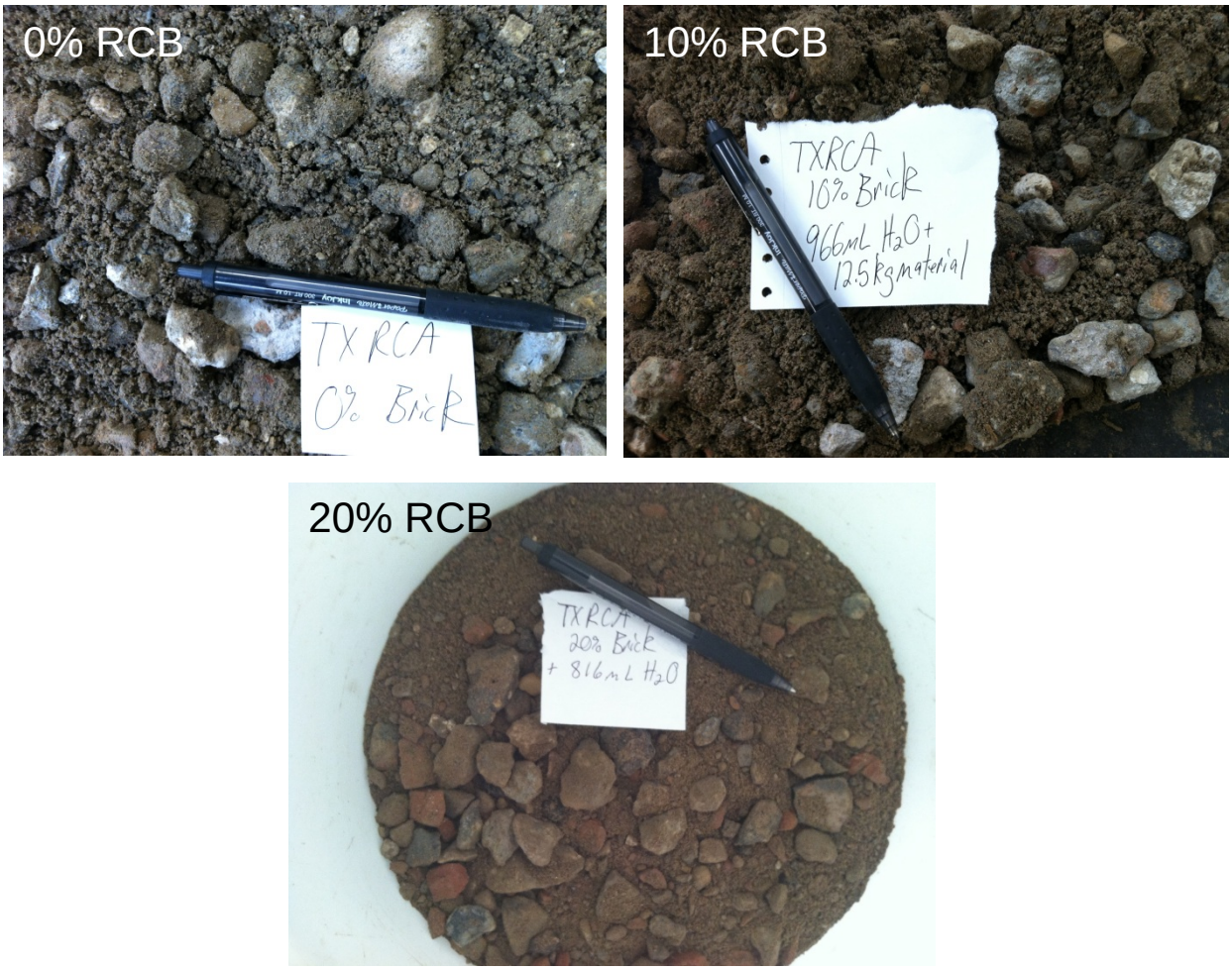

Figure 2.10 0%, 10%, and 20%, RCB with TX RCA at OMC

Figure 2.11 30% RCB with MN RCA Compacted for Resilient Modulus Test

3. REFERENCES

AASHTO. (2002). Standard Specification for Reclaimed Concrete Aggregate for Unbound Soil-Aggregate Base Course. In *American Association of State Highway and Transportation Officials*

AASHTO. (2009). "Standard Method of Test for Resistance of Coarse Aggregate to Degradation by Abrasion in the Micro-Deval Apparatus." Washington, D.C.

ACPA. *Recycling Concrete Pavements*. American Concrete Pavement Association, 2009.

Amrhein, J.E. (1998). "Reinforced Masonry Engineering Handbook: Clay and Concrete Masonry." 5th Edition. CRC Press, Boca Raton, NY.

ARA. *Guide for Mechanistic-Emprical Design on New and Rehabilitated Pavement Structures.* Publication NCHRP Project 1-37A, NCHRP, 2004.

Arm, M. "Self-cementing Properties of Crushed Demolished Concrete in Unbound Layers: Results from Triaxial Tests and Field Tests." *Waste Management*, Vol. 21, No.3, 2001, pp. 235-239.

Arulrajah. A., Piratheepan, J., Aatheesan, T., and Bo, M.W. (2011). "Geotechnical Properties of Recycled Crushed Brick in Pavement Applications." *Journal of Materials in Civil Engineering*, Vol. 23, No. 10, 1444-1452.

ASTM. (2003). "Standard Test Methods for Wetting and Drying Compacted Soil-Cement Mixtures." West Conshohocken, PA.

ASTM. (2007). "Standard Test Method for Particle-Size Analysis of Soils." West Conshohocken, PA.

Attia, M., and Abdelrahman, M. (2010) "Modeling the Effect of Moisture on Resilient Modulus of Untreated Reclaimed Asphalt Pavement." In *Transportation Research Record: Journal of the Transportation Research Board*, No. 2167, Transportation Research Board of the National Accademies, Washington, D.C., pp. 30-40.

Ba, M., Fall, M., Samb, F., Sarr, D., and Ndiaye, M. (2011). "Resilient Modulus of Unbound Aggregate Base Courses from Senegal (West Africa)." *Open Journal of Civil Engineering*, 1, 1-6.

Barksdale, R. D., and Itani S.Y. (1989) "Influence of Aggregate Shape on Base Behavior." *Transportation Research Record*, No.1227, Transportation Research Board of the National Accademies, Washington, D.C., pp. 173-182.

Bejarano, M.O, Harvey, J.T., and Lane, L. (2003). "In-Situ Recycling of Asphalt Concrete as Base Material in California." *Proc. 82nd Annual Meeting, Transportation Research Board*, Washigton, D.C, pp. 22.

Bennert, T., Papp, W.J., Jr., Maher A., and Gucunski, N. (2000). "Utilization of Construction and Demolition Debris Under Traffic-Type Loading in Base and Subbase Applications." *Transportation Research Record: Journal of the Transportation Research Board*, No. 1714, Transportation Research Board of the National Accademies, Washington, D.C., pp. 33-39.

Bozyurt, O. (2011) "Behavior of Recycled Asphalt Pavement and Recycled Concrete Aggregate as Unbound Road Base." MS thesis. Department of Civil and Environmental Engineering, University of Wisconsin, Madison.

Bozyurt, 0., Son, Y., Edil, T.B., Tinjum, J.M., Benson, C.H. (2011). "Task IB: Relationship Between Resilient Modulus and Composition of RCA or RAP." TPF-5 (129) Recycled Unbound Materials Pooled Fund Task Report.

Camargo, F. F., Edil. T.B., and Benson, C.H. (2009). "Strength and Stiffness of Recycled Base Materials Blended with Fly Ash." *Transportation Research Board 88th Annual Meeting*,Washigton, D.C.

Camargo, F.F., Benson, C.H., and Edil, T.B. (2012). "An Assessment of Resilient Modulus Testing: Internal and External Deflection Measurements." *Geotechnical Testing Journal,* Vol. 35, No. 6, 9 pages.

Cameron, D.A., Azam, A.H., and Rahman, M.M. (2012). "Recycled Clay Masonry and Recycled Concrete Aggregate Blends in Pavement." *GeoCongress 2012*, Oakland, CA, 1532-1541.

Carpenter, A.C., Gardner, K.H., Fopiano, J., Benson, C.H., Edil, T.B. (2007). "Life Cycle Based Risk Assessment of Recycled Materials in Roadway Construction." *Waste Management*, *27*, 1458-1464.

Chini, A. R., Kuo, S.S., Armaghani, J. M., and Duxbury, J.P. (2001). "Test of Recycled Concrete Aggregatenin Accelerated Test Track." *Transportation Research Record : Journal of Transportation Engineering* , No. 6, Transportation Research Board of the National Accademies, Washington, D.C., pp. 486-492.

Debieb, F. and Kenai, S. (2008). "The Use of Coarse and Fine Crushed Bricks as Aggregate in Concrete." *Construction and Building Materials*, Vol. 22, 886-893.

Ebrahimi, A. (2011). "Deformational Behavior of Fouled Railway Ballast." PhD Dissertation. Department of Civil and Environmental Engineering, University of Wisconsin, Madison.

Federal Highway Administration, "Highway Statistics 2003 - Usage Factors for Major Highway Construction Materials and Labor." http://www.fhwa.dot.gov/policy/ohim/hs03/htm/pt4.htm (accessed May 15, 2012)

FHWA. (2008). *User Guideline for Byproducts and Secondary Use Materials in Pavement Construction.* Publication FHWA-RD-97-148. FHWA, U.S. Department of Transportation.

FHWA. (2011). *Reclaimed Asphalt Pavement in Asphalt Mixtures: State of the Practice.* Publication FHWA-HRT-11-021. FHWA, U.S. Department of Transportation.

Gokce, A., Nagataki, S., Saeki T., and Hisada, M. (2011). " Identification of Frost-susceptible Recycled Concrete Aggregates for Durability of Concrete." *Construction and Building Materials*, Vol. 25, pp. 2426-2431.

GREENBOOK. (2009). Construction Materials, Section 200-Rock Materials. In *Greenbook Standard Specifications for Public Works Construction*.

Griffin, R.L., Simpson, W.C., and Miles, T.K. (1959). "Influence of Composition of paving Asphalt on Viscosity, Viscosity-Temperature Susceptibility, and Durability." *Journal of Chemical and Engineering Data*, Vol. 4, No. 4, 349-354.

Guthri, S.W., Cooley, D., and Eggett, D.L. (2007). "Effects of Reclaimed Asphalt Pavement on Mechanical Properties of Base Materials." *Transportation Research Record: Journal of the Transportation Research Board*, No. 2005, Transportation Research Board of the National Accademies, Washington, D.C., pp. 44-52.

Heydinger, A. G., Xie, Q. L., Randolph, B. W. and Gupta, J. D. (1996). "Analysis of Resilient Modulus od dense and Open-graded Aggregates." *Transportation Research Board*, Washington, D.C., No.1547, 1-6.

Horvath, A. (2003). "Life-Cycle Environmental and Economic Assessment of Using Recycled Materials for Asphalt Pavements." *University of California Technical Report,* 29p.

Huang, Y.H. (2003). "Pavement Analysis and Design." 2nd Edition. Prentice Hall, Upper Saddle River, NJ.

Jong, D.-T., Bosscher, P. J., and Benson, C.H. (1998). "Field Assessment of Changes in Pavement Moduli Caused by Freezing and Thawing." *Transportation Research Record: Journal of the Transportation Research Board*, No.1615, Transportation Research Board of the National Accademies, Washington, D.C., pp. 41-48.

Juan, M. S., and Gutierrez, P. A. (2009). "Study on the Influence of Attached Mortar Content on the Properties of Recycled Concrete Aggregate." *Construction and Building Materials*, Vol. 23, pp.872-877.

Kim, W., and Labuz, J.F. (2007). "Resilient Modulus and Strength of Base Course with Recycled Bituminous Material." *Minnesota Department of Transportation Report No. MN/RC-2007-05*, *1-270.*

Kim, W., Labuz, J.F., and Dai, S. (2007). "Resilient Modulus of Base Course Containing Recycled Asphalt Pavement." In *Transportation Research Record: Journal of the Transportation Research Board,* No. 2005, Transportation Research Board of the National Accademies, Washington, D.C., pp. 27-35.

Kootstra, B. R., Ebrahimi, A., Edil T.B., and Benson, C.H. (2010). Plastic Deformation of Recycled Base Materials. *GeoFlorida 2010: Advances in Analysis, Modeling & Design*, pp.2682-2691.

Kuo, S.-S., Mahgoub, H.S., and Nazef, A. (2002). "Investigation of recycled concrete made with limestone aggregate for a base course in flexible pavement." *Transportation Research Record: Journal of the Transportation Research Board*, No. 1787, Transportation Research Board of the National Accademies, Washington, D.C., pp. 99-108.

Lee, S. J., Amirkhanian, S.N., Shatanawi. S., and Thodesen, C. (2008). “Influence of compaction temperature on rubberized asphalt mixes and binders.” *Can. J. Civ. Eng.*, 35, 908-917.

Lee, J. C., Edil, T.B., Benson, C.H., and Tinjum J.M. (2010). “Use of BE^{2}ST in-Highways for Green Highway Construction Rating in Wisconsin.” *Proceeding of The 1st T&DI Green Streets & Highway Conference*, Denver, Colorado.

Lekarp, F., Isacsson, U. and Dawson, A. (2000). “State of the Art.II: Premanent Strain Response of Unbound Aggregates.” *Journal of Transportation Engineernig ,* No.126, Washington, D.C., 76-83.

Marasteanu, M. O., and D. A. Anderson. (1996). “Time-Temperature Dependency of Asphalt Binders: An Improved Model.” *Proc., Association of Asphalt Paving Technologists*, Vol. 65, pp. 408–448.

Mishra, D., Tutumluer, E., and Butt, A.A. (2010). “Quantifying Effects of Particle Shape and Type and Amount of Fines on Unbound Aggregate Performance Through Controlled Gradation.” *Transportation Research Record: Journal of the Transportation Research Board*, No. 2167, Transportation Research Board of the National Accademies, Washington, D.C., pp 61-71.

Molenaar, A. A. A., and van Niekerk, A.A. (2002). “Effects of Gradation, Composition, and Degree of Compaction on the Mechanical Characteristics of Recycled Unbound Materials.” *Transportation Research Record: Journal of the Transportation Research Board*, No. 1787,Transportation Research Board of the National Accademies, Washington, D.C., pp. 73-82.

Moosazedh, J., and Witczak, M.W. (1981). “Prediction of subgrade moduli for soil that exhibits nonlinear behavior.” *Transportation Research Record: Journal of the Transportation Research Board,* No.810, Transportation Research Board of the National Accademies, Washington, D.C., pp. 9-17.

NAPA. (2009). “How to Increase RAP Usage and Ensure Pavement Performance.” National Asphalt Pavement Association.

Nataatmadja, A. and Tan, Y. L. (2001). “Resilient Reponse of Recycled Concrete Road Aggregates.” *Journal of Transportation Engineering,* No.127, Washington, D.C., 450-453.

NCHRP. (2004). “Laboratory Determination of Resilient Modulus for Flexible Pavement Design.” NCHRP Research Results Digest.

Nokkaew, K., Tinjum, J.M., and Benson, C.H. (2011). *“*Hydraulic Properties of Recycled Asphalt Pavement and Recycled Concrete Aggregate.” GeoCongress, ASCE.

Pan, T., Tutumluer, E., and Anochie-Boateng, J. (2006). “Aggregate Morphology Affecting Resilient Behavior of Unbound Granular Materials.” *Trasnportation Research Record: Journal of the Transportation Research Board*, No.1952, Transportation Research Board of the National Accademies, Washington, D.C., pp. 12-20.

Park, T. (2003) “Application of Construction and Building Debris as Base and Subbase Materials in Rigid Pavement.” *Transportation Research Record :Journal of Transportation Engineering* , No. 129, Transportation Research Board of the National Accademies, Washington, D.C., pp. 558-563.

Poon, C.-S., Qiao, X.C., and Chan, D. (2006). “The Cause and Influence of Self-Cementing Properties of Fine Recycled Concrete Aggregates on the Properties of Unbound Sub-Base.” *Waste Management*, Vol.26, No.10, pp. 1166-1172.

Pucci, M. J. (2010). “Development of a Multi-Measurement Confined Free-Free Resonant Column Device and Initial Studies.” MS thesis, Department of Civil, Architectural and Environmental Engineering, University of Texas, Austin.

Read, J. and Whiteoak, D. (2003). “The Shell Bitumen Handbook, Fifth Edition.” *Thomas Telford Publishing*, London, UK.

Roberts, F. L., Kandhal, P. S., Brown, E. R., Lee, D. Y. and Kennedy, T. W. (1996). “Hot Mix Asphalt Materials, Mixture Design, and Construction.” *National Asphalt Paving Association Education Foundation*. Lanham, MD.

Robinson, G.R., Jr. and Brown, W.M. (2002). “Sociocultural Dimensions of Supply and Demand for Natural Aggregate-Examples from the Mid-Atlantic Region, United States.” US Geological Survey Open-File Report 02-350.

Rosa, M. (2006). “Effect of Freeze and Thaw Cycling on Soils Stabilized using Fly Ash.” MS thesis. Department of Civil and Environmental Engineering, University of Wisconsin, Madison.

Saeed, A., Hammons, M. I., Feldman, D.R., and Poole, T. (2006). "Evaluation, Design and Construction Techniques for Airfield Concrete Pavement Used as Recycled Material for Base." Publication IPRF-07-g-002-03-5. IPRF.

Schaertl, G. J., (2010). "Scaling and Equivalency of Bench-Scale Tests to Field Scale Condition." MS thesis. Department of Civil and Environmental Engineering, University of Wisconsin, Madison.

Schuettpelz, C. C., Fratta, D., and Edil, T. B. (2010). "Mechanistic method for determining the resilient modulus of base course materials based on elastic wave measurements." *Journal of Geotechnical and Geoenvironmental Engineering*. Vol. 136, No. 8, pp. 1086-1094.

Tian, P., Zaman, M. M., and Laguros, J.G. (1998). Gradation and Moisture Effects on Resilient Moduli of Aggregate Bases.In *Transportation Research Record: Journal of the Transportation Research Board,* No.1619, Transportation Research Board of the Natonal Accademies, Washington, D.C., pp.75-84.

Toros, U., and Hiltunen, D.R. (2008) "Effects of Moisture and Time on Stiffness of Unbound Aggregate Base Course Materials." *Transportation Research Record: Journal of the Transportation Research Board*, No.2059, Transportation Research Board of the National Accademies, Washington, D.C., pp. 41-51.

USGS. (2010). *Crushed Stone: Statistical Compendium U.S. Geological Survey.* U.S. Geological Survey,Reston, VA.

USGS Publication. (2011). "Crushed Stone Statistics and Information" http://minerals.usgs.gov/minerals/pubs/commodity/stone_crushed/myb1-2010-stonc.pdf (Accessed May 15, 2012)

Wen, H., Mengqi, W., and Uhlmeyer, J. (2011). "Evaluation of The Effects of Climatic Conditions on Modulus of Base Materials with Recycled Asphalt Pavement." *Journal of ASTM International*, Vol. 8, No. 10, 1-13.

West, R. C., Watson, D.E., Turner, P.A., and Casola, J. R. (2010). "Mixing and Compaction Temperatures of Asphalt Binders in Hot-mix Asphalt." *National Cooperative Highway Research Program*, Report No. 648, Trans. Res. Board, Washington, DC.

Williams, R. R., and Nazarian, S. (2007). "Correlation of Resilient and Seismic Modulus Test Results." *Journal of Materials in Civil Engineering*, Vol 19, No.12, ASCE, pp. 1026-1032.

Wilburn, D.R., and Goonan, T.G. (1998). "Aggregates from Natural and Recycled Sources." U.S. Geological Survey Circular 1176, 36p. http://greenwood.cr.usgs.gov/pub/ciculars/c1176/ (Accessed July 25, 2012)

Wu, Y., Parker, F. and Kandhal, P. S. (1998). "Aggregate Toughness/Abrasion Resistance and Durability/Soundness Tests Related to Aspahlt Concrete Performance in Pavements." *Transportation Research Record,* No.1638, Washington, D.C., 85-93.

Yang, J., Du, Q., and Bao, Y. (2011). "Concrete with Recycled Concrete Aggregate and Crushed Clay Bricks." *Construction and Building Materials*, Vol. 25, 1935-1945.

Zaman, M. M., and Laguros, J.-H., Zhu, J.G. (1999). "Durability Effects on Resilient Moduli of Stabilized Aggregate Base." *Transportation Research Record: Journal of the Transportation Research Board*, No. 687, Transportation Research Board of the National Accademies, Washington, D.C., pp. 29-39.

APPENDIX

Throughout the Recycled Unbound Materials Pooled Fund Project, approximately four individuals have conducted resilient modulus tests on similar materials. Although the material was prepared the same way (95% dry density and 100% optimum moisture content), discrepancies in the calculated summary resilient modulus values were found. Table A.1 and Table A.2 show the values of summary resilient modulus for material collected from the same sample, but prepared by different individuals. It also shows the fluctuation in SRM from user to user through the standard deviation and coefficient of variation. For some material the coefficient of variation is rather high (> 90%), while other materials it is low (4%). By viewing Figure A.1 and A.2, it can be observed that external LVDT summary resilient modulus values have overall lower coefficients of variation between different users when compared to internal LVDT summary resilient modulus. This difference in SRM between users on the same material has been investigated thoroughly and was determined to be a problem with calibration of the LVDTs and a physical difference of LVDTs used for each test. For example, Son used interior LVDTs that were unable to record displacements high enough to run an entire resilient modulus test without stopping the test and readjusting the LVDTs. This could have caused error in both his interior and exterior LVDT summary resilient modulus values.

For the studies described in this thesis, all resilient modulus data used was collected from tests performed by the author. No previous data was used except for the comparison in this Appendix. For this study, only four samples had enough material for replicate tests to be performed. Those materials were Class 5, Basalt, CA RCA, and TX

RCA. For those tests, coefficients of variation were determined and plotted as Figure A.3 for internal summary resilient modulus values and Figure A.4 for external summary resilient modulus values. The coefficients of variation in this study were less than 24% for internal summary resilient modulus values and less than 20% for external summary resilient modulus, both much lower than those of previous studies compared to this study.

Table A.1 Internal and External SRM Statistical Analysis on Replicate Specimens Prepared by Shedivy

		Internal LVDT Data				External LVDT Data			
Material	**M_r Tester**	**NCHRP SRM (MPa)**	**Average (MPa)**	**σ (MPa)**	**C_v**	**NCHRP SRM (Mpa)**	**Average (MPa)**	**σ (MPa)**	**C_v**
Class 5	Shedivy	123	154	36	23%	91	113	19	17%
	Shedivy	115				100			
	Shedivy	129				97			
Basalt	Shedivy	180	197	28	14%	131	130	8	7%
	Shedivy	192				121			
	Shedivy	187				135			
CA RCA	Shedivy	181	197	33	17%	121	123	17	14%
	Shedivy	246				140			
TX RCA	Shedivy	188	180	11	6%	99	115	22	19%
	Shedivy	172				130			

Note: Average is the mean, σ is the standard deviation, and C_v is the coefficient of variation

Table A.2 Internal and External SRM Statistical Analysis for Natural Aggregate and RAP Replicate Tests Completed on the Same Material Prepared across Multiple Studies (Ba et al. 2011, Bozyurt 2011)

		Internal LVDT Data				External LVDT Data			
Material	**M_r Tester**	**NCHRP SRM (MPa)**	**Average (MPa)**	**σ (MPa)**	**C_v**	**NCHRP SRM (MPa)**	**Average (MPa)**	**σ (MPa)**	**C_v**
Class 5	Shedivy	123	218	140	64%	91	131	40	31%
	Shedivy	115				100			
	Shedivy	129				97			
	Bozyurt	237				182			
	Bozyurt	221				169			
	Son	484				144			
Basalt	Shedivy	180	224	52	23%	131	138	13	9%
	Shedivy	192				121			
	Shedivy	187				135			
	Ba	274				148			
	Ba	286				153			
TX RAP	Shedivy	269	453	169	37%	200	225	89	39%
	Bozyurt	600				323			
	Son	490				151			
NJ RAP	Shedivy	290	503	301	60%	166	187	29	16%
	Son	715				207			
CO RAP	Shedivy	228	269	212	79%	151	167	14	8%
	Bozyurt	309				172			
	Son	629				177			
MN RAP	Bozyurt	387	526	197	37%	223	199	35	17%
	Son	665				174			

Note: Average is the mean, σ is the standard deviation, and C_v is the coefficient of variation

Table A.3 Internal and External SRM Statistical Analysis for RCA Replicate Tests Completed on the Same Material Prepared across Multiple Studies (Ba et al. 2011, Bozyurt 2011)

		Internal LVDT Data				External LVDT Data			
Material	**M_r Tester**	**NCHRP SRM (MPa)**	**Average (MPa)**	**σ (MPa)**	**C_v**	**NCHRP SRM (MPa)**	**Average (MPa)**	**σ (MPa)**	**C_v**
CA RCA	Shedivy	181	369	184	50%	121	170	57	34%
	Shedivy	246				140			
	Bozyurt	487				251			
	Son	563				166			
NJ RCA	Shedivy	157	420	372	89%	85	144	83	58%
	Son	683				203			
TX RCA	Shedivy	188	299	150	50%	99	153	56	37%
	Shedivy	172				130			
	Bozyurt	346				231			
	Son	490				151			
OH RCA	Shedivy	223	345	157	46%	149	170	28	17%
	Bozyurt	289				202			
	Son	522				158			
MN RCA	Shedivy	134	391	363	93%	109	150	57	38%
	Son	648				190			
MI RCA	Bozyurt	293	504	298	59%	180	176	6	4%
	Son	715				171			
CO RCA	Bozyurt	265	393	180	46%	224	193	44	23%
	Son	520				162			

Note: Average is the mean, σ is the standard deviation, and C_v is the coefficient of variation

Table A.4 SRM and Power model fitting parameters k_1 and k_2 for base materials after 0, 5, 10 and 20 F-T cycles

Material	States	Freeze-Thaw Cycles	External			Internal			SRM_0/ SRM_N
			k_1	k_2	SRM (MPa)	k_1	k_2	SRM (MPa)	
Class 5 Aggregate	MN	0	66.2	0.20	191	129.2	0.15	281	1.0
		5	59.1	0.21	186	59.1	0.28	261	0.9
		10	35.5	0.30	177	34.7	0.36	240	0.9
		20	24.8	0.34	153	24.7	0.41	223	0.8
RCA	CA	0	119.4	0.15	262	273.6	0.13	550	1.0
		5	74.8	0.21	227	113.4	0.27	489	0.9
		10	99.1	0.20	282	185.7	0.21	578	1.1
	MI	0	32.7	0.34	199	107.2	0.25	400	1.0
		5	22.8	0.39	191	55.3	0.35	361	0.9
		10	47.8	0.32	257	177.5	0.18	472	1.2
		20	83.6	0.22	268	388.7	0.07	553	1.4
	TX	0	74.6	0.23	258	236.1	0.13	464	1.0
		5	43.6	0.30	211	76.8	0.32	419	0.9
		10	44.6	0.31	236	120.8	0.26	471	1.0
		20	81.1	0.24	289	150.2	0.28	601	1.3
RAP	CA	0	122.5	0.14	256	348.8	0.06	473	1.0
		5	122.5	0.13	249	147.9	0.20	436	0.9
		10	76.6	0.20	223	136.2	0.19	379	0.8
		20	66.0	0.21	203	122.8	0.18	323	0.7
	MN	0	93.9	0.174	238	236.1	0.127	464	1.0
		5	57.6	0.25	220	85.8	0.27	361	0.8
		10	54.0	0.25	200	80.2	0.27	344	0.7
		20	31.2	0.33	180	57.3	0.32	314	0.7
	TX	0	156.6	0.14	334	358.7	0.12	686	1.0
		5	155.2	0.12	287	344.1	0.10	585	0.9
		10	88.6	0.21	272	259.1	0.15	566	0.8
		20	63.6	0.26	254	103.2	0.29	497	0.7

Table A.5 LA Abrasion Results

Specimens	**LA Abrasion Loss (%)**
Class 5 Natural Aggregate	23
MN RCA (Bozyurt 2011)	30
RCB (Arulrajah et al. 2011)	36

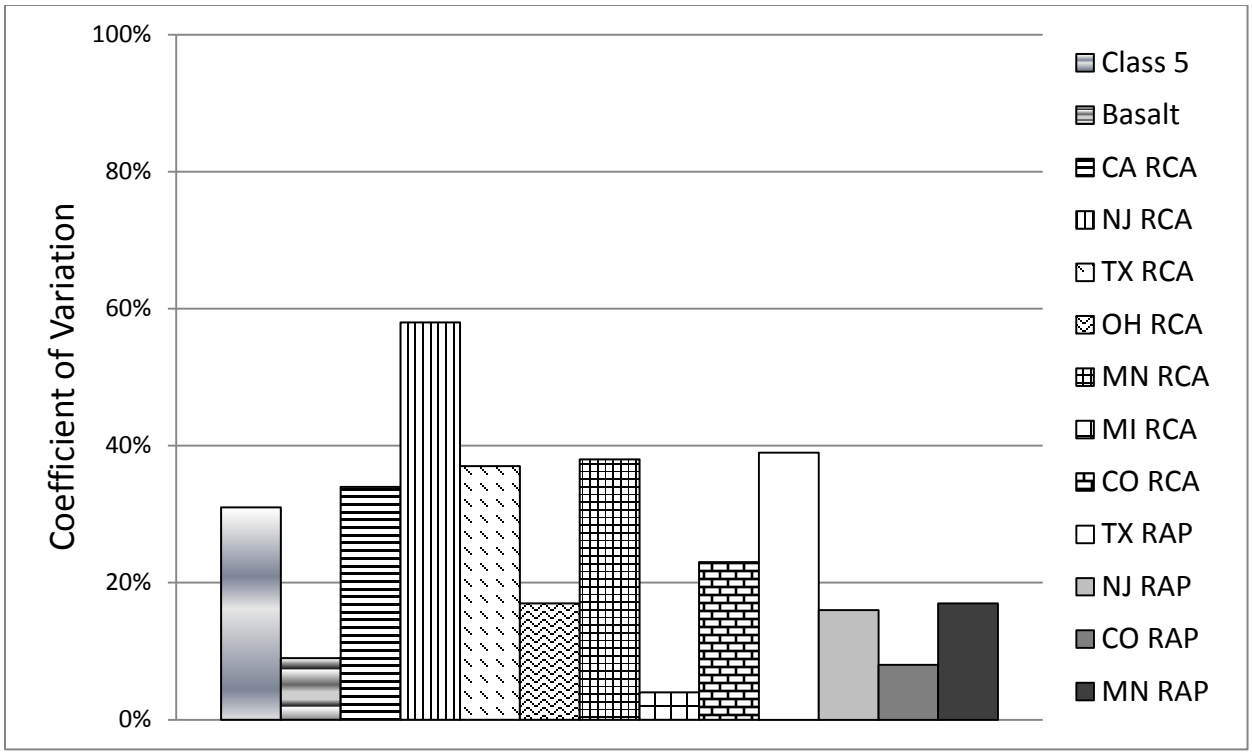

Figure A.1 External SRM Coefficients of Variation for Replicate Specimens Prepared Across Multiple Studies (Ba et al. 2011, Bozyurt 2011)

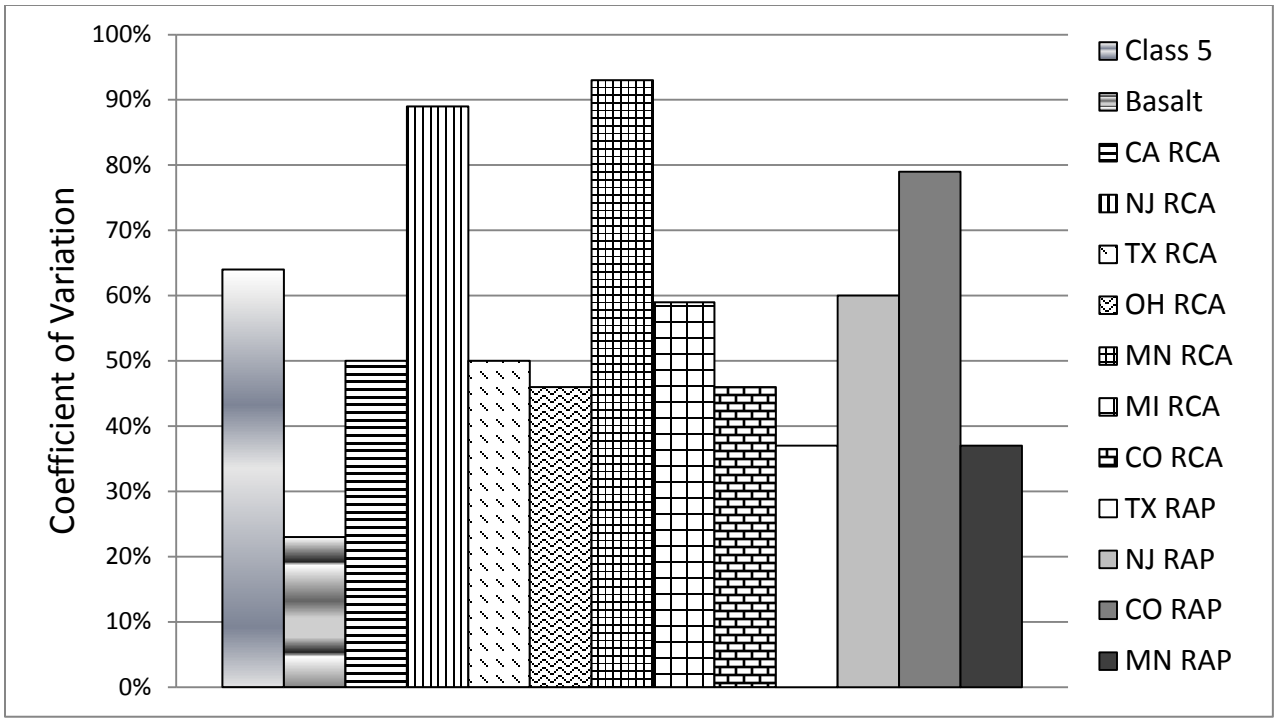

Figure A.2 Internal SRM Coefficients of Variation for Replicate Specimens Prepared Across Multiple Studies (Ba et al. 2011, Bozyurt 2011)

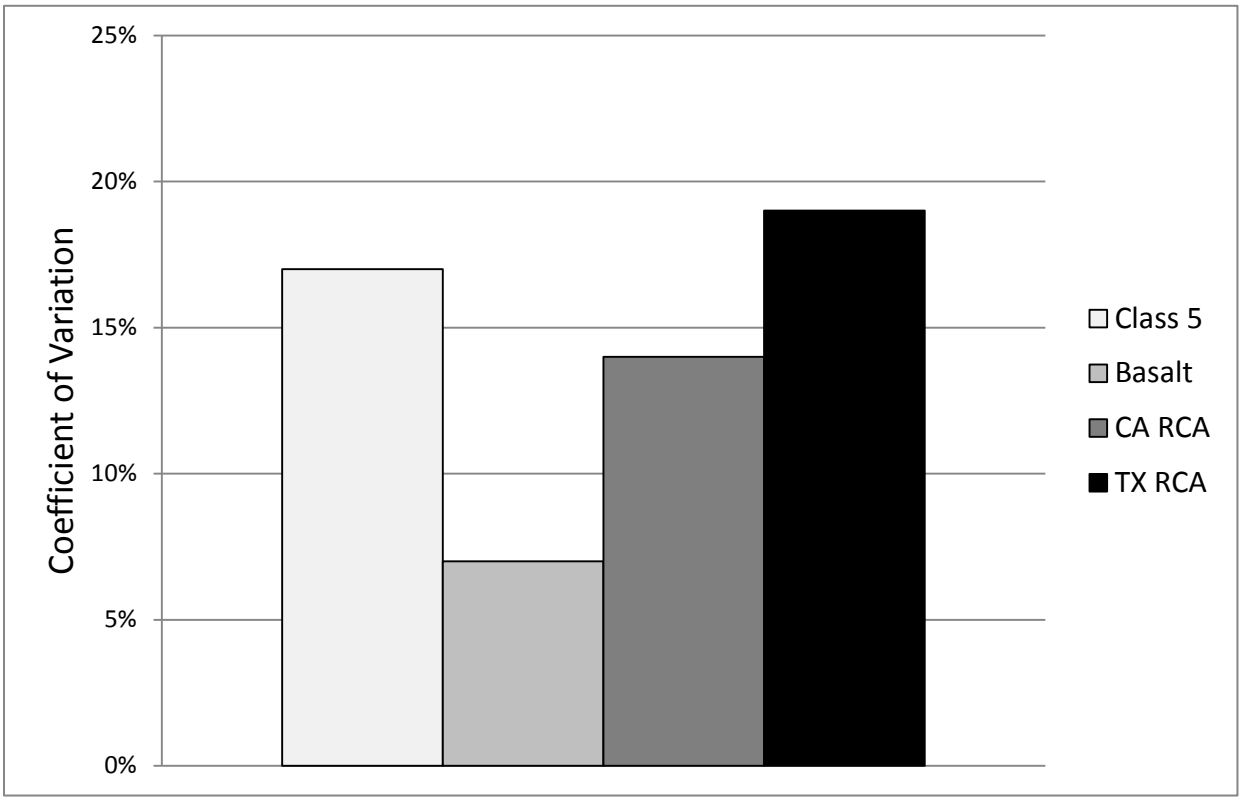

Figure A.3 External SRM Coefficients of Variation for Replicate Specimens Prepared by Shedivy

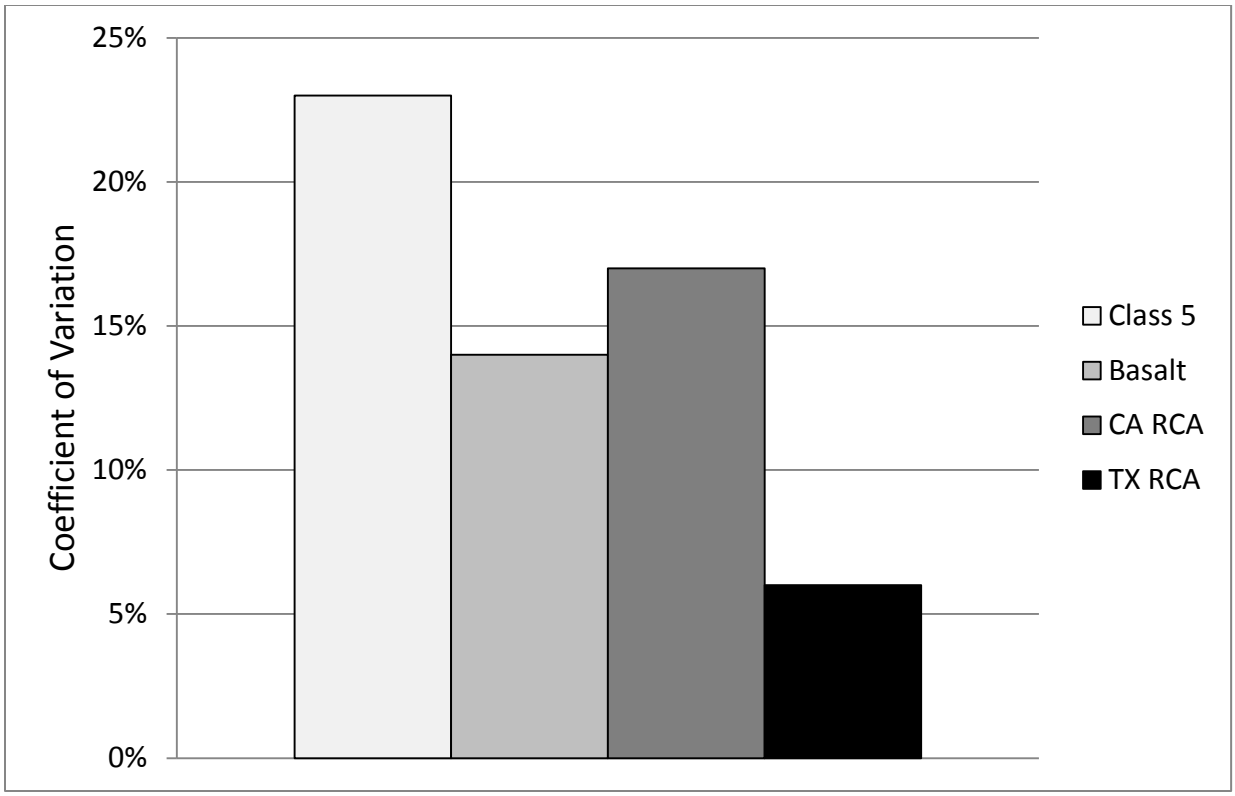

Figure A.4 Internal SRM Coefficients of Variation for Replicate Specimens Prepared by Shedivy

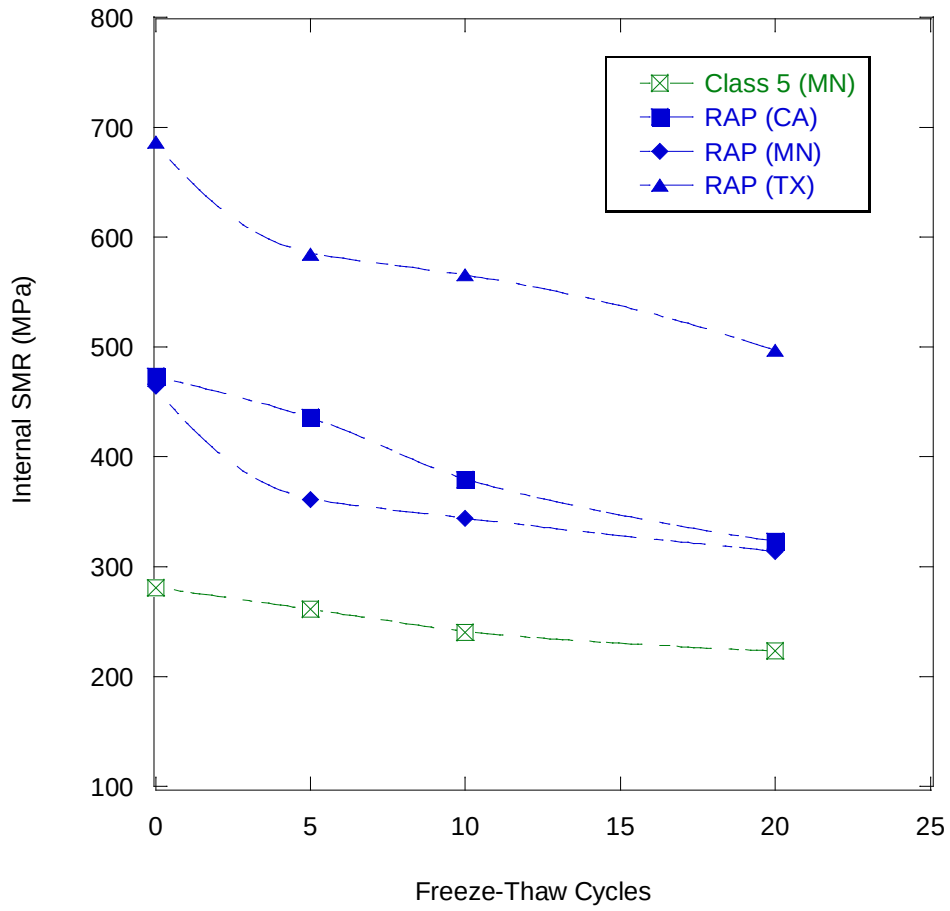

Figure A.5 Summary Resilient Modulus (SRM) of RAP and Class 5 Aggregate after 0, 5, 10 and 20 Freeze-Thaw Cycles (Bozyurt 2011)

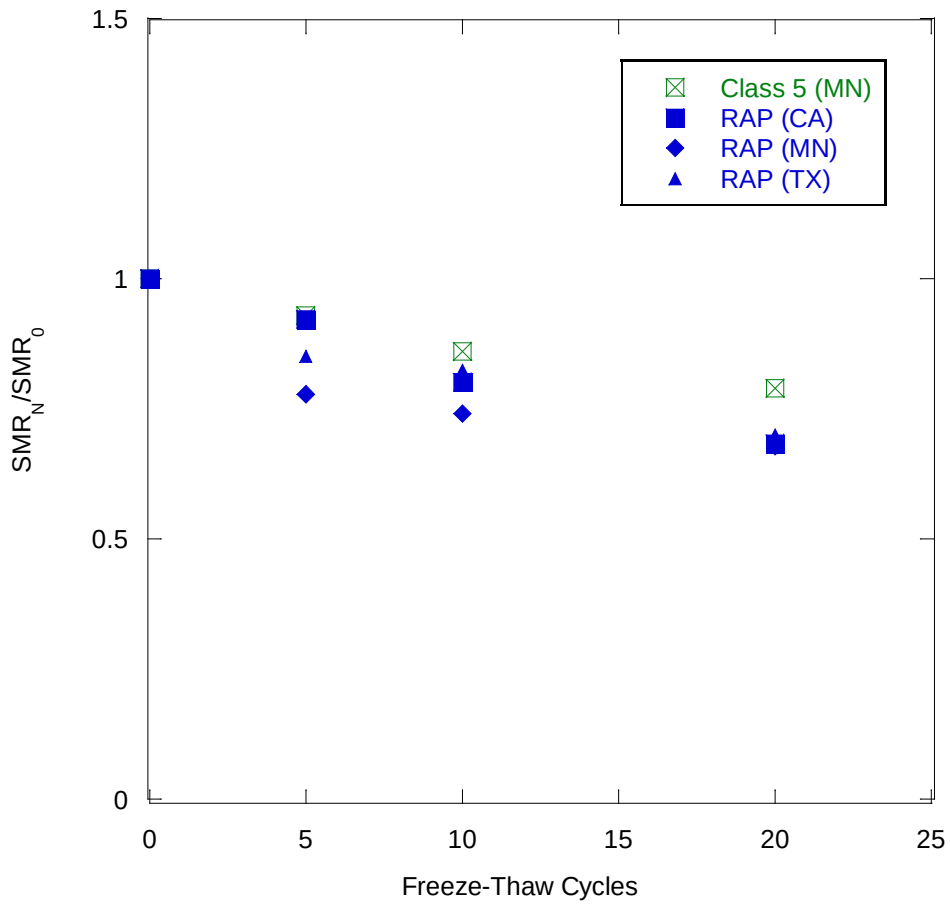

Figure A.6 Normalized Summary Resilient Modulus (SRM) of RAP and Class 5 Aggregate after 0, 5, 10 and 20 Freeze-Thaw Cycles (Bozyurt 2011)

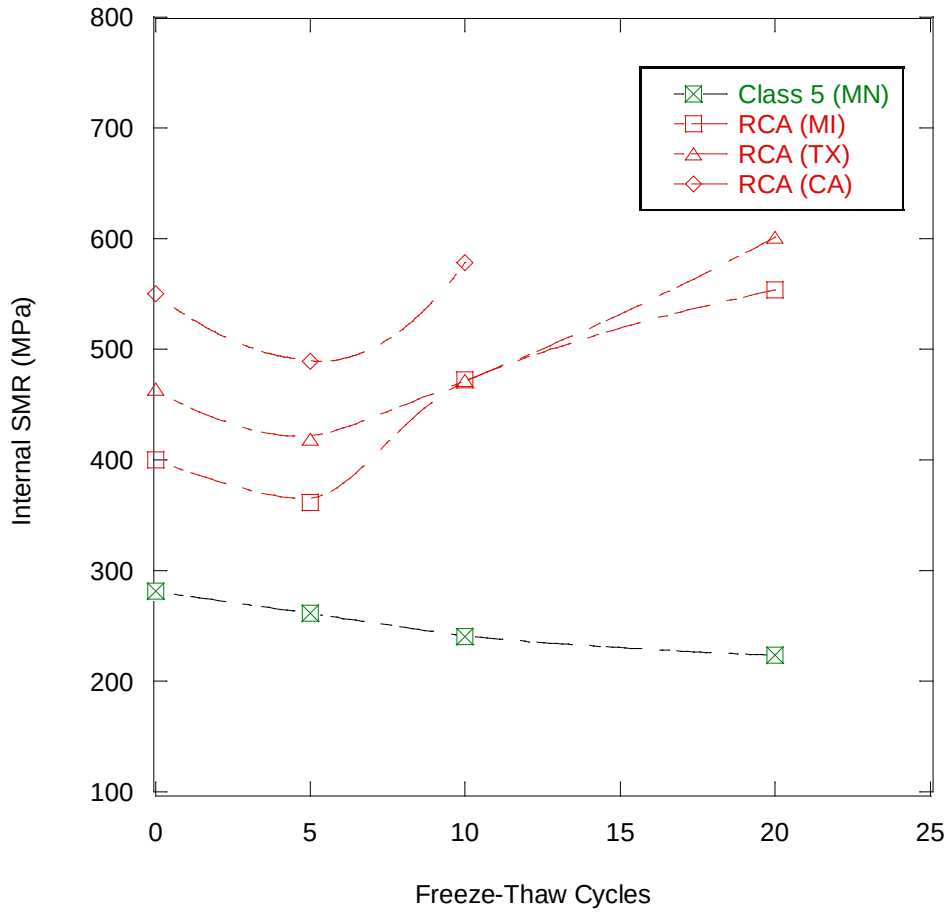

Figure A.7 Normalized Summary Resilient Modulus (SRM) of RCA and Class 5 Aggregate after 0, 5, 10 and 20 Freeze-Thaw Cycles (Bozyurt 2011)

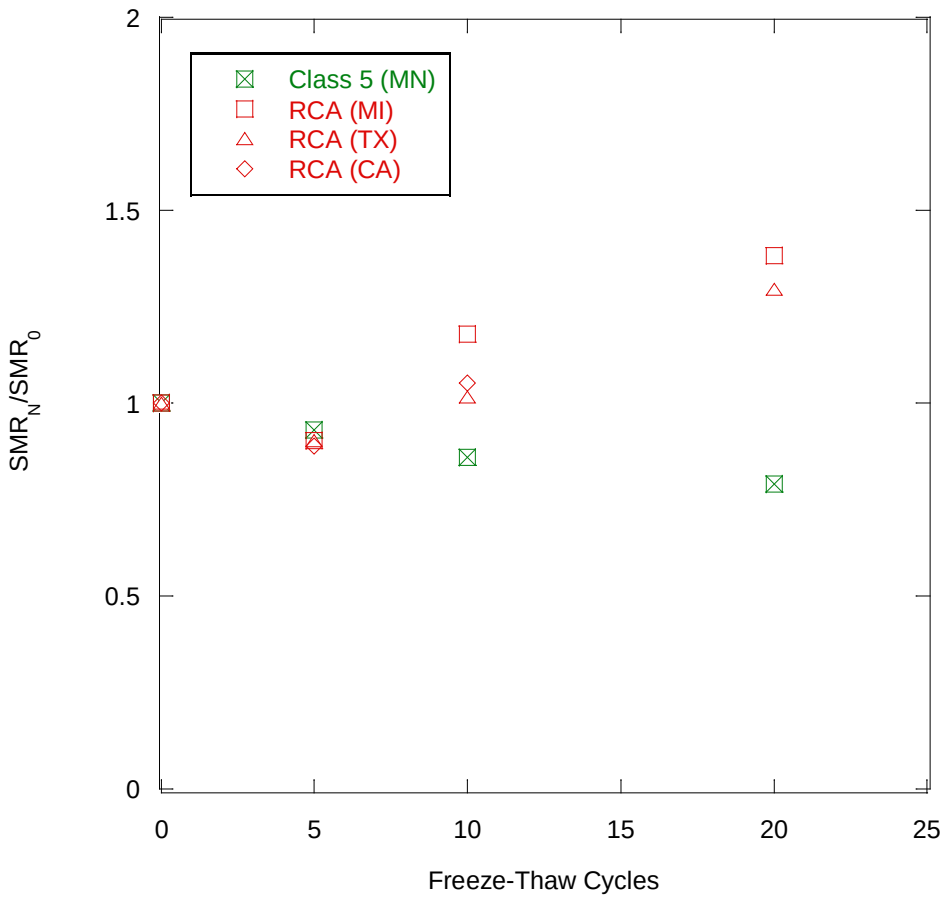

Figure A.8 Normalized Summary Resilient Modulus (SRM) of RCA and Class 5 Aggregate after 0, 5, 10 and 20 Freeze-Thaw Cycles (Bozyurt 2011)

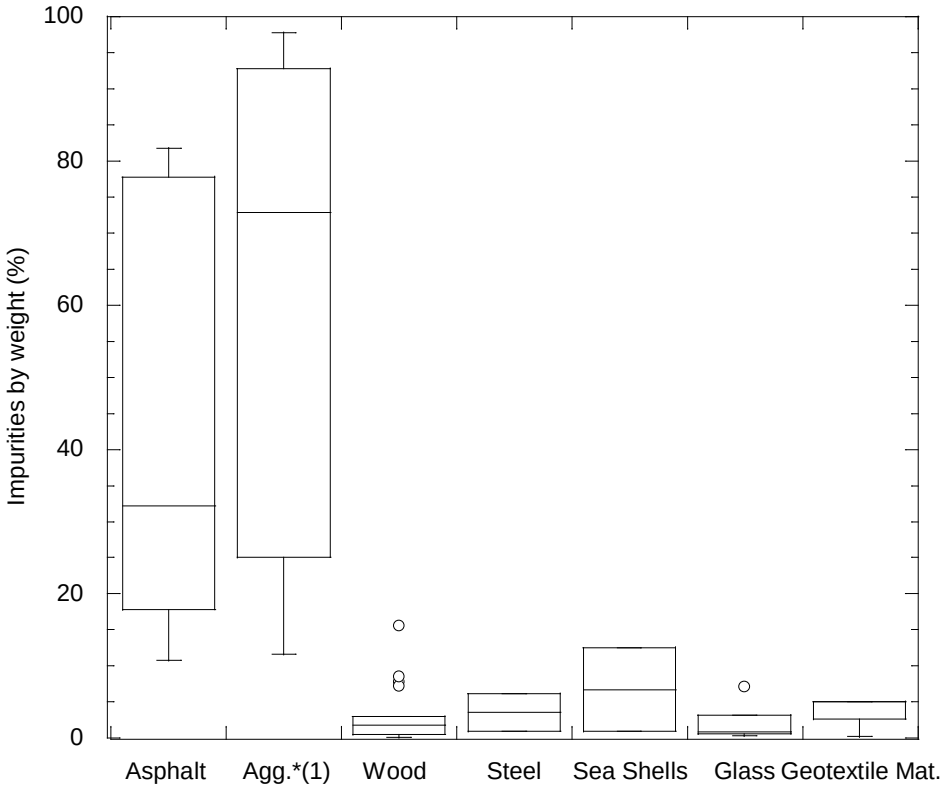

*(1): Aggregates with plastic fibers

Figure A.9 Distribution of Impurities by Weight Percentage (Bozyurt 2011)

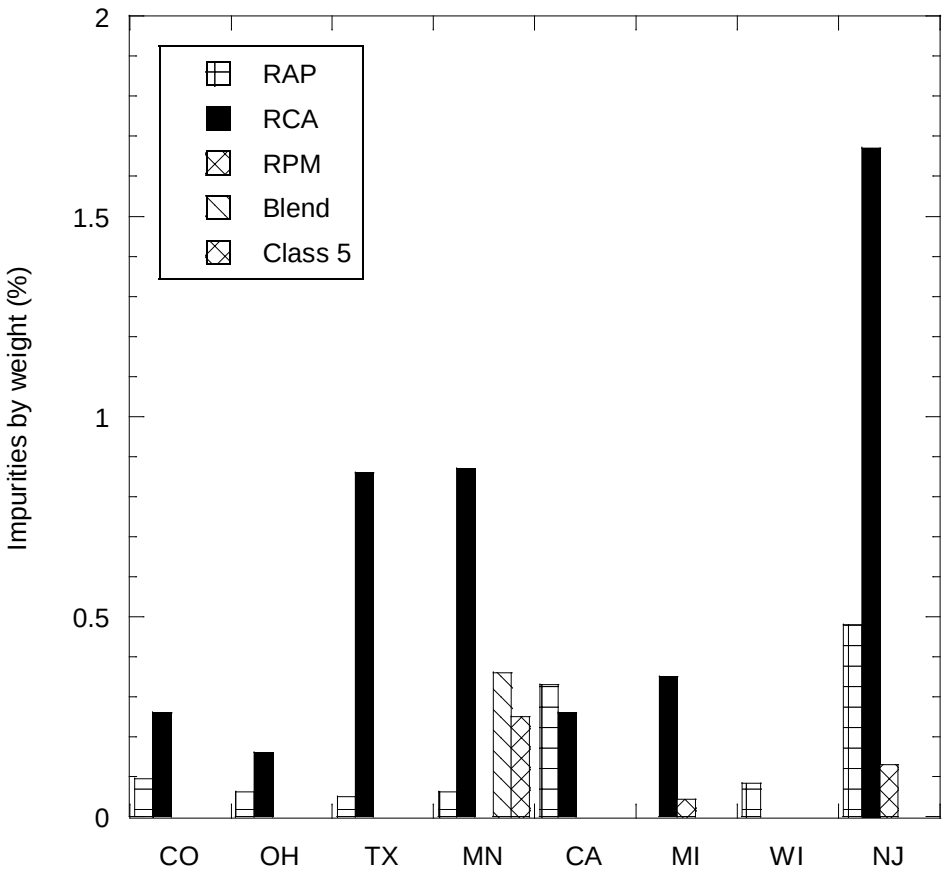

Figure A.10 Percent Impurities found in Recycled Material from Different States (Bozyurt 2011)

Figure A.11 Deleterious Material found in RCA: Sea Shells and Steel (Bozyurt 2011)

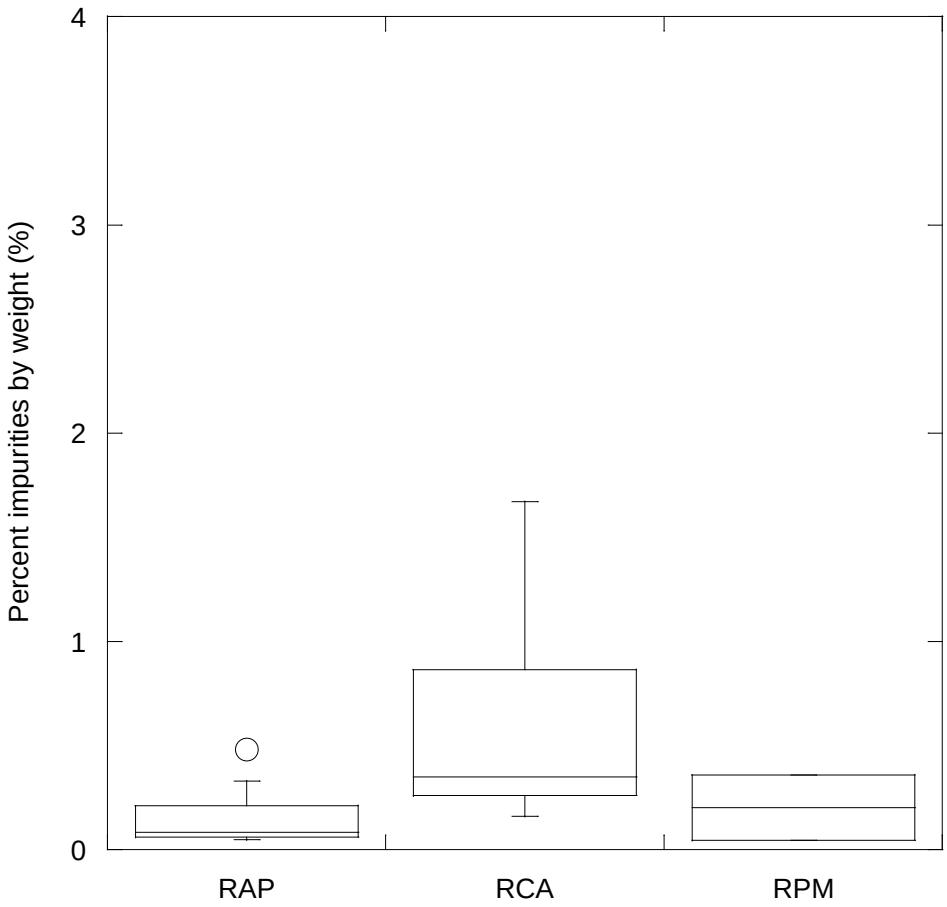

Figure A.12 Average Impurity Percentage by Weight for Recycled Material (Bozyurt 2011)

Figure A.13 Deleterious Material found in RAP: Pavement Markings and Wood Chips (Bozyurt 2011)